EPIGENETIC REGULATION OF HORMONAL RESPONSE

THESIS FOR THE DEGREE OF DOCTOR OF PHILOSOPHY (Ph.D.)

by

BÁLINT LÁSZLÓ BÁLINT M.D.

DEPARTMENT OF BIOCHEMISTRY AND MOLECULAR BIOLOGY
MEDICAL AND HEALTH SCIENCE CENTER
UNIVERSITY OF DEBRECEN
DEBRECEN, 2005

CONTENTS

1. A HORMONVÁLASZ EPIGENETIKAI SZABÁLYOZÁSA

A magreceptorok ligandfüggő transzkripciós faktorok, zsíroldékony molekulák, hormonok és anyagcseretermékek sejten belüli érzékelői. Munkacsoportunk fő érdeklődési területét a magreceptoroknak azon alcsoportja képezi, mely heterodimert alkot az RXR molekulával, a 9-cisz-retinsav receptorával. E magreceptorok kulcsszerepet játszanak a fejlődésben, anyagcserében és különböző patofiziológiás állapotokkal is kapcsolatba hozták őket, mint az ateroszklerózis és a diabétesz. Ezen magreceptorok közös jellemzője, hogy DNS-kötött érzékelői az intra- és extracelluláris lipideknek. A magreceptorok genomi szintre fordítják a sejt zsíroldékony környezetének változásait.

Ezen jellegzetességük alapján nano-kapcsolókként értelmezhetjük őket, melyek megváltoztatják a kromatin állapotát, és genomi programokat indítanak be a sejt lipidkörnyezetében bekövetkezett változásokra adott válaszként.

A HL-60 sejtvonal egy kiterjedten vizsgált mieloid leukémia sejtvonal, mely fiziológiás és farmakológiás behatásokra különböző irányokba differenciálódhat. A differenciáció során két különálló szakaszt különböztetünk meg. Az első szakasz egy átmeneti állapot vagy alapozási lépés, míg a második szakasz kései folyamatok sorozata, melyeknek vége a differenciációs útvonalbéli elköteleződés és a terminális differenciáció. E lépésre jellemző a magstruktúra átalakulása és néhány sejtciklusra kiterjedő memória. Az alapozási lépés során lejátszódó molekuláris folyamatokról és ezek szerepéről a későbbi génexpresszió szabályozásában igen keveset tudunk.

A differenciációt meghatározó molekuláris mechanizmusokat részben a kromatin állapota határozza meg. A kromatin strukúra döntő szerepet játszik a génexpresszió szabályozásában, mivel meghatározza a transzkripciós faktorok hozzáférését a DNS-hez. Magát a kromatin szerkezetét két enzimcsoport határozza meg: egyrészt az ATP függő kromatin átalakító enzimek (remodelling), másrészt a kromatin módosító enzimek csoportja. Ez utóbbiak felelősek a hisztonvégek poszttranszlációs módosításáért. A „hiszton-kód“ elmélet szerint a hiszonvégeken létrejövő kovalens módosítások fenntartják és szabályozzák a génexpressziós mintázatokat. A kovalensen módosított hisztonvégekről korábban leírták, hogy chromo- és bromodomén tartalmú fehérjék kötőhelyei lehetnek. Feltételezések szerint ezek a hisztonkötő fehérjék biztosítják a funkcionális kapcsot a módosított hisztonvégek és a transzkripció iniciáció effektorai között.

A kromatin immunprecipitációs technika segítségével (angolul: Chromatin immunoprecipitation: ChIP) in vivo fehérje:DNS kölcsönhatásokat vizsgálhatunk kromatin szinten. Adott fehérje elleni antitestek használatával a fehérje által kötött DNS darabok könyvtárát hozhatjuk létre és vizsgálhatjuk.

A HL-60 sejt differenciációja során létrejövő alapozási lépés molekuláris mechanizmusainak vizsgálata céljából elkészítettük a szöveti tranzglutamináz promóterének hisztonvég módosítási térképét. A szöveti tranzglutamináz expressziója ezen differenciáció során nagymértékben fokozódik. A promóter térképét három

különböző állapotban vettük fel kiindulási állapotban: az alapozási lépés során, melyet egy rövid DMSO vagy D-vitamin kezeléssel hoztunk létre, és differenciált állapotban, melyet az alapozásban résztvevő sejtek retinoid kezelésével hoztunk létre.

Az alapozás és a transzkripció során különálló kromatin szintű folyamatokat sikerült azonosítanunk. Az alapozás nagymértékű oldallánc-metilációs változásokat okoz: a H3 oldallánc K4 csoportjának metilációja csökken a promóteren, illetve a H4 oldallánc R3 csoportjának metilációja fokozódik az enhanszeren. A hiszton fehérjék arginin metilációja különös jelentőségű az alapozási állapot létrehozásában, mivel farmakológiai gátlása magát az alapozást is megszüntette.

Eredményeink alapján új modelljét javasoljuk a retinoid válaszkészség szabályozásának mieloid leukémia sejtekben. A szöveti transzglutamináz retinoid függő indukciója során sikerült egy új szerepét azonosítani a korábban leírt, de kevéssé karakterizált H4R3 metilációnak.

A H4R3 metiláció a differenciáció alapozási fázisára jellemző, és megelőzi a gén aktiválódását. E módosítás egy transzkripcionálisan még kikapcsolt, de „érzékenyített" állapotot jelöl, melynek következtében a módosított hisztonok jobb szubsztrátjaivá válnak a hiszton acetiltranszferázoknak. E mechanizmus felelős a fokozott retinoid válaszkészségért. A hisztonok preacetilációja meggátolja H4R3 metiláció kialakulását.

A javasolt modell egybecseng a hisztonkód elmélettel, mely szerint a módosított hisztonvégek fizikai hordozói a sejtmemóriának. Transzkripciós faktorok kötődését biztosítva ezek a hisztonvég módosulások génexpressziós kapcsolókként is felfoghatóak. Adataink a H4R3 metilációnak egy új szerepet tulajdonítanak, mely potenciálisan farmakológiailag módosítható és felhasználható a hormonhatás szabályozására.

H4R3 metiláció további vizsgálata céljából klónoztuk a módosítást tartalmazó kromatin darabokat, majd szekvenálás és in silico analízis után megállapítottuk, hogy a találatok mindegyike introni vagy gének 5' végéhez közeli lokalizációjú volt. Ezen lokalizációk feldúsulást mutattak a következő konzervált transzkripciós faktor kötőhelyekben: POU2F1, MEF-2 és FOXL1. Az így azonosított genomi lókuszok szignalizációs útvonalakban és fejlődési folyamatokban szerepet játszó gének közelében voltak. Ezen lókuszok további vizsgálata új szerepeit tisztázhatja a H4R3 metilációnak.

Munkám második részeként vizsgálati rendszeremet kiterjesztettem egy zárt rendszerből (egyedi promóterek vizsgálata) egy nyitott rendszerré (klónozás és szekvenálás). A módszer segítségével H4R3 metilációs helyeket térképeztünk a genomban. A módszert sikeresen alkalmazták eddigiekben transzkripciós faktor kötőhelyek azonosítására (Weinmann et al. 2001).

A genomi lokalizációs analízis egyesíti a kromatin immunprecipitációs módszert a microarray technikával (Weinmann et al. 2002). A módszer segítségével teljes genomi kontextusban vizsgálható, miként befolyásolja az epigenetikai környezet egy gén transzkripcióját.

Vizsgálatainkhoz egy 12000 CpG szigetet tartalmazó DNS chipet használtunk, és magreceptor kötődést, valamint H4 acetilációs státuszt vizsgáltunk. Az eredmények feldolgozását megkönnyítendő létrehoztunk egy bioinformatikai webfelületet, melynek segítségével a 12k CpG platformon begyűjtött adatokat tükrözhetjük Affymetrix platformon szerzett globális expressziós adatokra.

Összegzésként elmondhatjuk, hogy munkánk során azonosítottuk a szöveti transzglutamináz fokozott retinoid válaszkészgére jellemző epigenetikai változásokat. A fokozott válaszkészségre megnövekedett H4R3 és csökkent H3K4 metiláció jellemző. További kísérleteinkben teljes genomi megközelítésben vizsgáltuk a H4R3 és az acetilációs hisztonvégmódósításokat.

2. INTRODUCTION

Nuclear receptors are ligand activated transcription factors. They act as sensors of lipid soluble molecules, hormones or metabolites. Our main research interest focuses on a subclass of nuclear receptors that forms heterodimers with RXR, the 9-cis-retinoic acid receptor, with major implications in development and in certain diseases, such as atherosclerosis and diabetes. A common attribute of this subclass of nuclear receptors is that they are DNA-bound sensors of intra- or extracellular lipid soluble molecules. Nuclear receptors translate the lipid soluble small molecular environment of the cell into genomic actions. Thus, nuclear receptors can be viewed as molecular nano-switches that

change the status of the chromatin and open genomic scripts depending on the lipid environment of the cell.

2.1. Molecular determinants of the nuclear receptor action

The main structural parts of the nuclear receptors are the DNA binding domain (DBD) and the ligand bindig domain (LBD) and these are connected by a loose hinge region. The DBD is a well conserved zinc finger domain. The LBD is made of 12 alpha helices packed in three layers, forming a three-layered alpha helical sandwich. LBD-s are less well conserved and usually contain a ligand binding pocket. The ligand binding pockets determine the subtype of ligands that will activate the receptors, and their volume is widely variable. For example, PPARs have large ligand-binding pockets varying from 1300 cubic angstrom ($Å^3$) to 1500$Å^3$ depending on the isotype (Watkins et al. 2001), while RXRα and Vitamin D receptor has a ligand-binding pocket of 700$Å^3$ and 800$Å^3$, respectively. It has been proposed that some orphan receptors, such as RORα, do not have an open pocket, but bind a "structural lipid", a cholesterol molecule presumably constitutively, (Chai et al. 2001; Willson 2002; Kallen et al. 2004). Another orphan receptor, Nurr1 does not have ligand binding cavity at all, based on structural evidence (Wang et al. 2003). The concept of metabolic sensors is consistent with data demonstrating nuclear receptors acting as metabolic sensors, since the large ligand-binding pocket of some of them can bind structurally very different ligands. For example, the highly selective ligand Rosiglitazone fills only 25% of the large pocket of PPARγ, while GI262570, a tyrosine-based molecule that binds to the PPARγ/RXRα heterodimer, occupies approximately 40% of it (Gampe et al. 2000). On the other end we find RAR, in which all-trans retinoic acid fills 60% of a 441$Å^3$ pocket (Escriva et al. 2000) (Bourguet et al. 2000). More interestingly, according to structural data, eicosapentaenoic acid (EPA) is binding the pocket of PPARδ in two distinct conformations, filling a volume of 300 $Å^3$ (30% of the pocket) in each docking mode (Xu et al. 1999).

Nuclear receptors in their unliganded state bind corepressors (Nagy et al. 1997). The active form of these receptors is formed after ligand binds in their cavity. Ligand binding is stabilizing the structure of the protein (as a chemical skeleton) and helix 12 is

bent towards the core of the LBD (Benko et al. 2003). In the new conformational state, the receptor will be able to bind coactivators. This initiates a protein-protein interaction cascade that ultimately results in the transcription of the regulated gene (Metivier et al. 2003). During this process, coactivators recruit proteins with enzymatic activity, that induce changes in the phosphorylation, methylation and acetylation state of the histone tails, thus switching the chromatin into an activated state. The initial step for this cascade is the ligand-induced switch, which might produce a full spectrum of conformational states of the receptor (Nagy et al. 2004).

2.2. Molecular determinants regulating differentiation

Monocytes and the cells from this lineage provide an excellent model system to study cell differentiation and the involvement of nuclear receptors in health and disease. Nuclear receptors were shown to be involved in major diseases (Kliewer et al. 1999). RAR was implicated in leukemia through the PML-RAR fusion protein (Chen et al. 1994), PPAR-s in diabetes and atherosclerosis (Laffitte et al. 2002), vitamin D receptor (VDR) and estrogen receptors (ER) in osteoporosis (Thompson et al. 1999) and cancer. Complex regulation of metabolism seems to be also driven by some nuclear receptors: TR (tyroid hormone receptor) is a general integrator of metabolism, PPAR-s regulate adipogenesis and inflammation, LXR-s (Liver X Receptor), FXR (Farnesoid X Receptor) and SXR regulate cholesterol metabolism, bile acid and xenobiotic processing in the liver.

In the monocytic cell lineage, RAR and PPARγ were already identified as key regulators at different stages of development and terminal differentiation. The variety of cell lines available and the ease of preparing primary cells makes it straightforward to study myeloid differentiation. It is well documented that during cell differentiation the overall structure of chromatin is rearranged. Global acetylation levels drop and large chromosomal territories are changed from euchromatic to heterochromatic structure. Certain sets of genes are silenced, and their repressed state is maintained through multiple cell divisions by cellular memory. Equally importantly, during these events gene activation is responsible for the development of specialized functions, specific for each terminally differentiated cell type. As mentioned before, two nuclear receptors are

involved in the differentiation of monocytes at different stages: Retinoid receptors (RAR) and PPAR-s. The former is involved in the early stages of differentiation, while PPAR-s are key players of terminal differentiation of these cells. RAR was implicated in the development of leukemia through the chromosomal break and rearrangements resulting in a the PML-RAR fusion protein (Chen et al. 1994). On the other hand, PPARγ is markedly upregulated during monocyte-macrophage transition when these cells pass from circulation to periphery (Tontonoz et al. 1998). Although the marked nuclear rearrangement during the differentiation of this cell type is well known, the molecular determinants and the role of nuclear receptors in this process was not studied in this context.

The HL-60 cell line is a well-characterized M2 myeloid leukemia cell line that can be induced to undergo differentiation along different pathways to form monocytes or granulocytes, in response to a variety of physiological and pharmacological stimuli (Yen 1985; Collins et al. 1990). The process of myeloid differentiation itself involves two distinct and sequential steps (Yen 1985). The first is an identifiable intermediate state termed the precommitment or primed state, while the second is a series of late events leading to the onset of lineage-specific terminal differentiation. Altered nuclear structure and feature retention of phenotype, a form of cellular memory that can last for several cell cycles characterize primed cells. Very little is known about the molecular characteristics of the precommitment or primed state and it is particularly ill-defined how these molecular changes impact the regulation of gene expression. Some of the molecular mechanisms that drive differentiation of this cell line were shown to produce changes in chromatin structure (Ponton et al. 1996).

2.3. The histone code hypothesis

For cells undergoing differentiation, the phenotypic identity of a cell, as defined by its distinctive pattern of gene expression, has to be maintained through multiple cycles of DNA replication, chromatin assembly and repackaging. It has been suggested that there has to be some sort of cellular memory that provides a cell with an epigenetically coded identity that can be preserved during differentiation (Turner 2000) (Turner 2002).

In a human cell around 2m of DNA is packed and during each cell division its folded to considerably dense structure to perform the complicated manoeuvres of mitosis. This fact is impressive by itself and the further steps are also remarkable. After mitosis this compact DNA-protein complex, the chromosome, is specifically convoluted to perform its functional task namely to serve as template for the mRNA synthesis. The fact that the spindles of the nucleosomes, the histone octamers, are not only the physical carriers of the folded DNA but might serve as a functional structure that is able to regulate this folding and convolution is one of the most exciting finding of the past decades of molecular biology. The growing evidence supporting the hypothesis that the histone tails might be carriers of inherited information, settled the grounds of the novel field of epigenetics. By epigenetics we refer to the inheritance of information which is not directly embedded in the sequence of the double helix. The question of non-DNA carried inheritance was originally formulated around the so called “cytoplasmic” inheritance (for example see: (Beisson et al. 1965)). This question supported by many pieces of experimental evidence was answered mainly by proving the role of mitochondrial and other organelle (e.g. chloroplast) dependent, but still DNA based inheritance. The findings that proteins and in particular histones might be carriers of non-DNA coded, but inherited information initiated intensive studies trying to elucidate these mechanisms.

By now it seems to be widely accepted that the structure of the chromatin plays a fundamental role in regulating gene expression by controlling the access of transcription factors to the regulatory regions of genes. Two classes of enzymes are known to play a role in regulating chromatin structure, the ATP-dependent chromatin remodeling enzymes and the chromatin modifying enzymes. These latter ones are responsible for the post-translational modification of histone tails. Biological systems efficiently use posttranslational modifications of proteins in order to change rapidly and locally the activity of proteins involved in signaling (Pawson et al. 2000). These mechanisms are able to increase the number of effector molecules by as much as several orders of magnitude (Jenuwein 2001). Deciphering signaling networks have to take into consideration the wide variety of post-translational modifications, including palmitoylation, ubiquitination, sumoylation, acetylation, phosphorylation, and

methylation (Kabuyama et al. 2004). The question under debate nowadays is whether the widely accepted structural role of the chromatin is the only way by which chromatin participates in the control of gene expression or if the posttranslational variations on the histone tails code for a specific local information that might even set a “language”, the language of histone code modifications (Strahl et al. 2000).

According to the “histone code” hypothesis the covalent modifications of the histone tails maintain and modulate the patterns of gene expression by providing local instructions to the effector molecules about the information embedded in the particular genomic territory (Turner 2000; Imhof et al. 2001; Jenuwein et al. 2001). Reading of the code is performed by specialized proteins. Modified histone tails have been reported to form binding sites of specific classes of proteins; bromodomain–containing proteins as binding sites of acetylated lysine groups and chromodomain–containing proteins of methylated lysine residues (Marmorstein 2001) (Kanno et al. 2004). It is thought that these histone-binding proteins provide the functional link between the covalently modified histone tails and the effectors of transcription initiation.

It became widely accepted that DNA methylation on CpG islands and deacetylation of histone lysine side chains are linked to a silenced state of chromatin (Jones et al. 1998). Methylated cytidines create a binding site of methyl binding proteins (MBP). One of the best studied member of the group is MECP2. Localization of MECP2 was clearly linked to methylated DNA in the genome (Nan et al. 1996). MECP2 binds methylated DNA as shown by structural data (Wakefield et al. 1999) and mediates the anchoring of repressors such as HDAC-s (Jones et al. 1998). Interestingly, not only HDAC-s were linked to MECP2 but also TSA (Trichostatin A is an HDAC inhibitor) insensitive repression. MECP2 was found to have H3K4 methyltransferase activity (Fuks et al. 2003). By this, methylated DNA stretches are indeed instructing chromatin modifying enzymes to perform specific and local histone tail modifications.

The best studied modification of the histone tails is acetylation. Acetylation of histones H3 and H4 have been linked very early to the activation of gene expression (Pogo et al. 1966) (Libby 1968; Pogo et al. 1968). The positional role of the histone tail acetylation was later demonstrated in Drosophila by showing that H4Ac12 is localized in centromeric regions, H4Ac5 and H4Ac8 are distributed through multiple sites in the

genome and a single modification of the histone tail, namely H4Ac16 is specific to the hyperactivated male X chromosome (Turner et al. 1992; Bone et al. 1994; Smith et al. 2001). The effectors of these modifications are the histone acetyltransferases or HATs. In the case of Drosophila H4Ac16 modification, the MSL complex seem to contain the effectors (MYST family member HATs) and the entry point of the signal induction also. The entry point in this case is represented by non coding RNA molecules (roX1 and roX2). In mammalian cells, as reported recently (Agalioti et al. 2002) H4Ac8 is required for binding of SWI/SNF chromatin remodeling complex while H3Ac9 and H3Ac14 is critical for the recruitment of TFIID. The binding factors of the acetylated histone tails in mammalian cells were shown to be the bromodomain containing proteins (Kanno et al. 2004). The beauty of this finding is that bromodomains can be found in a variety of factors involved in transcription *per se*, like HAT proteins (PCAF), general transcription factors ($TAF_{II}250$) and chromatin remodeling enzymes (BRG1, member of the SWI/SNF complex). This finding might explain how the information coded in the sequence of particular regulatory regions, like the enhancer regions, is transferred to the histone tails and an ordered, sequential recruitment of other transcription regulators is initiated (Agalioti et al. 2002). These data and data generated in other systems were summarized as the acetylation code of the histone tails (Turner 2000; Agalioti et al. 2002).

Protein methylations were described early in the ‘70s, and the characterization of methylating enzymes in the ‘80s fuelled new studies of the processes mediated by methylation (Gallwitz 1971; Disa et al. 1986). Recently, a plethora of methylation substrates were identified (Boisvert et al. 2003) (Lee et al. 2002) (Wada et al. 2002) and the enzymes involved in demethylation were also described (Cuthbert et al. 2004; Shi et al. 2004; Wang et al. 2004).

The role of histone lysine methylations was extensively studied and reviewed (Kouzarides 2002; Lachner et al. 2002) (Jenuwein 2001). Some of these results suggest that methylations on lysines of the H3 tail have a positional value. Majority of the enzymes responsible for this modification contain a SET domain. There are more than 50 SET domain containing proteins in the mouse genome and they could be all considered as being putative histone lysine methyltransferases (Tachibana et al. 2005). If we take a closer look to H3K9 methylations we can see that at least five SET domain containing

methyltransferase proteins were shown to be responsible for this modification (Tachibana et al. 2005). These enzymes seem to have different biological roles. For example ESET is essential for preimplantation (Dodge et al. 2004), G9a for mid-gestation (Tachibana et al. 2002) while Suv39h2 for the developmental stage after day E12.5 (Peters et al. 2001) of mouse embryonic development. Mice lacking SUV39h show genomic instability and also increased tumor risk (Peters et al. 2001). The chromosomal territories targeted by these enzymes are also distinct. While H3K9 trimethylation of the pericentric heterochromatic territories is performed by Suv39h the mono- and di- methylations in the euchromatic regions is performed by G9a (Peters et al. 2001) (Rice et al. 2003). If the role in cell cycling of these modifications is inquired we can find that monomethylation of H3K9 can be found mainly in early replicating euchromatin, while di-and trimethylation in the same position might be characteristic to different types of heterochromatin (Wu et al. 2005). These modifications could be paraphrased as forming a code of silence (Rice et al. 2001).

The reading of methyl lysines in this code is performed by chromodomain containing proteins (Marmorstein 2001). The best studied chromodomain containing protein is HP1 (Heterochromatic protein 1). Methylation on H3K9 provides binding site for HP1 as shown by structural data (Nielsen et al. 2002). HP1 binding is the initial step in the silencing of large chromosomal territories through heterochromatinization of them (Bannister et al. 2001; Lachner et al. 2001; Nielsen et al. 2002).

Non SET domain containing methyltransferases might have roles also in the histone modification maze. Dot1L a non SET domain containing methyltransferase (Lacoste et al. 2002) that is methylating a non histone tail locus of the histone octamere (Ng et al. 2002; van Leeuwen et al. 2002). This lysine group is located on the outer surface, non DNA covered part of the spindle.

Removal of the H3K9 methylation mark was recently reported as being carried out by the same enzyme that was reported as being responsible for the removal of H3K4 methylation mark through an oxidation step performed by an amine oxidase enzyme LSD1 (Metzger et al. 2005) (Shi et al. 2004).

While methylation on H3K4 was in general linked with transcriptional activation, distinct roles were attributed to mono- di- and tri-methylation of this lysine residue (Santos-Rosa et al. 2002). In yeast, trimethylation can be unambiguously correlated with

active sites of transcription while dimethylation was also found on the chromatin of repressed genes (Santos-Rosa et al. 2002). In higher metazoans dimethylation stands for a 'poised' chromatin state and both di- and tri-methylation of H3K4 seem to be linked to active transcription (Schneider et al. 2004). The enzyme responsible for this modification is a SET domain containing protein, namely SET7 (Wang et al. 2001). Interestingly a cis correlation on H3 tail shows that methylation on H3K4 and H3K9 are mutually exclusive (Wang et al. 2001).

The other residues of the histone tails that can be methylated are the arginines. Three main forms of methylarginine have been identified in eukaryotes: N^G-monomethylarginine (MMA), N^GN^G (asymmetric) dimethylarginine (aDMA), and $N^GN'^G$ (symmetric) dimethylarginine (sDMA), all of which involve modification of guanidino nitrogen atoms (McBride et al. 2001).

The level of methylation on arginine residues depends on the level of methyl donor S-adenosyl-methionine (Adomet), the level of methyltransferases (PRMT-s) and the level of demethylases present in the cell at a specific point in time Methionine adenosyltransferase (EC 2.5.1.6) is a key enzyme of cellular metabolism and catalyzes the formation of S-adenosyl-methionine (Adomet) from l-methionine and ATP. Adomet is the main methyl donor of the cell, a precursor of polyamine synthesis of molecules such as spermine and spermidine (Moreira et al. 2004). An arginine group may be methylated to produce methyl-arginine, while the amino acid L-arginine may be oxidized by NOS to produce citrulline and NO, and may be hydrolyzed by arginase to produce ornithine and urea. Importantly, methyl-arginine groups may be de-iminated to form citrullinated proteins. Identification of protein substrates that may be methylated on arginine residues was carried out in several studies. Protein arrays, differential cloning and proteomic approaches were used to identify these substrates (Lee et al. 2002; Wada et al. 2002; Boisvert et al. 2003).

The enzymes involved in arginine methylation, members of the PRMT (protein arginine methyltransferase) protein family use as substrates arginine-glycine rich protein stretches (Wada et al. 2002) (Lee et al. 2002) and S-adenosine-methionine in order to catalyze the methylation reaction. Protein arginine methyltransferases are conserved

proteins from yeast to humans (Gary et al. 1996; McBride et al. 2001). They contain an S-adenosyl methionine (AdoMet) binding motif and a less conserved C-terminal domain.

PRMT1 is the main enzyme in the mammalian cell responsible for methylation of arginine residues (Tang et al. 2000). If one takes a closer look at the main arginine methyltransferase of the cell, PRMT1 could be considered as an apparently promiscuous protein. Methylation of STAT1 and NFAT, cofactors of nuclear receptors, DNA damage checkpoint control (Boisvert et al. 2005) and regulation of splicing was all described to involve PRMT1. One of the known methylation reactions mediated by this enzyme is the methylation on the tail of histone H4 arginine residue in position 3. Other members of the PRMT family involved in nuclear receptor signaling are PRMT2 and PRMT4 or CARM1. PRMT2 was shown to be a cofactor of estrogen receptor but until now no enzymatic activity of this protein was reported (Qi et al. 2002). On the other hand CARM1 was reported as being responsible for linking the group of p160 coactivators with arginine methyltransferase enzymatic activity (Chen et al. 1999). Several lines of evidence clarified that this enzyme is mainly responsible for the metylation of H3 arginine 17 (Ma et al. 2001; Schurter et al. 2001; Bauer et al. 2002). H4R3 methylation is specific to PRMT1 while CARM1 for the arginine methylation in position 17 of the H3 histone tail.

H4 Arginine 3 methylation is one of the least characterized histone tail modifications. Arginine methylation on both H4 and H3 tails has been shown to be related to nuclear receptor coactivation in several experimental systems. The family of p160 transcriptional coactivators (e.g. SRC1, GRIP1, ACTR) binds two members of the arginine methyltransferase family, PRMT1 and CARM1. Both these transferases have been implicated in the activation of NR dependent genes (Chen et al. 1999) (Strahl et al. 2001). The arginine methyltransferases modify histone tails and arginine side chains on other proteins as well (e.g. CBP, STAT) (Mowen et al. 2001; Xu et al. 2001; Chevillard-Briet et al. 2002). The PRMT1 enzyme has been shown in cotransfection studies to be a cofactor of nuclear receptor activated gene expression (Koh et al. 2001). In vitro studies have demonstrated that PRMT1 methylates H4 Arginine 3 and that once methylated, H4 is a better substrate for HAT-s. Vice versa, once acetylated, the histone tails lose their ability to become methylated by PRMT1 (Wang et al. 2001). The other factor implicated

in the regulation of arginine methylation is the enzyme called peptidyl arginine deiminase or PAD4. In HL-60 cells PAD4 was shown to be regulated by DMSO, vitamin D and retinoic acid (Nakashima et al. 1999). All of these agents have the potential of priming HL-60 cell differentiation (Yen et al. 1987; Yen et al. 1987). Recently this gene was found to be responsible for the removal of the methyl mark on H4R3 by conversion of it to a citrullinated histone H4 (Wang et al. 2004).

During murine embryonic development the expression of the PRMT1-reporter fusion gene was greatest along the midline of the neural plate and in the forming head fold from embryonic day 7.5 (E7.5) to E8.5 and in the developing central nervous system from E8.5 to E13.5. PRMT1-/- mice die between the embryonic day E4.5 and E6.5 between implantation and gastrulation, suggesting that the modification is crucial for organ development and the specific cell differentiantion pathways (Pawlak et al. 2000). Interestingly, PRMT1-/- ES cells are viable and are dividing, suggesting that this enzyme is not indispensable for life per se (Pawlak et al. 2000).

One of the most powerfull technique that was used to generate key findings of the field of epigenetics is chromatin immunoprecipitation (ChIP). Chromatin immunoprecipitation (ChIP) enables us to study in vivo DNA-protein interactions at the chromatin level, and DNA fragment libraries containing the DNA elements bound by a particular protein can be generated and studied with this method by using specific antibodies (Orlando 2000).

The epigenetic changes associated with both the priming and transcriptional activation occurring during retinoid-induced differentiation are clearly linked to the activity of retinoid receptors. In the absence of a ligand, RAR:RXR heterodimers, the mediators of the effects of retinoids on myeloid cell differentiation, are believed to bind to their cognate response elements and repress transcription. Liganding of these receptors results both in the loss of this repressive effect and the induction of transcriptional activity. While little detail is known of the molecular steps involved in the activation of transcription by retinoid receptors, significantly more is known about the activity of other members of the nuclear receptor superfamily. A general model of transcriptional activation, developed primarily from studies on estrogen and glucocorticoid receptor regulated genes (Becker et al. 2002; Metivier et al. 2003) suggests that liganding of the

receptors results in a sequential recruitment of proteins involved in transcriptional activation. According to the current concept the sequential recruitment of cofactors may be different from gene to gene (reviewed by M. P. Cosma (Cosma 2002)), but in all cases results in an orderly process of covalent modifications of the tails of histone proteins associated with the promoter and enhancer elements of the target gene. If we compare the knowledge accumulated in the field of epigenetics with the knowledge accumulated in the field of transcription regulation we can see that the field of epigenetics deepened mainly our understanding of transcriptional silencing. On the other hand several of the well characterized histone tail modifications can be clearly linked with transcriptional activation (e.g. acetylations in general, methylations on: H3K4, H3R17, H4R3). While H3K4 was linked to be a marker of active chromatin regions, the present knowledge about arginine methylations is mainly related with their role in transcriptional activation itself. The role of H4R3 methylation in defining the state of a chromatin region was not clearly defined yet. According to the histone code hypothesis histone tail modifications might be able to silence, sensitize or activate the chromatin in a specific region. Further studies need to be carried out in order to understand the dynamic changes taking place on the chromatin and especially how the sensitization of chromatin towards different specific signals is performed. One of the substrates for these modifications is in the position H4R3.

2.4. Genome-wide location analyses

In the second part of my project I have extended my experimental approach from studying a single promoter by QPCR to studying gene promoters genome-wide, using a high-throughput binding site survey together with DNA cloning and sequencing. This method was succesfully used before to map transcription factor binding sites in the genome (Weinmann et al. 2001). With this method we mapped genomic loci marked by H4R3 methylation during myeloid differentiation.

Chromatin immunoprecipitation studies previously established that PRMT1 is one of the first proteins involved at the chromatin level in the events, that in a concerted manner lead towards transcription (Metivier et al. 2003). To further characterize how

PRMT1 modulates gene expression at the chromatin level, we decided to isolate chromatin fragments that are methylated on histone arginine H4R3. For this we used a polyclonal antibody that recognizes specifically methylated H4R3 residues (Wang et al. 2004). The immunoprecipitated fragments were cloned and sequenced. We have shown that the immunoprecipitated fragments are more abundantly located in introns and a great majority of them contain conserved transcription factor binding sites. The locations identified were enriched in conserved transcription factor binding sites of POU2F1, MEF-2 and FOXL1 factors. A significant number of the genes in the proximity of the identified genomic loci are involved in signaling pathways and developmental processes, including immune response of myeloid cells.

In order to broaden the study of epigenetic changes to a high throughput platform, we decided to implement chromatin immunoprecipitation methods combined with microarray analysis (ChIP on Chip). We decided to study genomic binding sites of PPARs.

PPARs, as reported even in the first paper by Issemann and Green (Issemann et al. 1990), have lipid-lowering effect and produce massive peroxisome proliferation in rodents (hence their names: Peroxisome Proliferator Activated Receptors, PPAR). There are at least two major human diseases they were shown to be involved in, atherosclerosis and non-insulin dependent diabetes. Interestingly, but not surprisingly, two classes of compounds fibrates and thiazolidinediones (TZDs) were independently identified and tested for their possible beneficial effect in metabolic diseases without prior knowledge about their pharmacophores (Chang et al. 1983; Chang et al. 1983; Watts et al. 1999).

PPARs have been identified as ligand activated transcription factors belonging to the nuclear hormone receptor superfamily (Kliewer et al. 1999). There are three isoforms of PPARs: PPARα, PPARγ and PPARδ, called also β. The difference in the nomenclature of β and δ comes from their cloning. PPARβ was cloned from Xenopus by the Wahli group, while PPARδ was cloned from mouse by the Evans group. This latter was shown to be highly similar to the human receptor and became widely used in receptor studies with the name PPARδ.

There have been significant advance in our ability to identify systematically the genes occupied by various transcription factors. One of the first analyses carried out by

Peggy Farnham and colleagues identified binding sites for E2F using chromatin immunoprecipitation and sequencing (Weinmann et al. 2001). Other more recent significant studies include the genome wide localization studies for HNF binding sites (Odom et al. 2004) and for CREB binding sites (Zhang et al. 2005) used the combination of chromatin immunoprecipitation coupled to promoter microarray analysis. As an alternative to genomic arrays, Chip to SAGE method can be used. The benefit of this approach is that it is unbiased, but the analysis rather labor intensive. This method was used successfully to identify CREB binding sites in the genome (Impey et al. 2004). The results of all these studies show that genome-wide localization studies are essential for the understanding of global transcription changes that take place upon activation of particular transcription factors.

Using genomic location analysis approach for PPARs, we planned to integrate the large amount of global gene expression data with molecular determinants of chromatin state. The microarrays we used are from UHN (Toronto, CA), and contain 12 000 human CpG rich regions. By now our results show that ChIP on Chip is suitable for mapping regulatory sequences of PPARγ target genes. For this analysis we used two independent methods. First, we located PPARγ binding sites by using PPARγ specific antibodies. We found occupancy of approximately 1% of the spots represented on the CpG array and identified novel genes with lower level of induction by PPARγ specific ligands as potential target genes.

In an independent set of experiments we analyzed the changes in H4 acetylation of the chromatin regions represented on the CpG microarray after treatment with PPAR specific ligands. By this approach the hit rate for spots that showed an increase in H4 acetylation after PPARγ ligand treatment was 0.6%.

In order to correlate ChIP on Chip results with global gene expression data generated on the Affymerix platform, we developed a web-based bioinformatic interface in collaboration with the Hungarian Bioinformatics Institute.

2.5. Aims of the studies

1. To set up a system where one can analyse the regulated hormonal (retionoid) responsiveness.
2. To implement in our laboratory new techniques used in the field of epigenetic studies.
3. To map the epigenetic changes taking place on the promoter of TGM2 during different states of hormonal activation
4. To implement chip to clone technology, high throughput robotic PCR and Chip on chip analyses in order to move our studies to high throughput platforms.

3. MATERIALS AND METHODS

Reagents

All materials unless otherwise mentioned were purchased from Sigma Aldrich.

Cells, materials

HL-60/CDM-1 cells, a kind gift of Diane Lucas (Walter Reed Army Medical Center, Washington, D.C.), were cultured in suspension in RPMI 1640 medium supplemented with ITS (Sigma #I1884) using standard cell culture conditions. Monomac6 cells were cultured in suspension in RPMI 1640 medium supplemented with 10% FBS using

standard cell culture conditions. HT29 cells were received from Beatrice Desvergne (University of Lausanne) and were cultured in monolayer in DMEM medium supplemented 10% FBS using standard cell culture conditions similarly with 293T cells. Highly enriched monocytes (98% CD14+) were obtained from buffy coats of healthy donors by Ficoll gradient centrifugation and immunomagnetic cell sorting using anti-CD14-conjugated microbeads (VarioMACS; Miltenyi Biotec). Monocytes were cultured in RPMI 1640 supplemented with 10% FBS (Invitrogen), containing 800 U/ml GM-CSF (Leucomax) and 500 U/ml IL-4 (Peprotech).

HL60/CDM1 cells were treated with 9-cis retinoic acid in a concentration of 1 M dissolved in ethanol: DMSO (ratio??). Priming of cells was done with 1.25% DMSO or 10 nM Vitamin D for 16 hours. Blocking of methyltransferases was achieved by treatment with 10 M of adenosine dialdehyde (ADOX /Sigma #A7154) for the same period. After pretreatment media was replaced with fresh media and retinoic treatment was carried out. MonoMac6, HT29, 239T cells were treated with Rosiglitazone in a concentration of 1 M dissolved in ethanol: DMSO. If not specified, all materials were purchased from Sigma. Antibodies for flow cytometric analysis, as well as the appropriate control antibodies, were purchased from DAKO A/S, unless otherwise mentioned.

Plasmids

PcDNA3.1 hPRMT1 full-length wild type was cloned from the pGEX-HRMT1L2 (v2) (Scott et al. 1998) by PCR, introducing a BamHI site at the 5' end and a EcoRI site at the 3' end of the HMRT1L2 cDNA (deleting the stop codon at the same time). Subsequently, the HMRT1L2 cDNA was subcloned into the BamHI and EcoRI-double digested pcDNA3.1-B (Invitrogen), generating a C-terminal myc/his-tag. The point mutations S69A, G70A and T71A were introduced into pcDNA3.1 hPRMT1 via site-directed mutagenesis using the Quickchange kit (Stratagene), resulting in pcDNA3.1 PRMT1 full-length catalytic mutants. All constructs were verified by DNA sequencing. The constructs presented above were received from Uta Maria Bauer (University of Marburg). Mammalian expression vectors for PAD4 and the PAD4 C645S mutant were received from Yanming Wang and described previously (Wang et al. 2004). All other plasmids

used were described previously (Benko et al. 2003).

Transfection

HL-60 cells were transfected with AMAXA Electroporator System using 1 g of plasmid for 2 million cells according to the manufacturer's instructions (electroporation solution V and program V01).

293T cells were transfected with Polyethylene imine reagent. The method follows the steps of the jetPei (Qbiogene) transfection with modifications as done on the Gene Vectors EuroLab Course (Genethon, Evry) under the guidance of Anne Marie Douar. Briefly: Polyethileneimine (PEI) (Aldrich, cat. No.408727) working solution was prepared by dissolving 4,5 mg of pure PEI in 8 ml of deionized water. Solution was neutralized with HCl to pH 6,5-7,5 and the final volume adjusted to 10 ml. This solution was filtered (0,2µm pore), and was considered to be 10 mM of nitrogens. Before transfection, 239T cells were 40% confluent. Reagents were mixed as shown in the table below:

well format	DNA g	NaCl (150mM) to µl	PEI 10 mM µl	NaCl (150 mM)to µl	TOTAL VOLUME (µl)
96	0.25	10	0.5	10	20
48	0.5	25	1	25	50
24	1	50	2	50	100
12	2	50	4	50	100
6	3	100	6	100	200
60mm dish	5	250	10	250	500

The PEI solution was added dropwise to the DNA solution. We waited for 1 minute between adding each fraction of PEI solution to the DNA solution (one fraction of PEI solution was considered to be 1/5 of the total PEI solution used for the particular experiment). The solution was incubated for 15-30 minutes at room temperature. Meanwhile changed the media of the 293T cells to a 1% FBS media. Transfection complex was added dropwise to the cells and mixed with the media with gentle swirling.

After 5-7 hours of incubation in a 37 ºC, humidified CO_2 incubator, equal volume of 10% FBS media was added to the plates, and cells were analyzed after a further 16 hours of incubation.

βRARE tk Luc reporter plasmid was cotransfected with pCMV RARα full length, pCMV RXRα full length and βGal plasmid. PRMT1 wt, PRMT1 mut, PAD4 wt, PAD4 mut were added to the reporter plasmids.

Extraction of total RNA

Total RNA was extracted with Trizol Reagent (Invitrogen) according to the manufacturer‘s instructions.

Real Time QPCR

Total RNA was isolated with TRIZOL reagent (Invitrogen) and RNA was treated with Rnase-free DNase (Promega) before reverse transcription. Quantitative PCR analysis was performed using real-time PCR (ABI PRISM 7900 sequence detector, Applied Biosystems) performing 40 cycles of 95 ^{o}C for 12 sec and 60 ^{o}C for 1 min using TaqMan assays. All PCR reactions were done in triplicate with the appropiate control reactions. The comparative Ct method was used to quantify various PCR products. For the promoter assays the reactions were carried out similarly without the reverse transcription step. For standard calibration, DNA from the BAC clone RP5–1054A22 was used which contained the whole promoter of TGM2 and was received from the Sanger Centre, Clone Resources Group, Hinxton, UK. Primer sets used for these measurements are presented in Table 1.

For the 384-well plate format reverse transcriptase reactions were performed using random primers and the following conditions

RT reaction	Volume (for total of 40µl) µl
5x SSII buffer	8
100 mM DTT	4
2.5 mM dNTP	8
3□g/µl random hexamer (Invitrogen)	0.04
SSII enzyme (200 U/µl) (Invitrogen)	0.17
Total RNA (100	20

ng/µl)	

The reaction was carried out as it follows: 10 minutes at 25°C, 2 hours at 42°C and 10 minutes at 72°C. After this step mixture was diluted with 4 volumes of nuclease free water and aliquoted on a 384-well plate using a TECAN Genesis RSP 150 microfluidic pipeting robot. On each plate a „No amplification control" (sample without reverse transcriptase) and three replicates of each sample were aliquoted, mixed with equal amount of QPCR master mix (total reaction volume was 10 µl).

The QPCR master mix had the following composition:

Components	Volume (for total of 10µl) µl
Nuclease free water	2.1
$MgCl_2$ 25mM	1.2
10x buffer	1
2.5 mM dNTP	0.5
primer- 100 µM	0.0375
primer+ 100 µM	0.0375
probe 20 µM	0.0625
Taq polymerase 5U/µl	0.0625
cDNA from RT step	10

Chromatin Immunoprecipitation

Chromatin immunoprecipitation was carried out as described by Kuo and Allis (Kuo et al. 1999) with modifications. Briefly: cells were fixed with 1% formaldehyde for 10 min at room temperature. Adding chilled glycine to a final concentration of 150 mM stopped fixation. Cells were scraped and washed twice with ice-cold PBS that contained proteinase inhibitors (1 mM PMSF, 1 µg/µl aprotinin and 1 µg/µl pepstatin A). Nuclei were prepared by incubation for 10 minutes on ice in a buffer containing 5 mM Pipes pH8, 85 mM KCl, NP40 0.5% and proteinase inhibitors. After centrifugation with 3000g for 10 minutes at 4°C, nuclei were resuspended in sonication buffer (1% SDS, 0.1 M $NaHCO_3$ and proteinase inhibitors), lysed on ice for 10 minutes and sonicated on ice to an average fragment size of 300 basepairs. Cell debris was pelleted twice by centrifugation with 10000g for 30 min at 4°C in a bench-top centrifuge. Soluble chromatin was aliquoted, frozen in liquid nitrogen and stored at –70°C. For immunoprecipitation, chromatin was diluted 10-fold in an IP buffer (0.01%S DS, 1.1%

Triton X-100, 1.2 mM EDTA, 16.7 mM Tris pH8.1, 16.7 mM NaCl and proteinase inhibitors). 1 ml of diluted chromatin was precleared twice with 40 µl blocked protein A-sepharose beads. Immunoprecipitation was carried out with specific antibodies recognizing modified histones (purchased from Upstate Biotech and Abcam): Upstate: #06–866 Anti Acetyl H4 2 µl/IP, #07–213 Anti dimethyl H4 Arg3 6µl/IP, #07–030 Anti dimethyl H3 Lys 4 5µl/IP, #07 212 Anti dimethyl H3 Lys9 5µl/IP, and from Abcam: # ab5823 H4 methyl R3 antibody 5µl/IP, #413–200 Pan dimethyl arginine 5µl/IP. Diluted and precleared chromatin was incubated with the antibodies overnight, on a rotating plate at 4°C. Complexes were collected with 40 µl blocked protein A Agarose (Upstate #16–157). An aliquot of the no-antibody control supernatant was used to measure and calculate the input DNA. Beads were pelleted, washed twice with each of the following buffers: buffer A (low salt= 0.1% SDS, 1% Triton X-100, 2 mM EDTA, 20 mM Tris pH8.1, 150 mM NaCl), buffer B (high salt= 0.1% SDS, 1% Triton X-100, 2 mM EDTA, 20 mM Tris pH8.1, 500 mM NaCl), buffer C (0.25 M LiCl, 1% NP40, 1% sodium deoxycholate, 1mM EDTA, 10 mM Tris pH8.1) and TE buffer (10 mM Tris, 10 mM EDTA, pH8). Immunoprecipitated nucleosomes were eluted twice from the beads with elution buffer (1% SDS, 0.1 M $NaHCO_3$) and eluates were combined. Crosslinks were reversed by incubating for 6 hours at 65°C after adding 20 µl 5 M NaCl. Eluate was combined with 10 µl of 0.5 M EDTA, 20 µl 1 M Tris pH 6.5 and 2 µg Proteinase K, and incubated for 1 hour at 45°C. DNA was recovered after phenol: chloroform extraction and ethanol precipitation using 20 µg of glycogen as a carrier. DNA was resuspended in 50 µl of 50 ng/µl yeast tRNA (Invitrogen). 2 µl of this solution was used for real time QPCR in a 25 µl reaction volume. All measurements were done in triplicates. All chromatin results were verified from independent chromatin preparations.

Native ChIP

For native ChIP we performed ChIP as described above with modifications. Cells were not fixed with formaldehyde and glycine was not added to the media, but cells were washed twice with cold PBS and lysed in sonication buffer. If nuclei were isolated prior to lysis, the cells were resuspended in a buffer containing 5 mM Pipes pH8, 85 mM KCl, NP40 0.5%, 100 mM beta-mercaptoetanol, 1 mM dithiothreitol and proteinase inhibitors.

From this step on ChIP was performed as described above. All steps were performed in cold room, and all buffers contained proteinase inhibitors.

ChIP-Western

For ChIP -Western analysis we performed chromatin immunoprecipitation as described above, with the difference that all washing steps were performed with solutions using proteinase inhibitors. After washing the beads, they were resuspended in Protein loading buffer (Fermentas) and boiled for 30 minutes. The material was analyzed with standard Western Blot technique on a 12% polyacrylamide gel with SDS-PAGE. To assess the presence of PPARγ we used different antibodies that the one used for ChIP. As a positive control, we used PPARγ immunoprecipitated with an affinity purified antibody received from Peter Tontonoz (UCLA, LA).

Ligation and Plasmid Preparation

Protruding ends of the isolated DNA fragments were filled by Klenow treatment as follows. The DNA fragments from 10 independent chromatin immunoprecipitations were mixed, divided in 10 aliquots, supplemented with 0.5 µl of 2.5 mM dNTP, 3U Klenow (Fermentas) enzyme, 3.5 µl 10X Klenow buffer in a total of 35 µl reaction volume. Reaction was carried out at room temperature for 10 minutes and stopped by incubation for 10 minutes at 75 C°.

Ligation was performed with 15U (0.5 µl) T4 DNA Ligase (Fermentas) with addition of PEG at 16 C° overnight with a vector: insert ratio of 10:1, according to the manufacturers recommendations. We used Zero Blunt® PCR cloning vector (Invitrogen). The ligation product was transformed in competent E. coli (DH5α), shaked in SOC medium at 37 °C for 2 hours and plated in kanamycin containing plates according to the manufacturers recommendations. On the second day colonies were isolated, plated on 96 well plates in liquid medium and let grow for 24 hours at 37°C. Medium was supplemented with 30% of glycerol and frozen at -70 °C. At the analysis of colonies an aliquot of the frozen medium was plated on kanamycin containing plates and individual colonies were grown up. Plasmids were isolated with Miniprep Wizard (Promega) according to the manufacturers recommendations. The size of the insert was verified with

XbaI and BamHI double digestion and PCR with M13 primers. Results were visualized by standard agarose gel electrophoresis in a 2% agarose containing gel.

Sequencing

Sequencing of the insert was performed with standard M13+ sequencing primer according to the manufacturers recommendations of the ABI Big Dye Terminator 2.1 kit.

In Silico Analysis

In silico analysis of the sequences was performed as it follows:

The sequences of plasmid origin were removed from the ends of the raw sequence and the resulting sequence was first analyzed with NCBI Blast (Altschul et al. 1990). Sequences that passed the quality control described in the Results section were further analyzed. In the second step the genomic location of the sequences was analyzed with BLAT program (Kent 2002) on the UCSC Human Genome Browser (Karolchik et al. 2003). Conserved regions, known genes, conserved transcription factor binding sites and the position of the analyzed sequence towards these genomic elements was monitored. For annotation we used PANTHER Analysis. The PANTHER (Protein ANalysis THrough Evolutionary Relationships) (Mi et al. 2005) (Thomas et al. 2003) database allows complex annotation of proteins and genes. We selected the data described as “Molecular functions” and “Biological processes” of the Version 5.0 (release date Jan. 1, 2005).

Cell cycle analysis

Cell cycle analysis was performed as described in Current Protocols in Cell Biology (1999) edited by Juan S. Bonifacio (et al.) Chapter 8.4.1. Briefly: cells were washed in PBS and fixed in 70% ethanol overnight. Fixed cells were then washed twice and resuspended in PI (propidium iodide) working solution (50 µg of propidium iodide, 20 µg/ml RN-ase, and 0.5% Tween 20 in PBS). After a 15-min incubation at 37°C, cells were analyzed on a Coulter flow cytometer and data were analyzed with WinMDI software.

Microarray analysis

For the Affymetrix global gene expression analysis, total RNA was isolated using the RNeasy kit (Qiagen). cRNA was generated from total RNA by using the SuperScript kit (Invitrogen) and the High Yield RNA transcription labeling kit (Enzo Diagnostics). Fragmented cRNA was hybridized to Affymetrix (Santa Clara, CA) arrays (HG_U133_plus2.0 chips) according to Affymetrix standard protocols. The Microarray Core Facility at EMBL, Heidelberg, performed preliminary data analysis.

For genomic location analysis studies primer elongation reaction was performed with the chromatin immunoprecipitation product using Sequenase enzyme, and subsequently PCR amplification was carried out (DeRisi Lab Protocol, UC San Francisco).

The goal of this procedure is to randomly amplify any given sample of DNA which as much representation as possible. It is not a "linear" method, but is useful to compare relative enrichment between two samples. This protocol has been used successfully to amplify genomic representations of less than 1 ng of DNA. The protocol consists of three sets of enzymatic reactions. In Round A, Sequenase is used to extend randomly annealed primers (Primer A) to generate templates for subsequent PCR. During Round B, the specific primer B is used to amplify the templates previously generated. Finally, Round C consists of additional PCR cycles to incorporate either amino allyl dUTP or Cy-dye-coupled nucleotide.

Materials:

Round A

Sequenase (13 units/µl) US Biochemical cat# 70775
5X Sequenase Buffer
Sequenase Dilution Buffer
3 mM dNTP mix
500ug/ml BSA
0.1 M DTT
40 pmol/µl Primer A: GTT TCC CAG TCA CGA TCN NNN NNN NN

Round B

10X PCR Buffer
25 mM MgCl2
100X dNTPs (20 mM each nucleotide)
5 U/µl Taq polymerase
100 pmol/µl Primer B: GTT TCC CAG TCA CGA TC

Round C

Same as Round B except that modified dNTP mix was used. 100X modified dNTP mix contained 25 mM dATP, 25 mM dCTP, 25 mM dGT,P 10 mM dTTP, 15 mM aminoallyl-dUTP or Cy-dUTP.

1. Round A Reactions

Denature template DNA/primer annealing

7 µL DNA
2 µL 5X Sequenase Buffer
1 µL Primer A (40 pmol/µl)

Total Volume = 10 µl
Heat 2 min at 94°C
Rapid cool to 10°C and hold 5 min at 10°C

Add Reaction Mixture to sample:

1 µL 5X Sequenase Buffer
1.5 µL 3 mM dNTP
0.75 µL 0.1 M DTT
1.5 µL 500 µg/µl BSA
0.3 µL Sequenase (13U/µl)
Total Volume = 5.05 µl

Ramp from 10°C to 37°C over 8 min. Hold at 37°C for 8 min; rapid ramp to 94°C and hold for 2 min.

Rapid ramp to 10°C and hold for 5 min at 10°C while adding 1.2 µl of diluted Sequenase (1:4 dilution)
Ramp from 10°C to 37°C over 8 min. Hold at 37°C for 8 min.

Dilute samples with water to final Volume = 60 µl.

2. Round B PCR

Round A Template 15µl
$MgCl_2$ 8µl
10X PCR Buffer 10µl
100 X dNTP 1µl
Primer B (100pmol/µl) 1µl
Taq 1µl
Water 63 µl

Round B Cycles: 30 sec 94°C 30 sec 40°C 30 sec 50°C 2 min 72°C	Run 15-35 cycles, depending on the amount of starting material. Run 5 µL on 1% agarose gel. A "smear" of DNA should be present between 500 bp –1 kb.

3. Round C

Use 10-15 µl of Round B to seed the Round C reaction: Round B Template 10-15µl MgCl2 8µl 10X PCR Buffer 10µl 100X aa-dNTP/cy-dNTP 1µl Primer B (100pmol/µl) 1µl Taq 1µl Water 63-68µl	30 sec 94°C 30 sec 40°C 30 sec 50°C 2 min 72°C (even longer extension times may improve yield if directly coupling Cy dyes) 25 cycles If aa-dNTPs were used in Round C, the sample must be desalted (to remove Tris buffer which interferes with the coupling) prior to dye coupling.

Labeling of the amplified fragment was performed with the protocol suggested by the developer of the CpG array (UHN, Toronto, Canada). Analysis was performed using GeneSpring 7.0 (Agilent).

Quantification of DNaseI sensitivity

Quantification of DNaseI sensitivity was performed with QPCR analysis as described previously (McArthur et al. 2001) with modifications. Briefly, cells were washed with ice cold PBS resuspended in lysis buffer (50 mM Tris-Cl pH7.9, 100 mM KCl, 5 mM $MgCl_2$, 0.05% saponin, 50% glycerol, 200 mM beta-mercaptoetanol) and incubated on ice for 10 minutes. Nuclei were recovered by centrifugation at 1300 g for 15 minutes at 4°C and resuspended in buffer A (50 mM Tris-Cl pH 7.9, 100 mM NaCl, 3 mM $MgCl_2$ 1 mM dithiothreitol and proteinase inhibitors). After centrifugation at 1300 g for 15 minutes at 4°C nuclei were resuspended in buffer A and divided into several aliquots. After this step, nuclei were treated with different concentrations of DNaseI for 20 minutes at 37°C. Reaction was stopped with 1/10 volume of 0.5M EDTA. After RNase and Proteinase K digestion, DNA was extracted with phenol/chloroform and precipitated

with absolute ethanol. Extracted DNA was treated with EcoRI, purified with PCR purification columns (Qiagen) and measured with QPCR for the specific promoter regions. Values were normalized to total DNA concentration in each sample as measured with spectrophotometer (A260 nm and A280 nm).

4. RESULTS

4.1. Retinoid regulation of tissue transglutaminase gene expression in naïve and primed myeloid leukemia cells

The expression of tissue transglutaminase type 2 (TGM2) is very tightly regulated in myeloid leukemia cells. In HL-60 cells, in the absence of exposure to retinoids, level of TGM2 mRNA is below the limits of detection of a sensitive real-time RT-QPCR assay (less than 10 copies per nanogram of total RNA). Exposure of cells to either natural or synthetic retinoid receptor agonists increases transglutaminase gene expression markedly (Davies et al. 1985). Priming of the cells by pretreatment with differentiating agents such

as vitamin D, or the polar–planar solvent dimethyl-sulfoxid (DMSO) increases retinoid-induced TGM2 expression. This experimental system (Figure 1A) allowed us to study the effects of priming on the expression of a specific gene, the induction of which is increased by the process of pre-commitment. We will refer to the un-primed and uncommitted cells as “naïve” and those that advanced to precommitment as “primed”.

The priming effect of both DMSO and vitamin D pretreatment was detectable on the retinoid response of TGM2, a molecular marker of myeloid cell differentiation and a direct target of retinoid receptors (Nagy et al. 1996). As seen on Figure 1E, priming with DMSO produced a marked increase in the expression of TGM2. To determine whether priming conferred some sort of transcriptional memory, we analyzed the expression of TGM2 after the priming agent was washed out, and the cells were treated with 9-cis retinoic acid one, two or three days following the wash. The priming effect of DMSO proved to be transient and declined rapidly, vanishing after two cell divisions (Figure 1E). Similarly, in the case of vitamin D priming, increase in the expression of TGM2 was detected, but with a smaller amplitude (Figure 1F). This effect decreased within two days after priming to the level of naïve cells. These experiments showed that the priming effect is transient, lasting for 24-48 hours. Since both DMSO and vitamin D produced similar effects, we decided to carry out our experiments with the more potent priming agent available, DMSO.

In order to provide a baseline for further studies, we determined the time–course of mRNA induction. Exposure of “naïve“ HL-60 cells to retinoids (9-cis retinoic acid) results in a very rapid (<2 hours) increase in transglutaminase gene expression (Figure 2A) that reached a plateau after 12 hours (data not shown). This induction is strikingly enhanced (approx. 100 fold) upon DMSO priming (Figure 2A and B). DMSO alone does not increase TGM2 expression (Figure 2A and B). It was apparent by comparing the induction in the naïve and primed cells that while the magnitude of the induction was very different (Figure 2B) the kinetics was very similar whether or not the cells had been primed (Figure 2A). Thus, priming resulted in a state characterized by greater induction of the target gene without an alteration in the time–course of the transcriptional response.

A key question is whether increased induction of transglutaminase expression in the primed cells is a result of a higher mRNA expression level in each individual cell or is due to an increase in the fraction of the cells responding to the inducer (retinoid). Since it has been already demonstrated that there is a correlation between TGM2 protein and mRNA levels in HL-60 cells (Chiocca et al. 1988; Davies et al. 1988; Davies et al. 1988; Davies et al. 1988; Chiocca et al. 1989), we addressed the issue of the induction of the enzyme by using a coupled immunohistochemical/flow cytometric analysis to evaluate the levels of TGM2 in individual cells prior to, and following retinoid treatment. Using these techniques, the basal level of TGM2 protein was undetectable in both untreated HL-60 cells and HL-60 cells treated with DMSO alone (Figure 2A). In naïve cells (as shown in Figure 2C and 2D) 9-cis retinoic acid induced detectable levels of TGM2 protein in 19.7% of the cells. The level of TGM2 protein was normally distributed in the population of cells with a mean fluorescence intensity of 305.05 A.U. When DMSO primed cells were treated with 9-cis RA, a much greater fraction of the population responded to the retinoid stimuli compared to the naïve, retinoid treated cells. Among primed cells 63.7% had detectable levels of TGM2 protein (Figure 2D) and this showed a normal distribution. The mean fluorescence intensity in primed, retinoid treated cells was not different (327.8 A.U.) from the level of fluorescence intensity in retinoid–treated naïve cells (305.0 A.U.). The mean fluorescence intensity of the entire cell population increased from 39.6 to 179.43 (A.U.) after DMSO priming and retinoid induction. The most likely explanation for these findings is that the maximal level of TGM2 expression by individual cells did not change after DMSO priming, but more cells gained competence to respond to retinoids with increased TGM2 expression. It appears that priming is likely to lower the threshold for induction of gene expression and differentiation, resulting in a larger percentage of cells able to respond. This is consistent with our previous findings shown in Figure 2A, namely that priming affects the amplitude, but not the dynamics of the response to retinoic acid.

4.2. Role of receptor levels and cell cycle distribution of cells in enhanced retinoid response

In order to investigate possible explanations for the increased frequency of response by primed cells we tested two obvious hypotheses. The first is that the effect of priming is to increase the level of expression of retinoid receptors in individual cells. To address this hypothesis we measured the levels of transcripts of RARα, β and γ, and RXRα, and γ in naïve and DMSO-primed HL-60 cells. There was no significant change in expression level of RARα, and there was only a slight increase (less than two-fold increase as measured by real-time RT-QPCR assay) in the level of RXRα mRNA, as the result of DMSO priming (Figure 3A). There was also no change in the levels of RARβ, and RXRγ mRNA (Figure 3A). The second hypothesis is that differentiation is linked to cell cycle arrest. We considered it possible that the change in the fraction of cells responding to retinoids following DMSO priming was linked to alterations in the distribution of cells in different stages of the cell cycle. It has previously been shown that priming HL-60 cells with DMSO for a period shorter than 24 hours does not significantly change its cell cycle distribution (Yen et al. 1998), but to be sure that something different was not happening in our cell population, we compared the distribution of cells in naïve and DMSO-primed populations. Our results confirmed the previously reported findings, i.e. that DMSO priming has only a minor effect on the distribution of cells: there was a slight increase in the number of cells in G1 (51% to 63%) that was compensated for slight decreases in the fraction of cells in S and M phase (from 27% to 20% and from 22% to 17%, respectively) (Figure 3 B and C).

To test whether the effect of priming on retinoid-regulated gene expression was restricted to HL-60 cells, we carried out comparable studies in a human macrophage–like cell line (monocytic leukemia cell line–FAB M5/MonoMac6 or MM6), and in the well–characterized NB4 and NB4R2 promyelocytic leukemia (FAB M3) cell lines. The two NB4 cell lines also allowed us to address the issue of retinoid receptor dependence. As shown in Figure 2E we have found that retinoid-induced expression of TGM2 was increased in DMSO primed MM6 cells compared to unprimed cells. In the NB4 cells, DMSO priming also increased retinoid-induced TGM2 expression (Figure 2F). The

NB4R2 cells have a mutation in the ligand binding domain of RARα that disrupts retinoid signaling (Duprez et al. 2000). In this cell line, TGM2 could not be induced after retinoid treatment either in naïve or in DMSO primed cells (Figure 2F). These findings demonstrated that the effects of priming on retinoid regulated gene expression are not unique to HL-60 cells but represent a generalized phenomenon at least among human myeloid leukemia cell lines.

4.3. Alterations in chromatin modifications in naïve and primed cells upon retinoid treatment

A precommitment state of HL-60 cells can be generated by short treatment (< 24 hours) with several differentiating agents (Yen et al. 1987). This transient primed state is not associated with growth arrest but is characterized by lack of lineage commitment, by altered nuclear structure and by the retention of a cellular memory that lasts for at least three rounds of cell division (Yen 1985; Yen et al. 1987). Changes in chromatin structure are major contributors to the regulation of transcriptional activity that can, through epigenetic modifications, provide transcriptional memory. We therefore investigated the question whether DMSO-priming had any demonstrable effects on either the DNA or histone components of chromatin associated with retinoid-regulated genes, such as TGM2. Previous studies from the Davies laboratory have identified a 1800 bp fragment in the 5‘-flanking DNA of the human TGM2 gene as containing the core promoter and the HR1 enhancer (Nagy et al. 1996). We therefore focused our attention on the effects of DMSO-priming on the chromatin and covalent modification of histones on this key regulatory sequence.

To find out whether priming is producing changes on the chromatin level at the regulatory regions of this gene, we performed a DNaseI hypersensitivity analysis of the promoter of TGM2. The promoter of RARβ is not inducible in this cell line by retinoid treatment, priming had no effect on RARβ expression (data not shown), and DNaseI hypersensitivity was not induced in the promoter by priming (Figure 4A). On the other hand, the core promoter of the TGM2 gene became more sensitive to DNaseI solely by

DMSO priming (Figure 4B), suggesting that priming induces changes at the chromatin level of TGM2.

4.4. Epigenetic map of the promoter of TGM2

The next step in our studies was to characterize the effects of DMSO priming on the post-translational modifications of histones associated with regions of the TGM2 gene promoter. We have used chromatin immunoprecipitation in combination with QPCR (real-time quantitative PCR with TaqMan® probes) to obtain accurate quantitation of the level of post-translational modification of specific histone tails in chromatin isolated from naïve and DMSO-primed HL-60 cells. By this method two-fold differences can be measured precisely in a range of five orders of magnitude (Figure 29 C). In our hands the method was clearly more reliable than the SYBR Green real-time QPCR method (Figure 29 A and B). We designed five promoter -specific probe sets spanning the 1800 bp fragment from the HR1 enhancer to the core promoter (see Figure 5). The AG and the TG rich tandem repeat regions embedded in the promoter were not covered in this analysis.

4.4.1. H4 and H3 Acetylation

We first examined the effect of retinoid treatment on H4 acetylation in naïve and DMSO-primed cells. In naïve cells retinoid treatment produced little change in the level of acetylation of H4 histones associated with the HR1 enhancer region of the transglutaminase promoter (Figure 4C). In primed cells, on the other hand, retinoid treatment for 2 hours resulted in increased levels of H4 acetylation at the HR1 enhancer, and a similar and significant increase in H3 acetylation at the core promoter. (data not shown). These findings demonstrate that after retinoid induction of transcription, histones associated with both the HR1 enhancer and the core promoter of TGM2 gene become highly acetylated in primed cells, but acetylated to much lesser extent in naïve cells. Due to the fact that this method is not suitable for analysis of individual cells, we can only state that after retinoid treatment of DMSO primed HL-60 cells the acetylation level of TGM2 promoter of the entire cell population is much higher than in naïve retinoid treated cells. The level of acetylation of the TGM2 promoter in naïve cells after retinoid

treatment is below the levels of detection limits of this method. Therefore, we cannot assess whether there is a small fraction of cells in which this region binds acetylated histones.

4.4.2. Histone acetylations and methylations

Based on these findings we carried out a more comprehensive analysis of the effects of DMSO-priming and retinoid-treatment of primed cells on histone modifications: acetylation of H3, H4 and methylation of H3K4, H3K9 and H4R3. (Figure 5). The upper two panels of this figure show the changes in histone acetylation that occurred in response to retinoid treatment. In the case of H4 acetylation, retinoid treatment of primed cells results in a significant and uniform increase in the level of acetylation of this histone in all five regions of the promoter. This increase in acetylation starts within 2 hours of the addition of the retinoid and reaches a plateau in 6 to 8 hours. Retinoid treatment also results in increased acetylation of H3, but, unlike H4 acetylation, this effect is not global but is restricted to histones associated with the core promoter.

The lower three panels of Figure 5 profile the effects of retinoid treatment on the pattern of histone tail methylation. In the case of H3K4, DMSO priming results in a marked decrease in the level of methylation of histones on the core promoter region as seen on the left bar graph of Figure 5 (for other regions H3K4 levels were lower by at least one order of magnitude - data not shown). DMSO priming does not have any marked effect on the K9 methylation of H3 in any region of the TGM2 promoter. Retinoid treatment does induce transient changes in the methylation of this histone in most regions of the promoter and these changes are most prominent in histones associated with the distal enhancer (HR1) region of the promoter. While DMSO priming decreases methylation of the H3 histone side chains (K4), it increases the level of methylation on the H4 histone (R3). The effect is selective, being most marked on histones associated with the distal regions of the promoter, particularly the HR1 enhancer, and less marked for the histones associated with the proximal regions and the core of the promoter. Retinoid treatment induces a rapid increase in H4R3 methylation that peaks at about 2 hours, then rapidly returns to baseline.

These results demonstrate that the priming of HL-60 cells produced in a coordinated set of histone modifications that are likely to be linked to alterations in chromatin structure. The most prominent effects were suppression of H3K4 methylation at the core promoter, and the increased methylation of the R3 residue of H4 on histones associated with the distal regulatory regions of the promoter. Furthermore, although DMSO-priming had little effect on either H3 or H4 acetylation, retinoid treatment results in a marked and generalized increase in H4 acetylation and a more localized increase in H3 acetylation at the core promoter region.

4.4.3. Changes in H3 phosphorylation status.

In naïve state H3S10 phosphorylation was detectable all over the promoter at high levels. These levels showed a transient decrease upon gene activation, which probably correlated with opening of the closed chromatin structure (Figure 6 A). A transient peak in phospho-acetylation was detected prior to the start of mRNA synthesis (Figure 6 B). After this peak the mRNA synthesis starts and phospho-acetylation decreases. We suggest that phospho-acetylation is a dynamic histone tail modification that occurs in the first phase of the transcription initiation.

4.5. Role of H4R3 methylation and H3K4 demethylation

The comparison of histone modifications between naïve and DMSO primed HL-60 cells indicated that reciprocal changes in side-chain modifications might be linked to the altered activation of gene expression associated with the precommitment process. To better understand the types of processes that might be involved in the observed alterations in histone methylation, we examined the time course for the changes in H4R3 and H3K4 methylation that followed the initiation of priming with DMSO. Naïve cells were treated with DMSO for 4 and 12 hours and the ChIP analysis was carried out to determine the level of H4R3 methylation of histones bound to the HR1 enhancer and H3K4 methylation of histones bound to the core promoter (Figure 7). There is a striking similarity between the reciprocal changes of H4R3 and H3K4 methylation. Both are substantially changed

within 4 hours of the initiation of DMSO priming and these changes remained until the end of the monitored period.

To test if there is a functional link between the changes in H4R3 methylation induced by priming and altered gene expression, we used adenosine dialdehyde (ADOX), an inhibitor of methyltransferases (Najbauer et al. 1993) (Tang et al. 2000) to suppress methylation. Co-treatment of HL-60 cells with ADOX and DMSO eliminated H4R3 methylation (Figure 9A) and also reduced arginine methylation in general on the studied enhancer element, as measured by ChIP QPCR analyses with an anti-Pan-methylated arginine antibody (Figure 9B). The decrease in H3K4 methylation induced by DMSO priming was not blocked with ADOX (Figure 9C). Inhibition of methylation with ADOX also blocked retinoid-induced acetylation of H4 histones (Figure 9D). In parallel with the inhibition H4R3 methylation and H4 acetylation, there was marked but not complete inhibition in the retinoic acid-induced expression of TGM2 (Figure 9E). It is important to note that co-treatment with ADOX and DMSO reduced, but did not completely block the induction of the transglutaminase gene. Collectively, these data suggest that the inhibition of methyltransferases by ADOX leads to the inhibition of H4 arginine3 methylation, and a concomitant decrease in retinoid-induced transglutaminase promoter activation. We speculate that the decrease in acetylation of H4 histones associated with the transglutaminase promoter is the consequences of the decrease in the retinoid-dependent activation of transcription of this gene. Moreover, the results we have obtained point to a strong correlation between H4 arginine3 methylation and the precommitment of HL-60 cells to terminal differentiation.

There were two main concerns with the results obtained in the previous studies and these pertained to how widespread the priming effect was (i.e. whether it was limited to the TGM2 gene or other retinoid regulated genes were also involved), and if DMSO induced a general induction in gene expression rather than effect only a subset of genes during priming. To address the issue whether DMSO-priming was limited to only one gene, we compared the induction of TGM2 to the induction of two other genes, CD38 and CYP27, regulated by retinoids in myeloid leukemia cells (Kishimoto et al. 1998) (Szanto et al. 2004). The expression of both CD38 and CYP27 was increased by 9-cis retinoic acid, and this induction is much greater in cells that had been primed by pre-

treatment with DMSO (Figure 9F). Co-treatment of the cells with different concentrations of ADOX and DMSO resulted in a dose-dependent suppression of retinoid-induced expression for both genes.

To address the issue of a potential general effect on transcription by DMSO and ADOX on primed gene expression, we used a general expression profiling approach. HL-60 cells were primed with DMSO or DMSO and ADOX for 16 hours and subsequently treated with 9-cis retinoic acid for 6 hours. RNA was then prepared from these cells and global expression profiles were determined using a 3200-feature human cDNA microarray. There was approximately the same number of genes (104 for DMSO and 111 for ADOX) induced >1.5 fold in the DMSO– and ADOX–treated cultures (Figure 10 A). These results confirmed that treatment of HL-60 cells with ADOX does not result in a generalized perturbation of the pre-existing patterns of gene expression. These experiments were performed in the laboratory of Laszlo Puskas, BRC, Szeged.

4.6. Modulation of transcription by altering the epigenetic context

In order to address the question of the more general effects of DMSO priming and ADOX on retinoid-regulated gene expression, we compared the profiles of retinoid-induced genes in RNA from control, naïve cells and retinoid-treated cells that had been primed with either DMSO alone, or DMSO and ADOX. We detected 38 genes s upregulated more than 1.5 fold by the treatment of naïve HL-60 cells with retinoids for 6 hours. Exposure of similar cells to retinoids following DMSO priming resulted in a substantially larger pool of genes (104) upregulated more than 1.5 fold compared to the DMSO-primed cells. Of the 75 retinoid-induced genes selectively up-regulated in DMSO-primed cells, the induction of 62 was blocked by co-adminsitration of ADOX with DMSO (Figure 10 B). These experiments suggested that neither DMSO nor ADOX had a widespread effect on transcription in these cells. Since methylation is involved not only in RNA production, but also in protein synthesis, we asked whether a ADOX, a general inhibitor of methyltransferases would produce a major rearrangement in the proteins of the studied cells. For this, the proteome of HL-60 cells and the effect of ADOX on the protein expression pattern was analysed with 2D electrophoresis and silver

staining. This measurment was performed by Andras Madi, member of the Signaling and Apoptosis Research Group of the Hungarian Academy of Sciences, Debrecen. We could not detect any substantial change in the protein composition of HL-60 cells after ADOX treatment with this method; in fact, there was less than 5% change in the number of spots detected. These data strongly suggest that ADOX is not a general inhibitor of RNA and protein synthesis under the these conditions (Figure 10). In order to gain a more mechanistic insight into this process and also to take advantage of recent developments in the field, we evaluated the role of the enzymes proposed to be responsible for H4R3 methylation. These are PRMT1, a methyltransferase, and PAD4, a peptidylarginine deiminase recently identified as the enzyme responsible for methyl arginine's conversion into citrullin and thereby "reversing" arginine methylation (Hagiwara et al. 2002; Cuthbert et al. 2004; Wang et al. 2004). We used gene-specific TaqMan assays and carried out real-time RT-QPCR analysis to determine the expression level of PRMT1 and PAD4 in the myeloid cell lines used in our studies, in the absence or presence of 9-cis retinoic acid. All cell lines expressed appreciable levels of the PRMT1 mRNA, and retinoid treatment did not appear to change it significantly (Figure 11A). PAD4 is expressed at low or not detectable levels in the six cell lines examined, but induced to high levels upon 2 days of retinoid treatment in NB4 and HL-60 cells, and to a lesser degree in KG1 and PLB cells (Figure 11B). Finally, we examined the expression level of PAD4 during priming and subsequent retinoid response in HL-60 cells. As shown on Figure 11C, PAD4 is induced by priming itself and further induced during in response to retionids.

These data established that both PRMT1 and PAD4 are present in HL-60 cells, and while PRMT1's expression level appears to be constant, PAD4 is changing dynamically during priming and retinoid stimulation, in agreement with previous findings (Nakashima et al. 1999). If one assumes that H4R3 methylation is the cause of the priming effect, a few predictions can be put forward and tested. One is that preacetylation of chromatin interferes with H4R3 methylation (Wang et al. 2001), therefore the priming is likely to be attenuated. We tested this by using Trichostatin A (TSA), a histone deacetylase inhibitor. TSA alone had no effect on TGM2 expression (Figure 12A). Increasing amount of TSA potentiated the retinoid's effect as anticipated, and as

previously demonstrated (Nagy et al. 1997). Importantly, the DMSO priming effect was completely abolished if cells were pretreated with TSA, suggesting that acetylation of histones interfering with H4R3 methylation eliminates the priming effect. These findings confirm previous reports on the interference of acetylation and H4R3 methylation (Wang et al. 2001). Another prediction is that activation of PAD4, the enzyme converting methyl arginine to citrulline also attenuates the priming effect. To test this prediction we used calcium ionophores to activate PAD4 in HL60 cells similarly as reported by Allis et al. (Wang et al. 2004). Cells, after priming but prior to retinoid induction were exposed to a short, 15 minutes treatment of 1 μM A23187 calcium ionophore. After this treatment cells were washed extensively and treated with 9-cis retinoic acid. The presence of A23187 reduced retinoid responsiveness and priming as shown on Figure 12B. The interpretation of these data are corroborated by chromatin immunprecipitation results. As shown in Figure 12C, both TSA pretreatment and PAD4 activation prevented/eliminated H4R3 methylation. Moreover, comparison of H4 acetylation and H4R3 methylation revealed that TSA treatment enhanced acetylation, while preventing H4 R3 methylation (Figure 12D and E). The third prediction we tested was that increased level of PRMT1, the methylase responsible for H4R3 methylation, would lead to increased priming. On one hand, transfection of PRMT1 does not induce gene expression in the absence of retinoid treatment (Figure 13A). On the other hand, increased PRMT1 expression can further induce the priming effect, although, importantly, it does not substitute for priming under the conditions used. Finally, we have evaluated the combined effect of transfected wild type or mutant PRMT1 and PAD4 on the retinoid regulated expression of TGM2, and also on the expression of a retinoid inducible reporter gene. As shown on Figure 13B and C, PRMT1's enzymatic activity is required for its co-activator activity. PAD4 does not act as a co-repressor, but its enzymatically inactive mutant synergizes with PRMT1 in enhancing transcription (Figure 13B). The combined results of these experiments suggest strongly that the priming effect involves H4R3 methylation and the level of H3R4 methylation is regulated by the activity of PRMT1 and PAD4.

4.7. Cloning of H4R3 methylated loci

A key arginine methyltransferase of the mammalian cell is PRMT1. One of the methylation reactions mediated by this enzyme is the H4R3 methylation (Tang et al. 2000). H4R3 methylation was shown to be linked with gene expression (Wang et al. 2001). Methylation of histones by PRMT1 makes them a better substrate for histone acetyltransferases and by this provides a mechanistic link between gene expression regulation and arginine methylation (Wang et al. 2001). We decided to map genomic loci of arginine methylation in a differentiation-primed myeloid leukemia cell line using an unbiased technique. The „ChIP to clone" strategy was used previously to identify binding sites of transcription factors (Weinmann et al. 2001). Transcription factors have consensus binding sites that can be identified with in silico analysis and several biochemical methods can be used to verify the binding. In the case of a transcriptional cofactor that binds to a whole array of sequence specific transcription factors, and has a well defined enzymatic activity, identification of the genomic loci it binds to can be problematic. However, the post-translational modification produced by such cofactor can be reliably utilized for such analysis. It was shown previously that post-translational histone modifications of specific loci are produced on much wider genomic areas than the localization of the transcription cofactors responsible for them (Bernstein et al. 2005) (An et al. 2004). The mechanism of this phenomenon has not been explained yet; nonetheless, we decided to use this observation in order to identify genomic loci marked by PRMT1 via H4R3 methylation. The localization of H4R3 methylated loci was achieved by using chromatin immunoprecipitation with an antibody raised against methylated H4 arginine (Wang et al. 2004). This antibody should bind specifically to genomic loci marked by PRMT1 (Tang et al. 2000; Wang et al. 2004).

The „ChIP to Clone" method is summarized in Figure 15. Briefly, HL60 cells were treated with 1.25% DMSO for 16 hours to achieve a differentiation-primed state characterized by increased H4R3 methylation. Cells were fixed with 1% formaldehyde, and sonicated to achieve an average DNA fragment size of 500 bp. Figure 16A shows the predominant DNA fragment size of the sheared chromatin. We used anti- H4R3-methyl antibody and protein A-agarose beads to immunoprecipitate mono- and di-nucleosomes carrying this modification. Beads were washed extensively, and immunoprecipitated DNA was purified. After isolation of DNA, protruding ends of the DNA elements were

filled to create blunt ends. The blunt-ended fragments were then cloned in a low background plasmid vector, and used to transform a suitable bacterial strain. Individual colonies were isolated, and plasmids were purified from the colonies. Insert-carrying clone were identified by restriction enzyme analysis and by standard PCR with vector specific M13 primers and agarose gel electrophoresis (Figure 16B). Further analysis was carried out after sequencing the plasmid inserts.

4.8. Sequencing and analyses of the cloned fragments

By sequencing 111 of these cloned sequences we found that 54 of the sequenced clones had DNA fragments substantially smaller than those which could originate from the immunoprecipitated nucleosomes. We considered these fragments junk DNA, since they were unlikely to originate from an immunoprecipitated nucleosome containing a DNA fragment of at least 140 bp, even though they were large enough to provide disruption of the lethal gene included in the plasmid.but. 57 clones contained fragments longer than 150 bp, corresponding to mono-, di- or trinucleosomes. Therefore, we decided to analyze in detail the genomic localization of these. First, we performed a BLAST analysis with the identified sequences. 48 of them were of human origin, 7 of bacterial origin and two of them of salmon origin. The bacterial sequences were probably due to contamination with bacterial genomic DNA fragments and the salmon DNA from the salmon sperm DNA used as a blocking agent for the protein A agarose beads.

We considered a match in the human genome a sequence with more than 95% identity with the query sequence used for BLAST analysis. At the further stages of the analyses of the sequences we used the following categories:

1. sequence with unique localization: a sequence with a unique match in the human genome
2. repetitive sequence: a sequence with a match in one of the known repetitive elements in the genome. In these cases the query sequence gave several thousand hits along various chromosomes.
3. repeated sequences with unique localization: those sequences that were found several times in our library but had a unique genomic localization.

From the 48 human sequences 38 of them provided us with a perfect match, meaning that the whole length of our query sequence could be aligned with more than 98% identity to a human sequence. In one case we found a duplicate location with identical score but both of these locations were in gene poor regions. The 38 human sequences contained 26 unique sequences, 12 repeated unique sequences and 10 repetitive sequences. From the 10 repetitive sequences we found 6 unique repetitive sequences and 4 that were repetition of a single clone from the 6 previously mentioned. We decided to further analyze the genomic localization of the 26 unique sequence hits with the UCSC genome browser. From the 26 analyzed sequences we found 14 that localized in the vicinity of known genes. We set up a cut-off value of 10 kb for the analyses of proximity of genes. 9 of the sequences were found in introns, one at an intron/exon overlap, and 4 within 5 kb from 5‘ ends of genes. One hit was at 5‘ of a predicted promoter. 12 of them had no genes within 10 kb. 6 of these had regions with conserved TF binding sites within 5 kb. Table 2 presents the names of the 14 identified genes, their locations on chromosomes, the location of immunoprecipitated fragment, relative to the gene, and the conserved transcription factor binding sites within 1 kb relative to the immunoprecipitated fragment.

The PANTHER (Protein ANalysis THrough Evolutionary Relationships) (Mi et al. 2005) (Thomas et al. 2003) database allows complex annotation of proteins and genes. We selected the data described as “Molecular functions” and “Biological processes” of the Version 5.0 (release date Jan. 1, 2005). This annotation allowed us to align the identified genes along biological processes as shown in Table 3. Signaling, cell differentiation, immune response and development are frequently associated with the identified genes.

Next we decided to analyze the conserved transcription factor binding sites (TFBS) in the 5 kb region of the 26 identified immunoprecipitated fragments, regardless whether they were located in the proximity of genes or not. We found 39 conserved TFBS, with 12 of them being present more than one time. In Table 4 we present those 6 TFBS that were present at least three times in this list, with their corresponding transcription factors, according to the Biobase library (Matys et al. 2003). Two of these were published to have connections with the family of protein arginine

methyltransferases, namely MEF2 with PRMT4 (or CARM1) (Chen et al. 2002) and FOXO as being an inducer of BTG1 the activator of PRMT1 (Bakker et al. 2004).

4.9. Genomic location analyses studies

The transcriptional regulatory networks operated by nuclear hormone receptors are largely unknown. To gain insights into the regulatory pathways operated by orphan nuclear receptor heterodimers and their coregulators, genome-wide localization studies need to be carried out. Genomic location analysis, a method that involves the combination of chromatin immunoprecipitation (ChIP) with high throughput DNA detection methods, such as microarrays, enables us to correlate the epigenetic context of specific genes with their transcriptional activity in a whole genome context (Weinmann et al. 2002). It became apparent fairly early to us that the global expression analyses need to be complemented with genome-wide localization studies of nuclear receptor binding sites in order to identify the details of target gene activation.

In close collaboration with the Debrecen Clinical Genome Center and the Hungarian Bioinformatics Institute Inc. we have carried out ChIP on chip analysis. For these studies, initially we employed a microarray that contains 12 000 CpG enriched loci of the human genome, and analyzed the PPARγ binding sites and histone acetylation (H4 acetylation) status of the putative regulatory regions spotted on this microarray. This array was developed by UHN, Toronto, and is described in more detail in the next section.

For the chromatin IP of nuclear receptors we developed a series of TaqMan (Q-RT-PCR) assays for well-validated target gene response elements. TaqMan assays for the response elements of FABP4, CD36, LXRα, RAOH, RARβ, and CD38 have been developed. In parallel we screened several antibodies raised against RXR, RAR and PPARγ and selected a subset of these antibodies in order to perform Chip on chip experiments (Figure 20).

ChIP-Western technique was used to screen the PPARγ antibodies available. Interestingly but not surprisingly, we were able to immunoprecipitate PPARγ with anti-RXR antibodies as well (Figure 21). As a part of the optimization process, we assessed

the effect of fixation time on the ChIP efficiency by PPARγ antibodies. As seen on Figure 19A and B, we were able to immunoprecipitate a much larger fraction of the LXRα PPAR-RE fragment by using 15 minutes fixation time. As negative controls we used the „No antibody control", and to assess the specificity we measured the RAR-RE of the CD38 gene.

The DNA used for ChIP had an average fragment length of 500 bp. This corresponds to approximately 3 nucleosomes, and is in concordance with the average fragments spotted on the microarray. We tested two published methods used for amplification of DNA. The one used by the Farnham laboratory performes a blunt end ligation of a linker and subsequent linker PCR. For this ligation step it was suggested to create blunt end fragments from the ChIP DNA using a Klenow end-fill reaction (Figure 22). We tested this method but found it to be less suitable for amplification of DNA than the one suggested by De Risi laboratory. This latter one is using a primer extension reaction with a primer that has a degenerated 3' end and a specific 5'end. After the initial primer extension reaction, carried out with a Sequenase enzyme, subsequent PCR reaction is performed during the amplification step with a primer that is complementary to the specific 5'end of the initial primer used for the primer extension reaction (Figure 23).

On the CpG platform we analyzed fragments bound by PPARγ antibody. The number of spots enriched by PPARγ was in average 1%. This is in agreement with the observations of Young and his colleagues (Odom et al. 2004) regarding members of the HNF transcription factor family.

Several new putative binding sites of PPARγ were identified. As an example, we will refer to the Hes1 gene (Figure 24),which is induced by rosiglitazone according to global gene expression data (Istvan Szatmari, personal communication), albeit at low levels. Such low level induction is not considered significant in a stringent global gene expression data analysis (Figure 24 B). On the other hand, the genomic fragment spotted on the CpG array is enriched in PPARγ bound fragments, and this locus was previously described as being a retinoid response element of Hes1. (Figure 23E)

To test whether ChIP on Chip approach is suitable for functional analysis, we performed H4 acetylation studies using a cell line, which is known as being more PPARβ

responsive (HT29). We performed these studies in collaboration with Beatrice Desvergne (University of Lausanne). The work was done in our laboratory together with Matthew Hall, member of the Desvergne laboratory. We treated cells with PPARβ and PPARγ specific ligands and performed native ChIP as described in the Methods section. After amplification, labeling and hybridization we scanned the arrays and analyzed them using GeneSpring software (Figure 25A). We performed triplicates for each condition and compared the acetylation pattern to the „No Antibody Controls" and to the input sample. Using this approach the hit rate for spots that showed an increase in H4 acetylation after PPARγ ligand treatment and PPARβ ligand treatment was 0.6% and 0.8%, respectively (Figure 25B). These results confirm the previous observation that these cells are more prone to PPARβ ligand activation (Figure 25B). We found also that subsets of regulatory regions are becoming acetylated by ligand activation of both PPAR isotypes, PPARγ and PPARβ (Figure 25C).

After this step we decided to switch to the tiling array platform. Tiling arrays cover the human genome except the repetitive sequences. The goal of these experiments was to perform ChIP on Chip with H4 acetylation antibodies and hybridize on a tiling array that covers the ENCODE regions on a single array. In the initial phase we used the global gene expression data sets of Lajos Szeles from our laboratory to define the shortest time frame that is producing a marked change in the global gene expression pattern. We used human primary monocytes and first-day Immature Dendritic Cells (IDC) to compare the acetylation patterns and their correlation with the change in gene expression. We isolated a set of 8 samples of monocytes and first day IDC-s. From this set we selected 4 pairs of samples according to their changes in a number of genes used as markers and measured by QPCR (Figure 26). We labeled three sample sets and performed global gene expression analysis on the Affymetrix platform (Figure 27 and 28). 1770 genes showed at least three fold decrease when cells differentiated from monocytes to first day IDC-s, and 24 of these were located in the Encode regions. 1346 genes with higher raw values than 200 showed at least twofold decrease during this transition. 1640 genes showed at least threefold increase during the monocyte-IDC transition, and 22 of these were located in the Encode regions. 1294 genes with higher raw values than 200 showed at least two fold increase during this transition.

In the next phase we performed ChIP with anti-H4 acetylated antibodies on the chromatin isolated from these monocytes and first day IDC-s. Purified DNA was amplified and sent to the EMBL Genecore, Heidelberg.

4.10. The CpG Annotation bioinformatic interface

In order to efficiently mine the data obtained from the 12K CpG microarray platform, we developed a web-based annotation tool to link genomic location analyses data of the 12K CpG microarray with the global gene expression data obtained on the Affymetrix gene chips.

This interface allows users to identify the location in the genome of the enriched loci. The results for the query loci are interconnected with the UCSC genome browser and the Ensembl database. This interface allows the conversion of CpG array lists to Affymetrix lists of the genes located in the close proximity of the CpG island spotted on the array.

The microarray developed by University Health Network (Human CpG 12K Array) is described at: http://www.microarray.ca/products/types.html. The DNA spotted on this array is from the CpG library produced by Sally Cross in the laboratory of Adrian Bird at The Wellcome Trust Centre (Cross et al. 1994). Sanger Institute has performed the initial terminal sequencing of the clones, and information about the original sequencing data can be found at http://www.sanger.ac.uk/HGP/cgi.shtml. Recently the library was re-sequenced by Larry Heisler (Sandy Der Laboratory, University of Toronto) and the new set of sequence can be downloaded from the Der Laboratory website: http://derlab.med.utoronto.ca/ CpGIslands/

For identification of the Human CpG 12K Array spots we used the so-called “96 well location” that can be found in the fourth column of the CpG12k1.gal file provided by the University Health Network (http://www.microarrays.ca/support/glists.html). Location of the CpG annotation window that uses the Sanger Clone set is: http://genomics.dote.hu/jetspeed/air/ CpG.jsp. Location of the CpG annotation window that uses the Larry Heisler sequence set is: http://genomics.dote.hu/jetspeed/air/ CpG2.jsp

The left input field can be used to search single “96 well location” identifiers. A

tab delimited text file can be used to upload a list of identifiers.

As a result, the identifier, the chromosome, the exact location on the chromosome and the score of the Blat hit will be seen in the first four columns of the results window. The UCSC link of our database in the „Location" position allows the identification of conserved regions and conserved putative transcription factor binding sites.

CpG islands

96-well location	Chromosome	Location	Score (fwd rev)	Towards p end 3		Towards p end 2		Towards p end 1		Towards q end 1		Towards q end 2		Towards q end 3	
				Name	Delta (kb)	Name	Delta (kb)	Name	Delta (kb)	Name	Delta (kb)	Name	Delta (kb)	Name	Delta (kb)
1a11	16	75781525 - 75781724	371 –	Not named	-955	Not named	-903	CNTNAP4	-772	NP_055755	5	ADAMTS18	169	Not named	543

Only the longest forward and reverse sequences were considered for each clone. These sequences were searched in the ENSEMBL human DNA database (entire chromosomes) with BLAT. The score is made of the total number of hits between the raw sequence data (for the longest forward and reverse sequences) and the ENSEMBL human DNA database. The forward and reverse hits within a distance of 5000 bp on the same chromosome were checked, and the pair with the maximum score (forward score+reverse score) was selected for each clone. The other columns show the 6 neighboring genes compared to the BLAT hit. There are 3 genes shown towards the p end of the chromosome and 3 towards the q end of the chromosome.

CpG islands

96-well location	Chromosome	Location	Score (fwd rev)	Towards p end 3		Towards p end 2		Towards p end 1		Towards q end 1		Towards q end 2		Towards q end 3	
				Name	Delta (kb)	Name	Delta (kb)	Name	Delta (kb)	Name	Delta (kb)	Name	Delta (kb)	Name	Delta (kb)
1a11	16	75781525 - 75781724	371 –	Not named	-955	Not named	-903	CNTNAP4	-772	NP_055755	5	ADAMTS18	169	Not named	543

In the "Name" column there is a link to the ENSEMBL Human Gene View page of the gene. The "Delta (kb)" column shows the distance between the center of the BLAT hit and the center of the entire gene, expressed in kilobases. We have not taken into consideration the length of the gene. Some of the hits are intragenic. The Affymetrix

codes (array "AFFY HG U133 PLUS 2") corresponding to the 6 neighboring genes can be obtained by uploading a tab delimited text file that contains the “96 well location” identifiers and selecting the operation "Get Affy code".

Istvan Andrejkovics and Endre Barta from the Hungarian Bioinformatics Institute performed the database development and web design.

5. DISCUSSION

5.1. Transcriptional memory and differentiation

The nuclear receptors are modulators of hormonal responses. Hormonal responses can be regulated on several levels. In the case of nuclear receptor-driven genes, several steps of the complex signal transduction pathways are shortcut by the fact that the signal molecule is lipophylic, thus entering into the nucleus directly to bind to the RXR-bound nuclear receptors (e.g. RAR, TR, VDR, PPAR). The ligands activate the receptors, binding site-

specifically to the DNA, and induce well-characterized conformational changes. Understanding the enhanced hormonal response of a population of cells could bring new insights in the physiological mechanisms that coordinate quick hormonal responses. In our experiments we planned to study the molecular determinants of this enhanced retinoid response.

The form of cellular memory that provides gene “silencing”, has been studied in detail (Grewal et al. 2003; Okamoto et al. 2004). However, the mechanisms that allow for either persistent activation of gene expression or a pre-sensitization to expression of specific genes have not been well characterized. We decided to study these mechanisms in the context of the regulation of gene expression.

When a gene is turned on, a concert of protein-protein interactions occur on the promoter of the gene. In the case of nuclear receptor-mediated transcriptional activation, the starting note of this concert is the recruitment of coactivators after ligand activation of the receptor. Several studies have been carried out that suggest a sequential recruitment of these transcription factors to promoters. In parallel with the recruitment of these proteins, ordered modifications are carried out on the histone tails.

To understand hormonal regulation, we have to take in consideration that hormones are soluble molecules that penetrate whole tissues or the entire organism. Their action is restricted mainly because their receptors are expressed only in particular cell types or tissues. Receptor isoforms also bring a further level of regulation, since their expression is regulated by promoters with different TF binding site architecture. We have analyzed what mechanisms might be responsible for changing the neutral state of the chromatin of potential target genes –into a chromatin that will be tuned towards the specific signal.

In the studies reported here we have set out to address a complex issue, namely to investigate the changes in epigenetic markers that are linked to the regulation of gene expression during retinoid -induced myeloid cell differentiation. We have chosen to work with the HL-60 cell line, because previous work from several laboratories have established that differentiation of these cells involves a two-step process that can be separated pharmacologically (Yen 1985; Yen et al. 1987; Yen et al. 1987; Collins et al. 1990). The first step, termed precommitment or priming involves a persistent state of pre-

sensitization that constitutes a well-defined model of cellular memory. The second step, which is also well characterized, involves selective activation of gene expression by inducers of terminal differentiation for this lineage, such as retinoids. We have then used the promoter of a well-characterized retinoid-regulated gene in this pathway, tissue transglutaminase – a key marker of retinoid response – to investigate the role of epigenetic modification of chromatin components in the establishment of the precommited state of differentiation of these cells. We have carried out a detailed analysis of the covalent modifications of histones bound to different regions of the transglutaminase promoter, during three distinct states of differentiation: the naïve state that occurs prior to the initiation of differentiation; the primed or precommited state that is induced by brief exposure of the naïve cells to Vitamin D or DMSO; and the differentiated state that occurs following the addition of a retinoid to the primed cells. In characterizing the precommited state, we found that it was a "threshold phenomenon". The increased induction of gene expression in primed versus naïve cells was not due to an increase in the transcriptional activation of individual cells, but rather due to an increase in the fraction of the population of cells that was able to respond to retinoids with activation of gene expression (Figure 2). This result is entirely consistent with a model that suggests that the development of epigenetic memory entails a persistent "marking" those cells that have been exposed to the memory inducer (in this case Vitamin D or DMSO).

The analysis of histone tail modifications during both priming and transcriptional activation revealed distinct mechanisms that mark both of these processes. Priming itself appears to be linked to major changes in histone side chain methylation. In particular, methylation of K4 on histone H3 (H3K4) associated with the core promoter is rapidly decreased after the initiation of priming (Figure 4 and 5). This decrease in H3K4 methylation level was not blocked by the methyltransferase inhibitor ADOX (Figure 6C), suggesting that a non-methyltransferase dependent pathway might be responsible for this effect. This observation is in agreement with the recent identification of the enzymes responsible for demethylation (Shi et al. 2004). According to Shi et al. demethylation is mediated by LSD1, a member of amine oxidase enzymes. Priming increases the methylation of arginine on histone H4 (H4R3), specifically on histones associated with a

prominent enhancer element in the transglutaminase promoter. Arginine methylation of histones seems particularly important to the induction of the primed state, since its elimination with a pharmacologic inhibitor of methyltransferases resulted in the loss of priming for the induction of tissue transglutaminase and several other retinoid-regulated genes (Figure 6).

Phosphorylation on H3 Serine 10 has been reported to be related with mitosis (Strahl et al. 2000), while H3 Serine 10 K14 phospho-acetylation with nuclear receptor activity (Li et al. 2002). We found that in naïve state high levels of H3 Serine 10 phosphorylation are detectable all over the promoter. The level of phosphorylation show a transient decrease upon gene activation, which probably correlates with opening of the closed chromatin structure. If we compare in our system the dynamics of acetylation, phospho-acetylation and phosphorylation of the H3 tail, we can see that these processes appear to be interconnected. We suggest that H3 S10 phosphorylation together with H3 K4 methylation are the histone tail modifications characteristic for the naïve state of this promoter. After gene activation a subset of nucleosomes enters in a highly dynamic state and these nucleosomes are in a dynamic change between the purely phosphorylated and purely acetylated states. A transient peak in phospho-acetylation can be seen prior to the start of mRNA synthesis and this corresponds to the formation of the pre-initiation complex. After this peak the mRNA synthesis starts, phospho-acetylation decreases, albeit both phosphorylation and acetylation reach their maximal state. We suggest that phospho-acetylation is a transient histone tail modification that occurs in the first dynamic phase of the pre-initiation.

Transcription of the transglutaminase gene in these myeloid cells is paralleled by a wave of histone tail acetylation that is most likely due to the recruitment of HAT containing complexes to the promoter. However, our studies have also demonstrated that activation of transcription is not only linked to histone acetylation, but also to some very selective effects on histone methylation. H3K4 methylation has been characterized in several systems and has generally been found to oppose H4K9 methylation and to mark areas of increased gene expression (Grewal et al. 2002; Elgin et al. 2003). We have found that this methylation pattern is concentrated in the core promoter and is reduced by

priming and increased by retinoid treatment. These data are in agreement with a purported role of H3K4 as a marker of positive gene expression.

5.2. Cross-talk between enhancer and core promoter

There is an apparent discrepancy between the epigenetic changes occurring on the HR1 enhancer and the core promoter, as revealed by our studies. While histone methylation of H4R3 on the enhancer element appears to play an important role in the establishment of the precommited state, histone acetylation seem to contribute to the activation of transcription. Retinoid activated transcription of the primed cells resulted in a marked increase in H4 acetylation, particularly in regions of the enhancer element, and a lesser increase in H3 acetylation of histones associated with the core promoter. There could be numerous reasons for this discrepancy. For example, acetylation and arginine methylation were shown by Roeder and colleagues to be detectable on larger promoter fragments than the regions in the proximity of acetyltransferases or methyltransferases (An et al. 2004). In addition to changes in acetylation, transcriptional activation of the transglutaminase gene results in increased H3 methylation (H3K4) of the core promoter and to a lesser and more transient extent, H3 methylation (H3K9) of the enhancer. H3K4 methylation was reported as being localized to core promoters and transcribed regions of active genes if studied by CHIP on Chip technique on larger genomic regions (Bernstein et al. 2005). If studied on individual promoters, the location of increased H3K4 methylation seems also to correlate with core promoters (An et al. 2004) (Hatzis et al. 2002). We have also found a clear and marked difference in the H3K4 levels (more than 50 times higher levels on the core promoter if compared to the enhancer HR1). Taken together, these results suggest a crosstalk between the promoter and enhancer of TGM2 with the activation of distinct enzymatic pathways both during priming and retinoid activation. This so far unsubstantiated crosstalk suggests a physical interaction between these regulatory DNA elements, an interaction that needs to be further investigated.

5.3. A role for histone 4 arginine 3 methylation in nuclear receptor signaling

These observations provide a plausible link between our observations that the pre-commitment state of HL-60 cells involves increased H4R3 methylation and increased retinoid-activated gene expression. In parallel with the increase of H4R3 methylation, the gene responsible for the removal of the methyl mark is also induced. Our transfection data (Figure 9) also suggest that PAD4 may not act as a transcriptional repressor per se, but some of its activity it is required along with PRMT1 for synergistic/cooperative activation of retinoid mediated transcription. This activity does not require, but is inhibited by its peptidyl arginine deiminase activity. The complex role of PAD4 in regulation of transcription is further supported by recent work of Stallcup and colleagues (Lee et al. 2005). According to their data, demethyl-imination of p300 by PAD4 is changing its activity to an activated or even hyperactive form. This change in p300 activity is modulated via the regulation of p300-GRIP1 interaction. We propose that priming-induced modifications of H4 arginine 3 could increase retinoid-induced gene activation by potentiating HAT activity on histones. This in turn would result in increased histone acetylation and increased transcriptional activation. Our data also suggest that the full activation can be achieved in two distinct ways. The first is by switching off HDAC activity with a HDAC inhibitor such as TSA. In this case the response to a retinoid signal will increase. The other way is by transforming the histone tails to become better substrates of HAT-s. Arginine methylation on H4R3 is making such a change. The two mechanisms are mutually exclusive and antagonistic. By this, the two parallel pathways provide a signal integration mechanism for the cell.

The most detailed characterization of the dynamics of nuclear receptor mediated transcriptional activation has been carried out by Gannon and colleagues (Metivier et al. 2003). By analyzing the estrogen receptor induced transcription on the pS2 gene, they described the ordered and sequential recruitment of specific cofactors and the resultant ordered sequence of histone tail modifications. According to their data, in the first “unproductive“ cycle PRMT1 binds to the receptor complex and subsequent H4R3 methylation occurs. In the second, “productive” cycle, recruitment of PRMT1 is followed by binding of HAT-s and extensive acetylation of the histones H3 and H4. We propose that the two phases of gene activation proposed by Gannon and colleagues (Metivier et

al. 2003) may be dissociated in HL-60 cell differentiation. Our results suggest that the transition to the precommited state (i.e. the priming of the cells) induces an increase in H4R3 methylation, but no change in H4 acetylation and no activation of transcription. This first cycle of HL-60 differentiation does not require liganding of the nuclear receptors, but occurs via an independent and uncharacterized Vitamin D or DMSO-dependent step. This step is providing a further signal integration node for the cell by integrating two independent signals in time and space.

5.4. Cloning of H4R3 metylated loci

We decided to further characterize the links between gene expression regulation and arginine methylation by PRMT1. We used chromatin immunoprecipitation to identify genomic loci marked by PRMT1 with H4R3 methylation. The isolated fragments were cloned into a low-background vector and isolated. After sequencing of 111 isolated clones, we identified 26 fragments that had a fragment size corresponding of mono, di- and tri-nucleosomes. 14 of these sequences were intronic or within 5 kb to 5‘ ends of known genes. Regulatory regions show a higher degree of conservation during evolution (Liu et al. 2004); therefore, identification of conserved transcription binding sites in the proximity of H4R3 arginine methylated chromatin stretches is a sign of the relevance of the specific loci. We found 39 conserved TFBS, with 12 of them being present more than one time. In table 3 we present those 6 TFBS that were present at least three times in this list, with their corresponding transcription factors, according to the Biobase library (Matys et al. 2003). Two of these were published to have connections with the family of protein arginine methyltransferases, namely MEF2 with PRMT4 (or CARM1) (Chen et al. 2002) and FOXO as being an inducer of BTG1 the activator of PRMT1 (Bakker et al. 2004).

To annotate the identified genes we used the PANTHER (Protein ANalysis THrough Evolutionary Relationships) (Mi et al. 2005) (Thomas et al. 2003) database. From the 14 genes 3 remained unclassified. The nine classified genes contained one structural protein (Collagen 9A1), one amino acid transporter (SLC36A1), all the other genes are involved in signaling, cell differentiation, immune response and development.

To illustrate the possible connection between the H4R3 modification and its role in regulation of immune responses by PRMTs, we summarize the known data regarding one of the identified sequence, the one located in the promoter of IL1α. IL1α was shown to be expressed in both blood polymorphonuclear (PMN) and mononuclear (MNL) cells (Lord et al. 1991). Moreover, IL1α in the presence of histamine or PGE2 controls the expression of IL1β (Vannier et al. 1993).

One of the genomic localizations identified by this screen is at 3 kb upstream from the transcription start site of the gene IL1α. This location is on chromosomal band 2q13. Two conserved transcription binding sites are found within 2 kb towards the 5 prime end of the gene V$FOXP1_01 V$BRN2_01 responsible for binding of FOX P1a and POU3F2. More interestingly, in the first intron, at 5 kb from our located sequence, two conserved transcription factor binding sites V$YY1_Q6 and V$COUP_01 are located that can bind YY1 and COUP TF, respectively.

PRMT1 was shown to interact with YY1, and this interaction results in histone arginine methylation (Rezai-Zadeh et al. 2003). YY1 forms a complex with PRMT1 mediated by DRBP76 (also called ILF3, Interleukin enhancer factor 3, (Rezai-Zadeh et al. 2003). This complex favors H4R3 methylation and subsequent acetylation. The activated gene is transcribed and RNA produced. Arginine methylation controls elongation also, via SPT5. SPT5, a regulator of elongation is also methylated on arginine residues by both PRMT1 and PRMT5, on partially overlapping methylation sites (Kwak et al. 2003).

At the RNA methyltransferase complex level, PRMT5 (JKB1-janus kinase binding protein1) and PRMT1 produce asymmetric and symmetric methyl arginines (Yanagida et al. 2004). After splicing and formation of mRNA, ILF3 through its RNA binding domain binds the formed mRNA and interacts with exportin5 (Brownawell et al. 2002). This interaction between ILF3 and cytokine mRNA was reported to stabilize the formed mRNA molecule (Shim et al. 2002). This stabilization is concomitant with the export from the nucleus via XPO5 (expontin 5), which is a Ran GTP mediated process (Brownawell et al. 2002; Gwizdek et al. 2004). This stabilization of cytokine mRNA during nuclear export was documented for IL2 mRNA molecule (Shim et al. 2002).

Quite interesting members of ILF family (ILF1 and ILF2) were published as being methylated on arginine residues in a proteomic approach (Boisvert et al. 2003), while ILF3 on a protein array (Lee et al. 2002). ILF3 was shown to be an activator of the methyltransferase activity of PRMT1 (Tang et al. 2000). Taking these data together, one may formulate an attractive hypothesis that arginine methylation seems to control the expression of IL1 cytokines at various levels from chromatin level through splicing and nuclear export till mRNA stabilization. Although these levels are separated in time and space according to the classical gene expression regulation point of view, the presence of PRMT1 at various levels fits well in the unified theory of gene expression (Orphanides et al. 2002) and arginine methylation might be a common regulator of these processes.

5.5. Genomic location analyzes studies

During our studies we found that the presence of the receptor and its ligand is not enough for the initialization of their characteristic genetic programs. How is the fully active state or the integration in the transcription factories achieved? Are there epigenetic markers of these events that could be monitored? Answering these questions would provide us with essential answers about diseases like atherosclerosis, diabetes or rheumatoid arthritis.

For identification of possible markers of these regulatory processes, we mapped epigenetic changes and protein-DNA interactions with the established ChIP on Chip method. First, we assessed PPARγ binding sites in the genome by using a 12K CpG microarray. The number of spots enriched by PPARγ was around 1%, and some of the identified loci could be aligned with new putative target genes. Genes regulated by PPARγ ligands but with low expression levels could be identified with this method. In the functional test performed we compared the changes in the acetylation patterns produced by PPARγ or PPARβ ligand activation. We found an increase H4 acetylation after PPARγ ligand treatment in 0.6% of the spots, when for PPARβ ligand treatment the enrichment was found in 0.8% of the spots. These data confirmed the previous finding that the cell line used for these studies namely HT29 is more susceptible to PPARβ activation. A subset of genes was under the control of both receptor isotypes.

Next, we decided to perform ChIP on Chip with H4 acetylation antibodies and a tiling array that covers the ENCODE regions of the human genome.

The National Human Genome Research Institute (NHGRI) started the Encode (Encyclopedia Of DNA Elements) project in September 2003, to identify all functional elements in the human genome sequence. The project also aims to develop new high throughput methods to identify functional elements. A set of regions representing approximately 1 percent (30 Mb) of the human genome has been selected as the target for this pilot project. The data generated needs to be released into public databases. Tiling arrays for the selected regions cover uniformly the whole genomic loci except the repetitive sequences. We decided to use the Affymetrix Encode microarray as a part of the Early Access Program, since these tiling arrays were commercially not available, but could be accessed on an advanced technology basis. In parallel, we utilized the same genomic (Encode) regions for the analyses of our samples, on a different technological platform, namely the Nimblegen platform.

We used human primary monocytes and first day Immature Dendritic Cells (IDC) to compare the acetylation patterns and their correlation with the change in gene expression. We have chosen this model system for the following reasons. We already have in our laboratory a large amount of global gene expression data available for these primary cells; these cells are very permissive towards PPAR and retinoid signaling; and lastly, the changes in gene expression between monocytes and first day IDC-s are large enough to be sure we will have significant changes in the Encode regions of the genome. First, we assessed the changes in gene expression during monocyte-IDC transition. We labeled samples from 3 donors that were selected from a set of 8 donor samples according to the changes in the expression of some marker genes. Using Affymetrix gene expression profiling we found more than 3000 genes that produced a more than three fold change in their expression during this transition. 46 of these genes are located in the Encode regions. This correlates with the selection of these regions, namely that they cover 1% of the entire genome. After performing chromatin immunoprecipitation with an antibody that recognizes H4 acetylated histone tails, we amplified the samples and checked the representation of the promoters of TGM2, CD38 and LXRα. We found the fragments to be present in both the monocytes and the IDC-s but not in the „No antibody

controls". The samples were labeled and hybridized at the EMBL Gene Core Lab, Heidelberg. This experiment shows that the levels of acetylation and the level of gene expression are not parallel as a general rule. The most interesting gene, as measured by QPCR, is TGM2, which has a clearly acetylated promoter in monocytes without any transcription. Details of this regulation are not clear and need to be further investigated.

Our data show that these methods can be used for both localization of specific transcription factors in the genome and for assessment of epigenetic changes related with gene activation.

6. SUMMARY

We propose a new model for the epigenetic regulation of retinoid response and differentiation competence in myeloid leukemia cells. In our studies, we were able to dissect some of the epigenetic changes taking place on a retinoid-regulated gene tissue transglutaminase type 2. We found that H4R3 methylation, a modification identified previously but without a well defined biological role, is a hallmark of the primed cell state and precedes gene activation. This modification represents a transcriptional silent (unproductive), but primed state that marks key histones and makes them better substrates for receptor bound histone acetyltransferases (HAT-s). We propose that this mechanism accounts for the increased susceptibility of the cell to respond to a terminal

differentiating agents, such as a retinoid, with increased gene expression and an increased potential for phenotypic differentiation. Preacetylated histones are refractory to this mechanism. This model is consistent with the proposal that histone tail modifications function as the physical mediators of cellular memory. By providing docking sites for transcription factors and marking histones for subsequent covalent modifications, these methylation reactions serve as silent switches of gene expression. Our findings suggest an active and physiological role for arginine 3 methylation on H4 tails in retinoid response and provide a model amenable to further investigation and potentially to pharmacological exploitation.

In order to further characterize the role of arginine methylation in signal integration and developmental processes we carried out mapping of the genomic loci marked by PRMT1 via histone H4 arginine 3 methylation. We used chromatin immunoprecipitation and cloning to isolate genomic loci marked by H4R3 methylation. After sequencing and in silico analysis we found that all of the genomic hits identified were intronic or at 5‘ end of specific genes. The locations identified were enriched in conserved transcription factor binding sites of POU2F1, MEF-2 and FOXL1 factors. A great number of the genes in the proximity of the identified genomic loci were involving signaling pathways and developmental processes. Further analysis of the identified loci needs to be performed in order to decipher the role of arginine methylation in regulating signaling pathways and gene expression.

In order to broaden the study of epigenetic changes from individual genes to a high throughput platform and to move our research to a genomic scale we decided to implement chromatin immunoprecipitation methods combined with microarray analysis (ChIP on Chip). Using this approach, we can integrate the gene expression patterns with molecular determinants of chromatin. By now our results show that ChIP on Chip is suitable for mapping regulatory sequences of PPARγ target genes. For this analysis we used two independent methods. First we located PPARγ binding sites by using PPARγ specific antibodies. We found occupancy of approximately 1% of the spots represented on the CpG array and identified novel genes with lower level of induction by PPARγ specific ligands as potential target genes. In an independent set of experiments we analyzed the changes in H4 acetylation of the chromatin regions represented on the CpG

microarray after treatment with PPAR specific ligands. By this approach the hit rate for spots that showed an increase in H4 acetylation after PPARγ ligand treatment was 0.6%.

Further investigations need to be performed in order to dissect on a genomic level the components involved in the complex regulation of hormonal responses.

7. ACKNOWLEDGEMENTS

What is the chief end of man? Man's chief end is to glorify God, and to enjoy him forever.
Question 1, Westminster Shorter Catechism

First of all I wish to thank the permanent support and continuous training received during my PhD studentship from my supervisor, Laszlo Nagy. He was an excellent teacher whose main goal was to lead me towards becoming a scientist. It was a worthwhile experience!

I am also grateful to professor Laszlo Fesus for the open academic research atmosphere of the Department of Biochemistry and Molecular Biology. His presence was always a guarantee of meanigful discussions.

Thanks to members of the Nagy Laboratory for their help: Szilvia Benko, Attila Szanto and Istvan Szatmari – they taught me the first molecular biology techniques; Lajos Szeles, Daniel Torocsik, Szilard Poliska, Peter Brazda, Attila Pap and Petra Gabor helped with thoughtful discussions and practical contribution. I also thank Ibolya Furtos and Marta Beladi for their excellent technical assistance.

I am grateful to Drs Peter Davies, Laszlo Tora, Mate Demeny, Zsuzsanna Nagy and Beata Scholtz for suggestions and comments regarding my work and techniques used in these studies. I would like to thank the EMBO Young Investigator PhD Programme and the EU NUC REC NET – EU FP5 training network for the international scientific environment I could be part of.

8. FIGURE LEGENDS

Figure1. Priming is enhancing retinoid response in HL-60 cells (A) Experiment outline. HL-60/CDM-1 cells were primed with 1.25% DMSO overnight. The control (naïve) cells received no priming. After overnight incubation, cells were washed, resuspended in fresh media and treated with 1 □M 9-cis retinoic acid. (B) Priming with DMSO or Vitamin D is enhancing 9-cis retinoic acid-dependent expression of Integrin CD11b. Cells were primed with 1.25% of DMSO or 100 nM Vitamin D. After overnight incubation and washing out

the priming agent, cells were treated with 1 μM 9-cis retinoic acid and analyzed with flow cytometry at the indicated time points, as described in Materials and Methods. Isotype controls had no change (not shown). (C) Priming with DMSO, or to a lesser extent with Vitamin D is enhancing 9-cis retinoic acid-dependent expression of Integrin CD11c. Cells were primed with 1.25% of DMSO or 100 nM Vitamin D. After overnight incubation and washing out of the priming agent cells were treated with 1 μM 9-cis retinoic acid and analyzed with flow cytometry at the indicated time points, as described in Materials and Methods. Isotype controls had no change (not shown). (D) Priming with DMSO but not with Vitamin D is enhancing 9-cis retinoic acid-dependent expression of Integrin CD18. Cells were primed with 1.25% of DMSO or 100 nM Vitamin D. After overnight incubation and washing out the priming agent, cells were treated with 1 μM 9-cis retinoic acid and analyzed with flow cytometry at the indicated time points, as described in Materials and Methods. Isotype controls had no change (not shown). (E) Fold increase of Tissue Transglutaminase type 2 mRNA (TGM2) induction compared to naïve, retinoid treated cells. Assessment of the maintenance in time of the priming effect: TGM2 mRNA was measured by real-time QPCR after priming with 1.25% DMSO and compared to naïve, retinoid treated cells. After overnight incubation and washing out the priming agent cells were treated with 1 μM 9-cis retinoic acid at different time points after the priming, as indicated. The retinoid treatment was 12-hour long in all cases. Values are the mean of three independent QPCR measurements ±SD. (F) Fold increase of TGM2 induction compared to naïve, retinoid treated cells. Assessment of the maintenance in time of the priming effect: TGM2 mRNA was measured by real-time QPCR after priming with 100 nM vitamin D and compared to naïve, retinoid treated cells. After overnight incubation and washing out the priming agent cells were treated with 1 μM 9-cis retinoic acid at different time points after the priming, as indicated. The retinoid treatment was 12-hour long in all cases. Values are the mean of three independent QPCR measurements ±SD.

Figure 2. TGM2 expression is enhanced by DMSO priming both at the RNA and protein level. This effect is not cell type specific. (A) 9-cis retinoic acid induction of TGM2 mRNA as measured by real-time QPCR. The expression of TGM2 mRNA in primed and

naïve cells are shown on the same graph with two different Y–axes, with a difference of two orders of magnitude of the scales. Transcript copy numbers were normalized for 36B4 transcript levels. Values are the mean of three independent QPCR measurements ±SD. (B) The fold difference in gene expression in naïve and primed cells. Copy numbers of TGM2 mRNA were determined by real-time QPCR and normalized for 36B4 transcript levels. Values are the mean of three independent QPCR measurements ±SD. (C) Intracellular immunostaining and flow cytometry analysis of retinoid treated HL-60 cells as described in Materials and Methods. The expression of TGM2 protein in naïve cells (shaded) and its isotype control (open) after retinoid induction. The percent of cells expressing TGM2 protein is shown on the graph along with the mean fluorescence intensity of the positive cells. Values are expressed in arbitrary units (A.U.). (D) Intracellular immunostaining and flow cytometry analysis of retinoid treated HL-60 cells as described in Materials and Methods. TGM2 expression in DMSO primed cells (shaded) along with its isotype control (open). The percent of cells expressing TGM2 is shown on the graph along with the mean fluorescence intensity of the positive cells, expressed in arbitrary units (A.U.). At least three independent determinations have been carried out. Data from a representative experiment are shown. (G) Effect of priming upon TGM2 induction by retinoids in MonoMac6 (MM6) cells. TGM2 copy numbers were normalized for cyclophyline transcript levels. Values are the mean of three independent QPCR measurements ±SD. (H) TGM2 induction in NB4 and RARα mutant NB4R2 cells in naïve and primed states. The mRNA copy numbers were normalized for cyclophyline transcript levels. Values are the means of three parallel QPCR measurements ±SD., and results were confirmed from at least three independent biological samples.

Figure 3. Retinoid receptor levels and cell cycle distribution of naïve and primed cells. (A) RXR alpha and RAR alpha mRNA levels measured by real time QPCR normalized for 36B4 in naïve and primed cells. Values are the mean of three independent QPCR measurements ±S.D. (B) DNA contents of naïve and primed cells measured by propidium-iodide staining and flowcytometric analysis as described in Materials and Methods. (C) Cell cycle distribution of naïve and primed cells shown in percentage of total population in the indicated cell phase.

Figure 4. Priming is producing changes on the chromatin level on the promoter of TGM2 (A) DNaseI sensitivity of TGM2 and RARβ promoters is similar in naïve cells. DNaseI hypersensitivity was measured as described in Materials and Methods. Values are the means of three independent QPCR measurements ±S.D of a representative experiment. (B) Priming with DMSO is changing DNaseI sensitivity on the promoter region of TGM2 but not on the RARβ promoter. DNaseI hypersensitivity was measured as described in Materials and Methods. Values are the means of three independent QPCR measurements ±S.D of a representative experiment. (C) Chromatin immunoprecipitation analysis of HR1 enhancer element of TGM2. H4 acetylation was measured as described in Materials and Methods. Acetylation level is expressed as percent of input DNA. All no antibody controls were lower than 0.2% of input DNA. Values are the means of three independent QPCR measurements of a representative experiment. Chromatin immunoprecipitation results were confirmed in at least three independent chromatin preparations.

Figure 5. Detailed map of histone tail modifications on the promoter/enhancer of TGM2. The bar graphs on the left show the effect of priming on the histone tails bound to the enhancer region HR1 (except H3K4 which is shown on the core promoter). The line graphs show the changes in histone tail modifications along the 1.8 kb studied fragment of the promoter/enhancer in primed cells after 9-cis retinoic acid treatment for the indicated period (hours). Copy numbers are expressed as percent of input. All no-antibody controls were lower than 0.2% of input DNA. Values are the means of three independent QPCR measurements of a representative experiment. Chromatin immunoprecipitation results were confirmed in at least three independent chromatin preps. The layout of the 1.8 kb human TGM2 promoter and the location of the various QPCR assays are shown on the bottom.

Figure 6. H3 Serine 10 Phosphorylation and H3 S10K14 Phospho-acetylation levels on the promoter of TGM2 as measured by chromatin immunoprecipitation. H3 Serine 10 phosphorylation and H3 S10K14 phospho-acetylation levels were measured as described in Materials and Methods. Values were normalized to input DNA and expressed copy

numbers. All noantibody controls were lower than 200 copies. Values are the means of three independent QPCR measurements of a representative experiment. Chromatin immunoprecipitation results were confirmed in at least three independent chromatin preparations.

Figure 7. Histone tail modifications during priming. (A) H4 arginine3 methylation levels detected by chromatin immunoprecipitation on the enhancer element (HR1) during priming with DMSO. (B) H3 lysine4 methylation levels detected by chromatin immunoprecipitation on the core promoter during priming with DMSO. Values are the means of three independent QPCR measurements of a representative experiment. Chromatin immunoprecipitation results were confirmed in at least three independent chromatin preparations.

Figure 8. H3 Lysine4 methylation studied by chromatin immunoprecipitation on the core promoter. H3 Lysine4 methylatylation in naïve, primed and primed methylation mute cells after retinoid treatment. All chromatin immunoprecipitation values are the means of three independent QPCR measurements of a representative experiment. Chromatin immunoprecipitation results were confirmed in at least three independent chromatin preparations.

Figure 9. Epigenetic changes on TGM2 promoter and mRNA expression upon priming in methylation mute cells (methyltransferases were blocked with 10 □M ADOX for 16 hours as described in Materials and Methods). Values are the means of three parallel QPCR measurements ±S.D. and results were confirmed from at least three independent biological samples. All chromatin immunoprecipitation values are the means of three independent QPCR measurements of a representative experiment. Chromatin immunoprecipitation results were confirmed in at least three independent chromatin preps. (A) H4 arginine 3 methylation levels determined by chromatin immunoprecipitation on the HR1 enhancer element. (B) Arginine methylation levels determined by chromatin immunoprecipitation on the HR1 enhancer element with an anti-pan methyl-arginine antibody (C) H3 Lysine4 methylatylation studied by chromatin

immunoprecipitation on the core promoter. (D) Chromatin immunoprecipitation analysis of H4 acetylation levels in naïve, primed and primed methylation mute cells on the enhancer element HR1 (E) TGM2 mRNA levels normalized for 36B4 copy numbers in naïve, primed and primed methylation mute cells (in the insert the structure of ADOX is shown). (F) TGM2, CD38 and CYP27 transcript levels after blocking methylation with ADOX in naïve and primed cells. ADOX was used in increasing concentrations as shown. The mRNA copy numbers were normalized for 36B4 transcript levels. Values are the means of three parallel QPCR measurements ±S.D. and results were confirmed from at least three independent biological samples.

Figure 10. Analysis of methylation mute cells on genomic and proteomic levels. (A) Blocking methyltransferases with ADOX is not blocking transcription. Both ADOX and DMSO induced approximately the same number of genes (111 for ADOX and 104 for DMSO). Global gene expression analysis was performed on a cDNA microarray that contained 3200 features in duplicates as described in Materials and Methods. (B) Number of genes with a higher than 1.5 fold increase in expression after retinoid induction in three different conditions: naïve, primed with DMSO or primed with DMSO in the presence of ADOX. Retinoid treated samples were compared to their appropriate controls (naïve, primed with DMSO or primed with DMSO in the presence of ADOX) Global gene expression analysis was performed on a cDNA microarray that contained 3200 features in duplicates. (C) Comparison on proteomic level of HL-60 cells and HL-60 cells treated with 10 □M ADOX for 16 hours. 2D electrophoresis, silver staining and analysis were performed as described in Materials and Methods.

Figure 11. Analysis of PRMT1 and PAD4 mRNA levels in different cell lines after retinoid treatment. (A) PRMT1 mRNA copy numbers were normalized for cyclophyline transcript levels. Values are the mean of three independent QPCR measurements ±S.D. (B) PAD4 mRNA copy numbers were normalized for cyclophyline transcript levels. Values are the mean of three independent QPCR measurements ±S.D. (C) Messenger RNA levels of PAD4 in 9-cis retinoic acid treated naïve and DMSO primed HL60 cells. Fold increase of mRNA levels during priming or retinoid treatment of primed cells are

shown on the arrows. PAD4 mRNA copy numbers were normalized for cyclophyline transcript levels. Values are the mean of three independent QPCR measurements ±S.D.

Figure 12. Modulation of TGM2 expression levels in HL60 cells. (A) TSA pretreatment for 1 hour of HL-60 cells is enhancing the retinoid response in naïve cells (50, 100 and 150 nM TSA was used). TSA pretreatment for 1 hour of HL60 cells before DMSO priming is reducing the effect of priming on TGM2 induction (50, 100 and 150 nM TSA was used). Arrow indicates the effect of pretreatment with 150 nM TSA on primed versus naïve retinoid treated cells. mRNA copy numbers were normalized for 36B4 transcript levels. Values are the mean of three independent QPCR measurements ±S.D. (B) Activation of PAD4 after priming by a 15 minutes treatment with 1 □M of the calcium ionophore, A23187, is reducing the priming effect. mRNA copy numbers were normalized for cyclophyline transcript levels. Values are the mean of three independent QPCR measurements ±S.D. (C) H4R3 methylation levels are changed during priming and modulated by pretreatment with 100 nM TSA for one hour or 15 minutes treatment with 1 □M of the calcium ionophore, A23187. H4R3 methylation was determined by chromatin immunoprecipitation on the HR1 enhancer element. Copy numbers are expressed as percent of input. (D) H4 acetylation levels in primed, retinoid treated cells and TSA pretreated, primed retinoid treated cells. Cells were pretreated with 100 nM TSA for one hour and H4 acetylation levels were determined by chromatin immunoprecipitation on the HR1 enhancer element. Copy numbers are expressed as percent of input. (E) H4R3 methylation levels in primed, retinoid treated cells and TSA pretreated, primed retinoid treated cells. Cells were pretreated with 100 nM TSA for one hour and H4R3 methylation levels were determined by chromatin immunoprecipitation on the HR1 enhancer element. Copy numbers are expressed as percent of input. All detected signals are above the no antibody control values. Values are the means of three independent QPCR measurements of a representative experiment. Chromatin immunoprecipitation results were confirmed in two independent chromatin preparations with two independent immunoprecipitations, respectively.

Figure 13. Effect of PRMT1 and PAD4 on retinoid regulated gene expression. (A)

Transfection of PRMT1 expression vector into HL-60 cells is increasing the TGM2 induction after retinoid treatment in primed cells, while the catalytic mutant has no effect on retinoid responsiveness. Cells were treated with 1μM 9 cis retinoic acid for 10 hours. mRNA copy numbers were normalized for cyclophyline transcript levels. Values are the mean of three independent QPCR measurements ±S.D. (B) Co-transfection of PAD4 and PRMT1 expression vectors and their catalytic mutants into HL-60 cells is modulating the TGM2 induction. Cells were treated with 1μM 9 cis retinoic acid for 24 hours. mRNA copy numbers were normalized for cyclophyline transcript levels. Values are the mean of two independent biological replicates and three independent QPCR measurements for each sample ±S.D. (C) Co-transfection of PAD4 and PRMT1 expression vectors and their catalytic mutants to 293T cells is modulating the luciferase expression on a βRARE tkLuc reporter system. Values were normalized for measured βgal values and expressed in arbitrary units (A. U.) as described in Materials and Methods. Values are the mean of three independent biological replicates ± S.D .

Figure 14. Proposed model of gene expression modulation by changes in H4 Arginine 3 methylation: PRMT1 and PAD4 regulate Arginine 3 methylation. Naïve state is characterized by lack of H4 Arginine methylation on the enhancer region. Priming results in increased H4 R3 methylation, while retinoid treatment leads to decreased H4R3 methylation and to the indicated changes in lysine acetylations. Pre-acetylation of histone tails prior to priming by TSA is likely to reduce the affinity of histone tails towards PRMT1 and by this prevents the enhanced retinoid responsiveness caused by priming. The activation of PAD4 after priming by calcium ionophore treatment leads to the removal of the methyl mark from H4R3 and abolishing the enhanced retinoid responsiveness caused by priming.

Figure 15. Overview of the ChIP to clone method. (1) Protein-DNA interactions in the cell result in specific post-translational modifications on the histone tails. (2) Protein-DNA interactions are fixed with 1% formaldehyde. (3) Chromatin is sheared by sonication to mono-, di- and tri-nucleosomes. (4) Specific antibodies against modified histone tails will bind the H4R3 methylated nucleosomes. (5) Antibodies bind to Protein

A beads. (6) Nucleosomes with methylated arginine residues are isolated by extensive washing and centrifugation of Protein A beads. (7) DNA is isolated (8) Isolated DNA fragments are cloned in a low background vector.

Figure 16. Fragment size distribution of sonicated DNA and cloned fragments (A) Average fragment size of the sonicated DNA. Lanes 1-3 show an increasing amount of purified sonicated DNA, while M refers to the molecular weight marker. (B) Cloned fragments are identified with vector-specific PCR using M13 primers. The product was analyzed by standard agarose gel electrophoresis (2% gel). Different lanes show different isolated clones and M refers to the molecular weight marker.

Figure 17. Distribution of different fragments after BLAST and BLAT analysis as described in the Results section. (A) 54 fragments from 111 analysed were of expected size (larger than 150 bp). (B) 48 of these 54 fragments were of human origin. (C) 26 human unique sequences were considered for BLAT analysis. (D) 14 hits are within 5 kb of known genes.

Figure 18. Genomic context of the identified H4R3 methylated site in the promoter of IL1α. Conserved transcription binding sites, and the cloned fragment are shown with arrays.

Figure 19. The effect of fixation time on the recovery of CD38 and LXRα response elements. (A) MonoMac 6 cells in control state or treated with 1 μM 9-cis retinoic acid for 12 hours were fixed with 1% formaldehyde for 10 and 15 minutes. Chromatin immunoprecipitation was performed with anti-RXR antibodies, and DNA was measured with TaqMan assays specific for CD38 and LXRα response elements. Values are the means of three parallel QPCR measurements. (B) MonoMac 6 cells in control state or treated with 1 μM 9-cis Retinoic Acid for 12 hours were fixed with 1% formaldehyde for 10 and 15 minutes. Chromatin immunoprecipitation was performed with anti-RAR antibodies and DNA measured with TaqMan assays specific for CD38 and LXRα response elements. Values are the means of three parallel QPCR measurements.

Figure 20. Chromatin immunoprecipitation of H4 acetylated nucleosomes and different transcription factors in MonoMac 6 cells. (A) MonoMac 6 cells in control state or treated with 1 μM LG268 and 1 μM Rosiglitazone for 12 hours were fixed with 1% formaldehyde for 15 minutes. Chromatin immunoprecipitation was performed with anti H4 acetylated specific antibodies and DNA measured with TaqMan assays specific for CD38 response elements. Values are the means of three parallel QPCR measurements. (B) MonoMac 6 cells in control state or treated with 1 μM 9 cis Retinoic Acid for 12 hours were fixed with 1% formaldehyde for 15 minutes. Chromatin immunoprecipitation was performed with anti H4 acetylated specific antibodies and DNA measured with TaqMan assays specific for CD38 response elements. Values are the means of three parallel QPCR measurements. (C) MonoMac 6 cells in control state or treated with 1 μM LG268 and 1 μM Rosiglitazone for 12 hours were fixed with 1% formaldehyde for 15 minutes. Chromatin immunoprecipitation was performed with anti-RXR, RAR and RNA Polymerase II specific antibodies and DNA was measured with TaqMan assays specific for CD38 response elements. Values are the means of three parallel QPCR measurements. (D) MonoMac 6 cells in control state or treated with 1 μM 9- cis retinoic acid for 12 hours were fixed with 1% formaldehyde for 15 minutes. Chromatin immunoprecipitation was performed with anti-RXR, RAR and Polymerase II specific antibodies and DNA was measured with TaqMan assays specific for CD38 response elements. Values are the means of three parallel QPCR measurements.

Figure 21. ChIP Western analyses of different PPARγ specific antibodies. ChIP Western was performed as described in Materials and Methods section. Blue arrow indicates the PPARγ immunoprecipitated with an anti-RXR antibody. Stars "*" indicate the presence of PPARγ specific band.

Figure 22. Amplification of DNA from Chromatin immunoprecipitation using the Farnham protocol. (A) Starting material copy numbers of TGM2 HR1 fragment in four different samples. (B) Copy numbers after the end-fill reaction, ligation reaction and DNA purification. (C) Copy numbers after performing the the first 25 cycle of PCR

amplification. (D) Copy numbers after the second run of 25 cycle of PCR amplification using as template an aliquot of the first PCR run.

Figure 23. Amplification of DNA from Chromatin immunoprecipitation using the De Risi protocol. After the first 25 cycles of PCR amplification we can see an amplification corresponding of two orders of magnitude (6 Ct) with a good representation of the starting material.

Figure 24. PPARγ ChIP on Chip performed as described in Materials and Methods on the 12K CpG array. (A.) A representative image from a scan. (B.) Hes1 levels in IDC treated with 1 □M Rosiglitazone for 6 or 12 hours. Values are from an Affymetrix global gene expression analysis. (C. and D) Location in the UCSC Genome Browser of the BLAT result is showing a conserved region near the Hes1 transcript. (E) A putative binding site with DR1 structure in the promoter of Hes1 identified by MacVector subsequence analysis.

Figure 25. ChIP on Chip analyses of changes in H4 acetylation levels after ligand treatment with PPARγ and PPARβ specific ligands for 24 hours of HT29 cell line. ChIP on Chip was performed as described in Materials and Methods on the 12K CpG array. (A.) Intensity distribution of the normalized intensity values of the spots. (B.) Venn diagram representation of fragments with an increase in H4 acetylation after ligand treatments. (C.) Venn diagram representation of fragments with a specific increase in H4 acetylation after ligand treatments with either PPARγ or PPARβ specific ligands.

Figure 26. QPCR analysis of two different marker genes in the monocyte and IDC sample pairs. ID1 and PPARγ were monitored using specific TaqMan assays. These samples were labeled for Affymetrix gene expression microarray analysis.

Figure 27. Monocyte IDC transition is producing a massive transcriptional change. (A) Gene tree of the genes with more than five fold change during the transition. (B)

Changing genes with more than five fold change during the transition are represented with normalized intensities on the Y axis.

Figure 28. Five clusters of genes identified during monocyte/IDC transition. Changing genes with more than five fold change during the transition are represented with normalized intensities on the Y axis.

Figure 29. Comparison of TaqMan and SYBR Green I real-time QPCR measurements with the same primer pairs and the same samples. (A.) Ampification plots of 4000, 2000, 1000, 400 copy number containing templates measured in triplicates with TaqMan assay for LXRα PPARRE. (B.) Ampification plots of 4000, 2000, 1000, 400 copy number containing templates measured in triplicates with SYBR Green I using primers specific for LXRα and PPARRE. (C.) Amplification plots from 300 000 copies to 3 copies and their double quantities as measured in triplicates with TaqMan assay for LXRα PPARRE.

Table 1. Real-time quantitative PCR oligo sets used in the presented experiments.

Table 2. Genes identified by cloning H4R3 methylated nucleosomes, their chromosomal locations, their position relative to the genes and the conserved transcription factor binding sites within 1 kb.

Table 3. PANTHER (Protein ANalysis THrough Evolutionary Relationships) analysis of the identified genes. Data described as “Molecular functions” and “Biological processes” are shown. One relevant reference is shown independently of PANTHER analysis

Table 4. Conserved transcription factor binding sites overrepresented in the regions identified by chromatin immunoprecipitation. The genomic context of 5 kb of all 26 identified immunoprecipitated fragments was analysed. 39 conserved TFBS were found, 12 of them beeing present more than one time. Here we present the 6 overrepresented TFBS with their corresponding transcription factors, according to the Biobase library and the number of their occurencies in the analyzed genomic locations.

9. REFERENCES

Agalioti, T., G. Chen, et al. (2002). "Deciphering the transcriptional histone acetylation code for a human gene." Cell **111**(3): 381-92.

Altschul, S. F., W. Gish, et al. (1990). "Basic local alignment search tool." J Mol Biol **215**(3): 403-10.

An, W., J. Kim, et al. (2004). "Ordered cooperative functions of PRMT1, p300, and CARM1 in transcriptional activation by p53." Cell **117**(6): 735-48.

Bakker, W. J., M. Blazquez-Domingo, et al. (2004). "FoxO3a regulates erythroid differentiation and induces BTG1, an activator of protein arginine methyl transferase 1." J Cell Biol **164**(2): 175-84.

Bannister, A. J., P. Zegerman, et al. (2001). "Selective recognition of methylated lysine 9 on histone H3 by the HP1 chromo domain." Nature **410**(6824): 120-4.

Bauer, U. M., S. Daujat, et al. (2002). "Methylation at arginine 17 of histone H3 is linked to gene activation." EMBO Rep **3**(1): 39-44.

Becker, M., C. Baumann, et al. (2002). "Dynamic behavior of transcription factors on a natural promoter in living cells." EMBO Rep **3**(12): 1188-94.

Beisson, J. and T. M. Sonneborn (1965). "Cytoplasmic Inheritance Of The Organization Of The Cell Cortex In Paramecium Aurelia." Proc Natl Acad Sci U S A **53**: 275-82.

Benko, S., J. D. Love, et al. (2003). "Molecular determinants of the balance between co-repressor and co-activator recruitment to the retinoic acid receptor." J Biol Chem **278**(44): 43797-806.

Bernstein, B. E., M. Kamal, et al. (2005). "Genomic maps and comparative analysis of histone modifications in human and mouse." Cell **120**(2): 169-81.

Boisvert, F. M., J. Cote, et al. (2003). "A Proteomic Analysis of Arginine-methylated Protein Complexes." Mol Cell Proteomics **2**(12): 1319-30.

Boisvert, F. M., U. Dery, et al. (2005). "Arginine methylation of MRE11 by PRMT1 is required for DNA damage checkpoint control." Genes Dev **19**(6): 671-6.

Bone, J. R., J. Lavender, et al. (1994). "Acetylated histone H4 on the male X chromosome is associated with dosage compensation in Drosophila." Genes Dev **8**(1): 96-104.

Bourguet, W., V. Vivat, et al. (2000). "Crystal structure of a heterodimeric complex of RAR and RXR ligand-binding domains." Mol Cell **5**(2): 289-98.

Brownawell, A. M. and I. G. Macara (2002). "Exportin-5, a novel karyopherin, mediates nuclear export of double-stranded RNA binding proteins." J Cell Biol **156**(1): 53-64.

Chai, X., W. Chen, et al. (2001). "Structure, promoter and chromosomal localization of rdh6." Gene **274**(1-2): 27-33.

Chang, A. Y., B. M. Wyse, et al. (1983). "Ciglitazone, a new hypoglycemic agent. II. Effect on glucose and lipid metabolisms and insulin binding in the adipose tissue of C57BL/6J-ob/ob and -+/? mice." Diabetes **32**(9): 839-45.

Chang, A. Y., B. M. Wyse, et al. (1983). "Ciglitazone, a new hypoglycemic agent. I. Studies in ob/ob and db/db mice, diabetic Chinese hamsters, and normal and streptozotocin-diabetic rats." Diabetes **32**(9): 830-8.

Chen, A., J. D. Licht, et al. (1994). "Retinoic acid is required for and potentiates differentiation of acute promyelocytic leukemia cells by nonretinoid agents." Blood **84**(7): 2122-9.

Chen, D., H. Ma, et al. (1999). "Regulation of transcription by a protein methyltransferase." Science **284**(5423): 2174-7.

Chen, S. L., K. A. Loffler, et al. (2002). "The coactivator-associated arginine methyltransferase is necessary for muscle differentiation: CARM1 coactivates myocyte enhancer factor-2." J Biol Chem **277**(6): 4324-33.

Chevillard-Briet, M., D. Trouche, et al. (2002). "Control of CBP co-activating activity by arginine methylation." Embo J **21**(20): 5457-66.

Chiocca, E. A., P. J. Davies, et al. (1988). "The molecular basis of retinoic acid action. Transcriptional regulation of tissue transglutaminase gene expression in macrophages." J Biol Chem **263**(23): 11584-9.

Chiocca, E. A., P. J. Davies, et al. (1989). "Regulation of tissue transglutaminase gene expression as a molecular model for retinoid effects on proliferation and differentiation." J Cell Biochem **39**(3): 293-304.

Collins, S. J., K. A. Robertson, et al. (1990). "Retinoic acid-induced granulocytic differentiation of HL-60 myeloid leukemia cells is mediated directly through the retinoic acid receptor (RAR-alpha)." Mol Cell Biol **10**(5): 2154-63.

Cosma, M. P. (2002). "Ordered recruitment: gene-specific mechanism of transcription activation." Mol Cell **10**(2): 227-36.

Cross, S. H., J. A. Charlton, et al. (1994). "Purification of CpG islands using a methylated DNA binding column." Nat Genet **6**(3): 236-44.

Cuthbert, G. L., S. Daujat, et al. (2004). "Histone deimination antagonizes arginine methylation." Cell **118**(5): 545-53.

Davies, P. J., J. P. Basilion, et al. (1988). "Retinoids as generalized regulators of cellular growth and differentiation." Am J Med Sci **296**(3): 164-70.

Davies, P. J., E. A. Chiocca, et al. (1988). "Transglutaminases and their regulation: implications for polyamine metabolism." Adv Exp Med Biol **250**: 391-401.

Davies, P. J., E. A. Chiocca, et al. (1988). "Retinoid--regulated expression of tissue transglutaminase in normal and leukemic myeloid cells." Adv Exp Med Biol **231**: 63-71.

Davies, P. J., M. P. Murtaugh, et al. (1985). "Retinoic acid-induced expression of tissue transglutaminase in human promyelocytic leukemia (HL-60) cells." J Biol Chem **260**(8): 5166-74.

Disa, S. G., A. Gupta, et al. (1986). "Site specificity of histone H4 methylation by wheat germ protein-arginine N-methyltransferase." Biochemistry **25**(9): 2443-8.

Dodge, J. E., Y. K. Kang, et al. (2004). "Histone H3-K9 methyltransferase ESET is essential for early development." Mol Cell Biol **24**(6): 2478-86.

Duprez, E., G. Benoit, et al. (2000). "A mutated PML/RARA found in the retinoid maturation resistant NB4 subclone, NB4-R2, blocks RARA and wild-type PML/RARA transcriptional activities." Leukemia **14**(2): 255-61.

Elgin, S. C. and S. I. Grewal (2003). "Heterochromatin: silence is golden." Curr Biol **13**(23): R895-8.

Escriva, H., F. Delaunay, et al. (2000). "Ligand binding and nuclear receptor evolution." Bioessays **22**(8): 717-27.

Fuks, F., P. J. Hurd, et al. (2003). "The methyl-CpG-binding protein MeCP2 links DNA methylation to histone methylation." J Biol Chem **278**(6): 4035-40.

Gallwitz, D. (1971). "Histone methylation. Partial purification of two histone-specific methyltransferases from rat thymus nuclei preferentially methylating histones F2a 1 and F3." Arch Biochem Biophys **145**(2): 650-7.

Gampe, R. T., Jr., V. G. Montana, et al. (2000). "Asymmetry in the PPARgamma/RXRalpha crystal structure reveals the molecular basis of heterodimerization among nuclear receptors." Mol Cell **5**(3): 545-55.

Gary, J. D., W. J. Lin, et al. (1996). "The predominant protein-arginine methyltransferase from Saccharomyces cerevisiae." J Biol Chem **271**(21): 12585-94.

Grewal, S. I. and S. C. Elgin (2002). "Heterochromatin: new possibilities for the inheritance of structure." Curr Opin Genet Dev **12**(2): 178-87.

Grewal, S. I. and D. Moazed (2003). "Heterochromatin and epigenetic control of gene expression." Science **301**(5634): 798-802.

Gwizdek, C., B. Ossareh-Nazari, et al. (2004). "Minihelix-containing RNAs mediate exportin-5-dependent nuclear export of the double-stranded RNA-binding protein ILF3." J Biol Chem **279**(2): 884-91.

Hagiwara, T., K. Nakashima, et al. (2002). "Deimination of arginine residues in nucleophosmin/B23 and histones in HL-60 granulocytes." Biochem Biophys Res Commun **290**(3): 979-83.

Hatzis, P. and I. Talianidis (2002). "Dynamics of enhancer-promoter communication during differentiation-induced gene activation." Mol Cell **10**(6): 1467-77.

Imhof, A. and P. B. Becker (2001). "Modifications of the histone N-terminal domains. Evidence for an "epigenetic code"?" Mol Biotechnol **17**(1): 1-13.

Impey, S., S. R. McCorkle, et al. (2004). "Defining the CREB regulon: a genome-wide analysis of transcription factor regulatory regions." Cell **119**(7): 1041-54.

Issemann, I. and S. Green (1990). "Activation of a member of the steroid hormone receptor superfamily by peroxisome proliferators." Nature **347**(6294): 645-50.

Jenuwein, T. (2001). "Re-SET-ting heterochromatin by histone methyltransferases." Trends Cell Biol **11**(6): 266-73.

Jenuwein, T. and C. D. Allis (2001). "Translating the histone code." Science **293**(5532): 1074-80.

Jones, P. L., G. J. Veenstra, et al. (1998). "Methylated DNA and MeCP2 recruit histone deacetylase to repress transcription." Nat Genet **19**(2): 187-91.

Kabuyama, Y., K. A. Resing, et al. (2004). "Applying proteomics to signaling networks." Curr Opin Genet Dev **14**(5): 492-8.

Kallen, J., J. M. Schlaeppi, et al. (2004). "Crystal structure of the human RORalpha Ligand binding domain in complex with cholesterol sulfate at 2.2 A." J Biol Chem **279**(14): 14033-8.

Kanno, T., Y. Kanno, et al. (2004). "Selective recognition of acetylated histones by bromodomain proteins visualized in living cells." Mol Cell **13**(1): 33-43.

Karolchik, D., R. Baertsch, et al. (2003). "The UCSC Genome Browser Database." Nucleic Acids Res **31**(1): 51-4.

Kent, W. J. (2002). "BLAT--the BLAST-like alignment tool." Genome Res **12**(4): 656-64.

Kishimoto, H., S. Hoshino, et al. (1998). "Molecular mechanism of human CD38 gene expression by retinoic acid. Identification of retinoic acid response element in the first intron." J Biol Chem **273**(25): 15429-34.

Kliewer, S. A., J. M. Lehmann, et al. (1999). "Orphan nuclear receptors: shifting endocrinology into reverse." Science **284**(5415): 757-60.

Koh, S. S., D. Chen, et al. (2001). "Synergistic enhancement of nuclear receptor function by p160 coactivators and two coactivators with protein methyltransferase activities." J Biol Chem **276**(2): 1089-98.

Kouzarides, T. (2002). "Histone methylation in transcriptional control." Curr Opin Genet Dev **12**(2): 198-209.

Kuo, M. H. and C. D. Allis (1999). "In vivo cross-linking and immunoprecipitation for studying dynamic Protein:DNA associations in a chromatin environment." Methods **19**(3): 425-33.

Kwak, Y. T., J. Guo, et al. (2003). "Methylation of SPT5 regulates its interaction with RNA polymerase II and transcriptional elongation properties." Mol Cell **11**(4): 1055-66.

Lachner, M. and T. Jenuwein (2002). "The many faces of histone lysine methylation." Curr Opin Cell Biol **14**(3): 286-98.

Lachner, M., D. O'Carroll, et al. (2001). "Methylation of histone H3 lysine 9 creates a binding site for HP1 proteins." Nature **410**(6824): 116-20.

Lacoste, N., R. T. Utley, et al. (2002). "Disruptor of telomeric silencing-1 is a chromatin-specific histone H3 methyltransferase." J Biol Chem **277**(34): 30421-4.

Laffitte, B. A. and P. Tontonoz (2002). "Orphan nuclear receptors find a home in the arterial wall." Curr Atheroscler Rep **4**(3): 213-21.

Lee, J. and M. T. Bedford (2002). "PABP1 identified as an arginine methyltransferase substrate using high-density protein arrays." EMBO Rep **3**(3): 268-73.

Lee, Y. H., S. A. Coonrod, et al. (2005). "Regulation of coactivator complex assembly and function by protein arginine methylation and demethylimination." Proc Natl Acad Sci U S A.

Li, J., Q. Lin, et al. (2002). "Involvement of histone methylation and phosphorylation in regulation of transcription by thyroid hormone receptor." Mol Cell Biol **22**(16): 5688-97.

Libby, P. R. (1968). "Histone acetylation by cell-free preparations from rat uterus: in vitro stimulation by estradiol-17 beta." Biochem Biophys Res Commun **31**(1): 59-65.

Liu, Y., X. S. Liu, et al. (2004). "Eukaryotic regulatory element conservation analysis and identification using comparative genomics." Genome Res **14**(3): 451-8.

Lord, P. C., L. M. Wilmoth, et al. (1991). "Expression of interleukin-1 alpha and beta genes by human blood polymorphonuclear leukocytes." J Clin Invest **87**(4): 1312-21.

Ma, H., C. T. Baumann, et al. (2001). "Hormone-dependent, CARM1-directed, arginine-specific methylation of histone H3 on a steroid-regulated promoter." Curr Biol **11**(24): 1981-5.

Marmorstein, R. (2001). "Protein modules that manipulate histone tails for chromatin regulation." Nat Rev Mol Cell Biol **2**(6): 422-32.

Matys, V., E. Fricke, et al. (2003). "TRANSFAC: transcriptional regulation, from patterns to profiles." Nucleic Acids Res **31**(1): 374-8.

McArthur, M., S. Gerum, et al. (2001). "Quantification of DNaseI-sensitivity by real-time PCR: quantitative analysis of DNaseI-hypersensitivity of the mouse beta-globin LCR." J Mol Biol **313**(1): 27-34.

McBride, A. E. and P. A. Silver (2001). "State of the arg: protein methylation at arginine comes of age." Cell **106**(1): 5-8.

Metivier, R., G. Penot, et al. (2003). "Estrogen receptor-alpha directs ordered, cyclical, and combinatorial recruitment of cofactors on a natural target promoter." Cell **115**(6): 751-63.

Metzger, E., M. Wissmann, et al. (2005). "LSD1 demethylates repressive histone marks to promote androgen-receptor-dependent transcription." Nature **437**(7057): 436-9.

Mi, H., B. Lazareva-Ulitsky, et al. (2005). "The PANTHER database of protein families, subfamilies, functions and pathways." Nucleic Acids Res **33 Database Issue**: D284-8.

Moreira, C., M. H. Tsuhako, et al. (2004). "Arginine metabolism during macrophage autocrine activation and infection with mouse hepatitis virus 3." Immunobiology **209**(8): 585-98.

Mowen, K. A., J. Tang, et al. (2001). "Arginine methylation of STAT1 modulates IFNalpha/beta-induced transcription." Cell **104**(5): 731-41.

Nagy, L., H. Y. Kao, et al. (1997). "Nuclear receptor repression mediated by a complex containing SMRT, mSin3A, and histone deacetylase." Cell **89**(3): 373-80.

Nagy, L., M. Saydak, et al. (1996). "Identification and characterization of a versatile retinoid response element (retinoic acid receptor response element-retinoid X receptor response element) in the mouse tissue transglutaminase gene promoter." J Biol Chem **271**(8): 4355-65.

Nagy, L. and J. W. Schwabe (2004). "Mechanism of the nuclear receptor molecular switch." Trends Biochem Sci **29**(6): 317-24.

Najbauer, J., B. A. Johnson, et al. (1993). "Peptides with sequences similar to glycine, arginine-rich motifs in proteins interacting with RNA are efficiently recognized by methyltransferase(s) modifying arginine in numerous proteins." J Biol Chem **268**(14): 10501-9.

Nakashima, K., T. Hagiwara, et al. (1999). "Molecular characterization of peptidylarginine deiminase in HL-60 cells induced by retinoic acid and 1alpha,25-dihydroxyvitamin D(3)." J Biol Chem **274**(39): 27786-92.

Nan, X., P. Tate, et al. (1996). "DNA methylation specifies chromosomal localization of MeCP2." Mol Cell Biol **16**(1): 414-21.

Ng, H. H., Q. Feng, et al. (2002). "Lysine methylation within the globular domain of histone H3 by Dot1 is important for telomeric silencing and Sir protein association." Genes Dev **16**(12): 1518-27.

Nielsen, P. R., D. Nietlispach, et al. (2002). "Structure of the HP1 chromodomain bound to histone H3 methylated at lysine 9." Nature **416**(6876): 103-7.

Odom, D. T., N. Zizlsperger, et al. (2004). "Control of pancreas and liver gene expression by HNF transcription factors." Science **303**(5662): 1378-81.

Okamoto, I., A. P. Otte, et al. (2004). "Epigenetic dynamics of imprinted X inactivation during early mouse development." Science **303**(5658): 644-9.

Orlando, V. (2000). "Mapping chromosomal proteins in vivo by formaldehyde-crosslinked-chromatin immunoprecipitation." Trends Biochem Sci **25**(3): 99-104.

Orphanides, G. and D. Reinberg (2002). "A unified theory of gene expression." Cell **108**(4): 439-51.

Pawlak, M. R., C. A. Scherer, et al. (2000). "Arginine N-methyltransferase 1 is required for early postimplantation mouse development, but cells deficient in the enzyme are viable." Mol Cell Biol **20**(13): 4859-69.

Pawson, T. and P. Nash (2000). "Protein-protein interactions define specificity in signal transduction." Genes Dev **14**(9): 1027-47.

Peters, A. H., D. O'Carroll, et al. (2001). "Loss of the Suv39h histone methyltransferases impairs mammalian heterochromatin and genome stability." Cell **107**(3): 323-37.

Pogo, B. G., V. G. Allfrey, et al. (1966). "RNA synthesis and histone acetylation during the course of gene activation in lymphocytes." Proc Natl Acad Sci U S A **55**(4): 805-12.

Pogo, B. G., A. O. Pogo, et al. (1968). "Changing patterns of histone acetylation and RNA synthesis in regeneration of the liver." Proc Natl Acad Sci U S A **59**(4): 1337-44.

Ponton, A., J. P. Thirion, et al. (1996). "Changes in chromatin conformation regulate the 5-lipoxygenase gene expression during differentiation of HL60 cells." Prostaglandins Leukot Essent Fatty Acids **55**(3): 139-43.

Qi, C., J. Chang, et al. (2002). "Identification of protein arginine methyltransferase 2 as a coactivator for estrogen receptor alpha." J Biol Chem **277**(32): 28624-30.

Rezai-Zadeh, N., X. Zhang, et al. (2003). "Targeted recruitment of a histone H4-specific methyltransferase by the transcription factor YY1." Genes Dev **17**(8): 1019-29.

Rice, J. C. and C. D. Allis (2001). "Code of silence." Nature **414**(6861): 258-61.

Rice, J. C., S. D. Briggs, et al. (2003). "Histone methyltransferases direct different degrees of methylation to define distinct chromatin domains." Mol Cell **12**(6): 1591-8.

Santos-Rosa, H., R. Schneider, et al. (2002). "Active genes are tri-methylated at K4 of histone H3." Nature **419**(6905): 407-11.

Schneider, R., A. J. Bannister, et al. (2004). "Histone H3 lysine 4 methylation patterns in higher eukaryotic genes." Nat Cell Biol **6**(1): 73-7.

Schurter, B. T., S. S. Koh, et al. (2001). "Methylation of histone H3 by coactivator-associated arginine methyltransferase 1." Biochemistry **40**(19): 5747-56.

Scott, H. S., S. E. Antonarakis, et al. (1998). "Identification and characterization of two putative human arginine methyltransferases (HRMT1L1 and HRMT1L2)." Genomics **48**(3): 330-40.

Shi, Y., F. Lan, et al. (2004). "Histone demethylation mediated by the nuclear amine oxidase homolog LSD1." Cell **119**(7): 941-53.

Shim, J., H. Lim, et al. (2002). "Nuclear export of NF90 is required for interleukin-2 mRNA stabilization." Mol Cell **10**(6): 1331-44.

Smith, E. R., C. D. Allis, et al. (2001). "Linking global histone acetylation to the transcription enhancement of X-chromosomal genes in Drosophila males." J Biol Chem **276**(34): 31483-6.

Strahl, B. D. and C. D. Allis (2000). "The language of covalent histone modifications." Nature **403**(6765): 41-5.

Strahl, B. D., S. D. Briggs, et al. (2001). "Methylation of histone H4 at arginine 3 occurs in vivo and is mediated by the nuclear receptor coactivator PRMT1." Curr Biol **11**(12): 996-1000.

Szanto, A., S. Benko, et al. (2004). "Transcriptional regulation of human CYP27 integrates retinoid, peroxisome proliferator-activated receptor, and liver X receptor signaling in macrophages." Mol Cell Biol **24**(18): 8154-66.

Tachibana, M., K. Sugimoto, et al. (2002). "G9a histone methyltransferase plays a dominant role in euchromatic histone H3 lysine 9 methylation and is essential for early embryogenesis." Genes Dev **16**(14): 1779-91.

Tachibana, M., J. Ueda, et al. (2005). "Histone methyltransferases G9a and GLP form heteromeric complexes and are both crucial for methylation of euchromatin at H3-K9." Genes Dev **19**(7): 815-26.

Tang, J., A. Frankel, et al. (2000). "PRMT1 is the predominant type I protein arginine methyltransferase in mammalian cells." J Biol Chem **275**(11): 7723-30.

Tang, J., P. N. Kao, et al. (2000). "Protein-arginine methyltransferase I, the predominant protein-arginine methyltransferase in cells, interacts with and is regulated by interleukin enhancer-binding factor 3." J Biol Chem **275**(26): 19866-76.

Thomas, P. D., M. J. Campbell, et al. (2003). "PANTHER: a library of protein families and subfamilies indexed by function." Genome Res **13**(9): 2129-41.

Thompson, P. D., J. C. Hsieh, et al. (1999). "Vitamin D receptor displays DNA binding and transactivation as a heterodimer with the retinoid X receptor, but not with the thyroid hormone receptor." J Cell Biochem **75**(3): 462-80.

Tontonoz, P., L. Nagy, et al. (1998). "PPARgamma promotes monocyte/macrophage differentiation and uptake of oxidized LDL." Cell **93**(2): 241-52.

Turner, B. M. (2000). "Histone acetylation and an epigenetic code." Bioessays **22**(9): 836-45.

Turner, B. M. (2002). "Cellular memory and the histone code." Cell **111**(3): 285-91.

Turner, B. M., A. J. Birley, et al. (1992). "Histone H4 isoforms acetylated at specific lysine residues define individual chromosomes and chromatin domains in Drosophila polytene nuclei." Cell **69**(2): 375-84.

van Leeuwen, F., P. R. Gafken, et al. (2002). "Dot1p modulates silencing in yeast by methylation of the nucleosome core." Cell **109**(6): 745-56.

Vannier, E. and C. A. Dinarello (1993). "Histamine enhances interleukin (IL)-1-induced IL-1 gene expression and protein synthesis via H2 receptors in peripheral blood mononuclear cells. Comparison with IL-1 receptor antagonist." J Clin Invest **92**(1): 281-7.

Wada, K., K. Inoue, et al. (2002). "Identification of methylated proteins by protein arginine N-methyltransferase 1, PRMT1, with a new expression cloning strategy." Biochim Biophys Acta **1591**(1-3): 1-10.

Wakefield, R. I., B. O. Smith, et al. (1999). "The solution structure of the domain from MeCP2 that binds to methylated DNA." J Mol Biol **291**(5): 1055-65.

Wang, H., R. Cao, et al. (2001). "Purification and functional characterization of a histone H3-lysine 4-specific methyltransferase." Mol Cell **8**(6): 1207-17.

Wang, H., Z. Q. Huang, et al. (2001). "Methylation of histone H4 at arginine 3 facilitating transcriptional activation by nuclear hormone receptor." Science **293**(5531): 853-7.

Wang, Y., J. Wysocka, et al. (2004). "Human PAD4 regulates histone arginine methylation levels via demethylimination." Science **306**(5694): 279-83.

Wang, Z., G. Benoit, et al. (2003). "Structure and function of Nurr1 identifies a class of ligand-independent nuclear receptors." Nature **423**(6939): 555-60.

Watkins, R. E., G. B. Wisely, et al. (2001). "The human nuclear xenobiotic receptor PXR: structural determinants of directed promiscuity." Science **292**(5525): 2329-33.

Watts, G. F. and S. B. Dimmitt (1999). "Fibrates, dyslipoproteinaemia and cardiovascular disease." Curr Opin Lipidol **10**(6): 561-74.

Weinmann, A. S., S. M. Bartley, et al. (2001). "Use of chromatin immunoprecipitation to clone novel E2F target promoters." Mol Cell Biol **21**(20): 6820-32.

Weinmann, A. S., P. S. Yan, et al. (2002). "Isolating human transcription factor targets by coupling chromatin immunoprecipitation and CpG island microarray analysis." Genes Dev **16**(2): 235-44.

Willson, T. M. (2002). "RORalpha: an orphan nuclear receptor on a high-cholesterol diet." Structure (Camb) **10**(12): 1605-6.

Wu, R., A. V. Terry, et al. (2005). "Differential subnuclear localization and replication timing of histone H3 lysine 9 methylation states." Mol Biol Cell **16**(6): 2872-81.

Xu, H. E., M. H. Lambert, et al. (1999). "Molecular recognition of fatty acids by peroxisome proliferator-activated receptors." Mol Cell **3**(3): 397-403.

Xu, W., H. Chen, et al. (2001). "A transcriptional switch mediated by cofactor methylation." Science **294**(5551): 2507-11.

Yanagida, M., T. Hayano, et al. (2004). "Human fibrillarin forms a sub-complex with splicing factor 2-associated p32, protein arginine methyltransferases, and tubulins alpha 3 and beta 1 that is independent of its association with preribosomal ribonucleoprotein complexes." J Biol Chem **279**(3): 1607-14.

Yen, A. (1985). "Control of HL-60 myeloid differentiation. Evidence of uncoupled growth and differentiation control, S-phase specificity, and two-step regulation." Exp Cell Res **156**(1): 198-212.

Yen, A., D. Brown, et al. (1987). "Precommitment states induced during HL-60 myeloid differentiation: possible similarities of retinoic acid- and DMSO-induced early events." Exp Cell Res **173**(1): 80-4.

Yen, A., M. Forbes, et al. (1987). "Control of HL-60 cell differentiation lineage specificity, a late event occurring after precommitment." Cancer Res **47**(1): 129-34.

Yen, A. and R. Sturgill (1998). "Hypophosphorylation of the RB protein in S and G2 as well as G1 during growth arrest." Exp Cell Res **241**(2): 324-31.

Zhang, X., D. T. Odom, et al. (2005). "Genome-wide analysis of cAMP-response element binding protein occupancy, phosphorylation, and target gene activation in human tissues." Proc Natl Acad Sci U S A **102**(12): 4459-64.

This thesis is built on the following publications:

Balint BL, Szanto A, Madi A, Bauer UM, Gabor P, Benko S, Puskas LG, Davies PJ, Nagy L.
Arginine methylation provides epigenetic transcription memory for retinoid-induced differentiation in myeloid cells.
Mol Cell Biol. 2005 Jul;25(13):5648-63.
IF: 8.142

Balint BL, Gabor P, Nagy L,
Genome-wide localization of histone 4 arginine 3 methylation
in a differentiation primed myeloid leukemia cell line
Immunobiology 2005 Aug 210 (2005) 141–152
IF: 1.773

Other publications:

Szanto A, Benko S, Szatmari I, Balint LB, Furtos I, Rühl R, Molnar C, Csiba L, Garuti R, Calandra S, Larsson H, Diczfalusy U, Nagy L: Transcriptional regulation of human CYP27 integrates retinoid, PPAR and LXR signaling in macrophages. Mol. Cell. Biol. (2004) 24: 8154-8166
IF: 8.142

Balint BL, Nagy L,
Selective modulators of PPAR activity as new therapeutic tools in metabolic

diseases
Current Drug Targets (accepted for publication on 28.04.2005.)
IF: 3.77

Lóránt Székvölgyi, Bálint L Bálint, László Imre, Katalin Goda, Miklós Szabó and Gábor Szabó,
ChIP-on-beads: a robust flow-cytometric method for the evaluation of chromatin immunoprecipitation results (Submitted for publication)

Balint LB, Nagy L: Genome wide location analysis of nuclear receptors
Abstract published in: The FEBS Journal vol 271 Suppl 1 July 2005
Abstract number K3-012

Posters:
First author of posters on the following meetings:

* IMP Spring Conference, Vienna, "Epigenetic Programming of the Genome" 2002 May: Epigenetic regulation of Tissue Transglutaminase Type 2,

* Meeting of the Hungarian Biochemical Society/ Keszthely, Hungary 2002 may: Egy retinoid indukálta gén epigenetikus szabályozása

* EMBO Conference on Nuclear Receptors, Villefranche sur Mer 2003 June: Epigenetic Regulation of Hormone Response

* EMBO Practical Course Naples: Deciphering Chromosomes by Chromatin

Immunoprecipitation 2003 september: In vivo Genomic Localization of Nuclear receptors

* Semmelweis Symposium: New Trends in Medical Genomics, Budapest, 2003 October: Epigenetic Regulation of Hormonal Response

*6-th Transcription Meeting, Heidelberg, EMBL 2004 September: Analysis of epigenetic determinants of hormonal in a Whole Genome approach

And: Arginine Methylation provides Epigenetic Transcription Memory for Differentiating Myeloid Cells

* EMBO-HHMI Joint Meeting Budapest 2004 December: Genome-wide Location Analysis of Nuclear Receptors

* Keystone Symposia PPAR/LXR Meeting, Vancouver, Canada, 2005 April: Genome-wide Location Analysis of Nuclear Receptors

* 30-th FEBS Congress, Budapest, Hungary, 2005 July: Genome-wide Location Analysis of Nuclear Receptors

* EMBO Symposium on Nuclear Receptors, Lake Garda, Italy, 2005 September: Lipid Sensors that Modify the Genome

Co-author:

*Meeting of the Hungarian Society for Cell Biology/ Eger, Hungary 2005 april (Co-author of poster with Lorant Szekvolgyi: DNS-fehérje interakciók az MLL-gén töréspont klaszter régiójában)

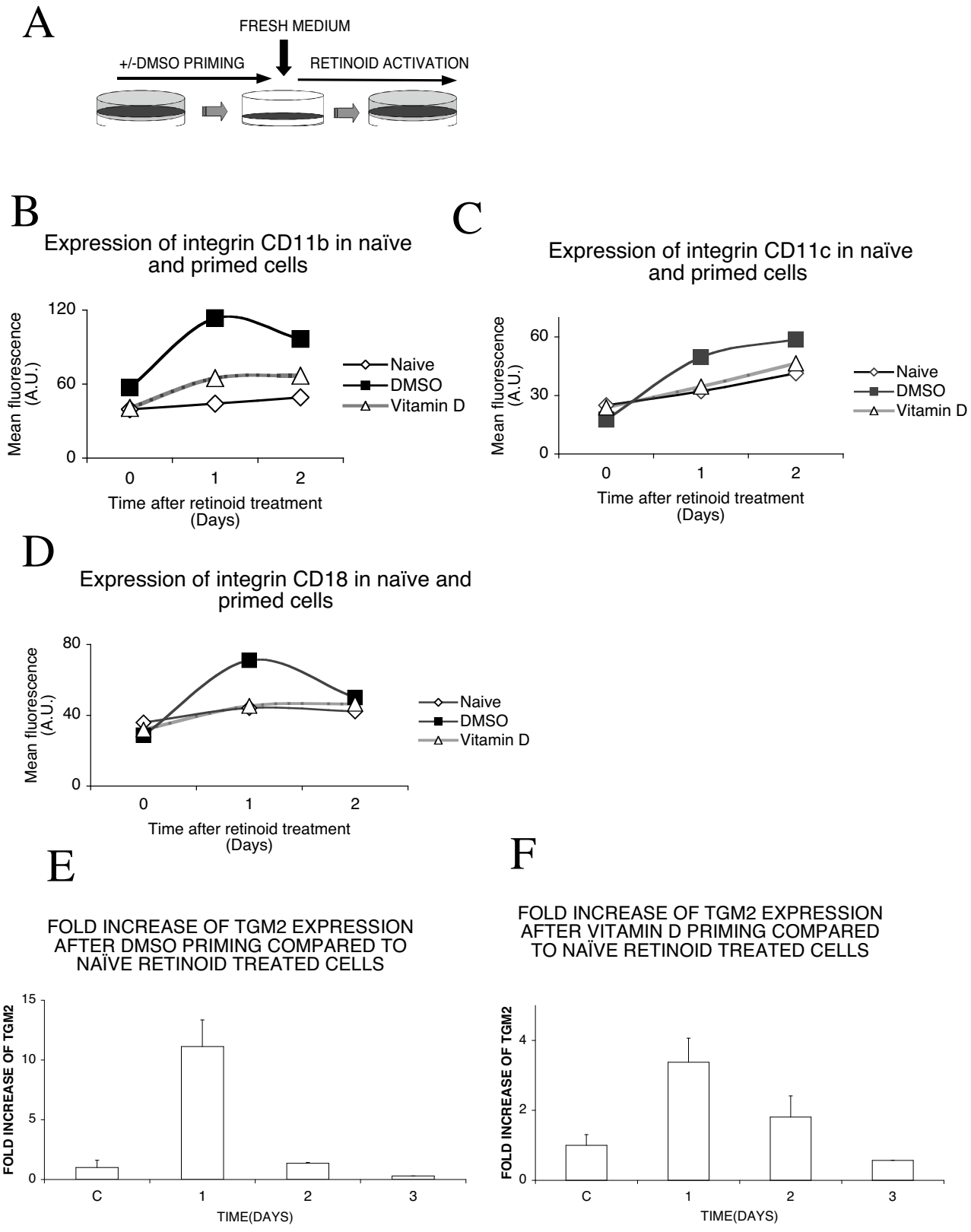
A
FRESH MEDIUM
+/-DMSO PRIMING
RETINOID ACTIVATION
B
Expression of integrin CD11b in naïve and primed cells
Mean fluorescence (A.U.)
120
60
0
0
1
2
Time after retinoid treatment (Days)
Naive
DMSO
Vitamin D
C
Expression of integrin CD11c in naïve and primed cells
Mean fluorescence (A.U.)
60
30
0
0
1
2
Time after retinoid treatment (Days)
Naive
DMSO
Vitamin D
D
Expression of integrin CD18 in naïve and primed cells
Mean fluorescence (A.U.)
80
40
0
0
1
2
Time after retinoid treatment (Days)
Naive
DMSO
Vitamin D
E
FOLD INCREASE OF TGM2 EXPRESSION AFTER DMSO PRIMING COMPARED TO NAÏVE RETINOID TREATED CELLS
FOLD INCREASE OF TGM2
15
10
5
0
C
1
2
3
TIME(DAYS)
F
FOLD INCREASE OF TGM2 EXPRESSION AFTER VITAMIN D PRIMING COMPARED TO NAÏVE RETINOID TREATED CELLS
FOLD INCREASE OF TGM2
4
2
0
C
1
2
3
TIME(DAYS)

Fig. 1

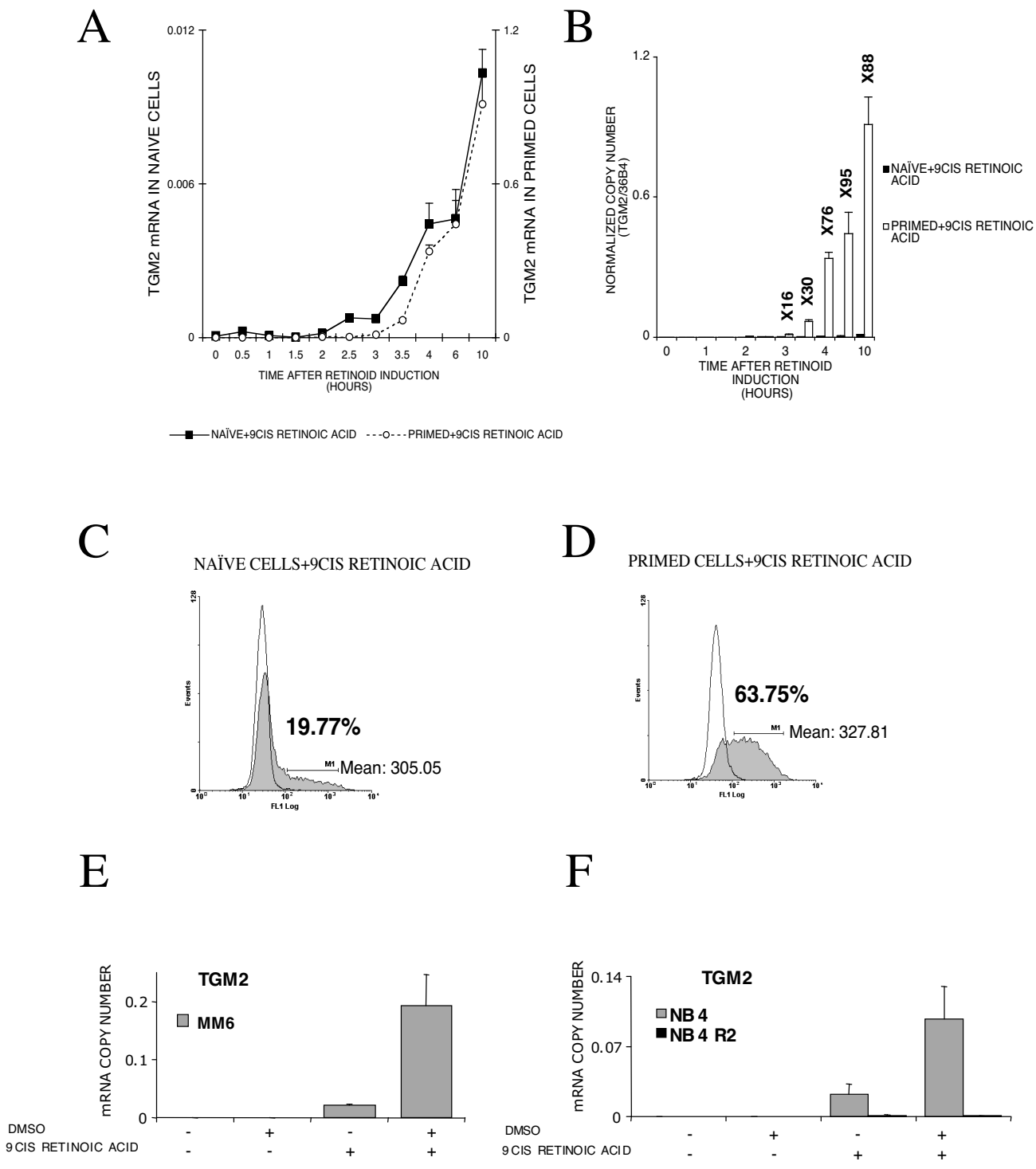
A
TGM2 mRNA IN NAIVE CELLS
TGM2 mRNA IN PRIMED CELLS
TIME AFTER RETINOID INDUCTION (HOURS)
NAÏVE+9CIS RETINOIC ACID
PRIMED+9CIS RETINOIC ACID
B
NORMALIZED COPY NUMBER (TGM2/36B4)
X16
X30
X76
X95
X88
TIME AFTER RETINOID INDUCTION (HOURS)
NAÏVE+9CIS RETINOIC ACID
PRIMED+9CIS RETINOIC ACID
C
NAÏVE CELLS+9CIS RETINOIC ACID
19.77%
Mean: 305.05
FL1 Log
D
PRIMED CELLS+9CIS RETINOIC ACID
63.75%
Mean: 327.81
FL1 Log
E
TGM2
MM6
mRNA COPY NUMBER
DMSO
9CIS RETINOIC ACID
F
TGM2
NB4
NB4 R2
mRNA COPY NUMBER
DMSO
9CIS RETINOIC ACID

Fig. 2

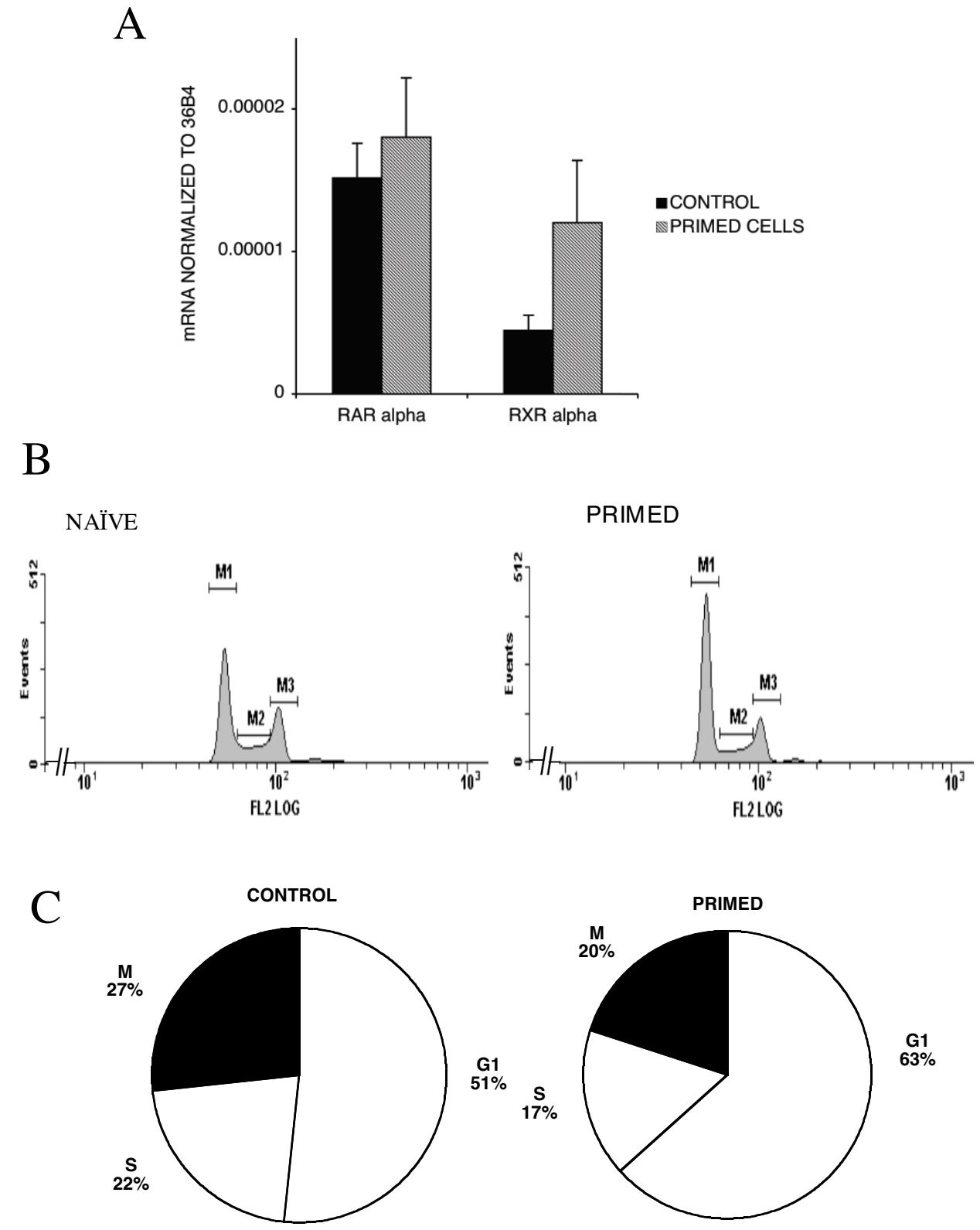
A
mRNA NORMALIZED TO 36B4
0.00002
0.00001
0
CONTROL
PRIMED CELLS
RAR alpha
RXR alpha
B
NAÏVE
PRIMED
Events
512
0
M1
M2
M3
10^1
10^2
10^3
FL2 LOG
C
CONTROL
M
27%
G1
51%
S
22%
PRIMED
M
20%
G1
63%
S
17%

Fig. 3

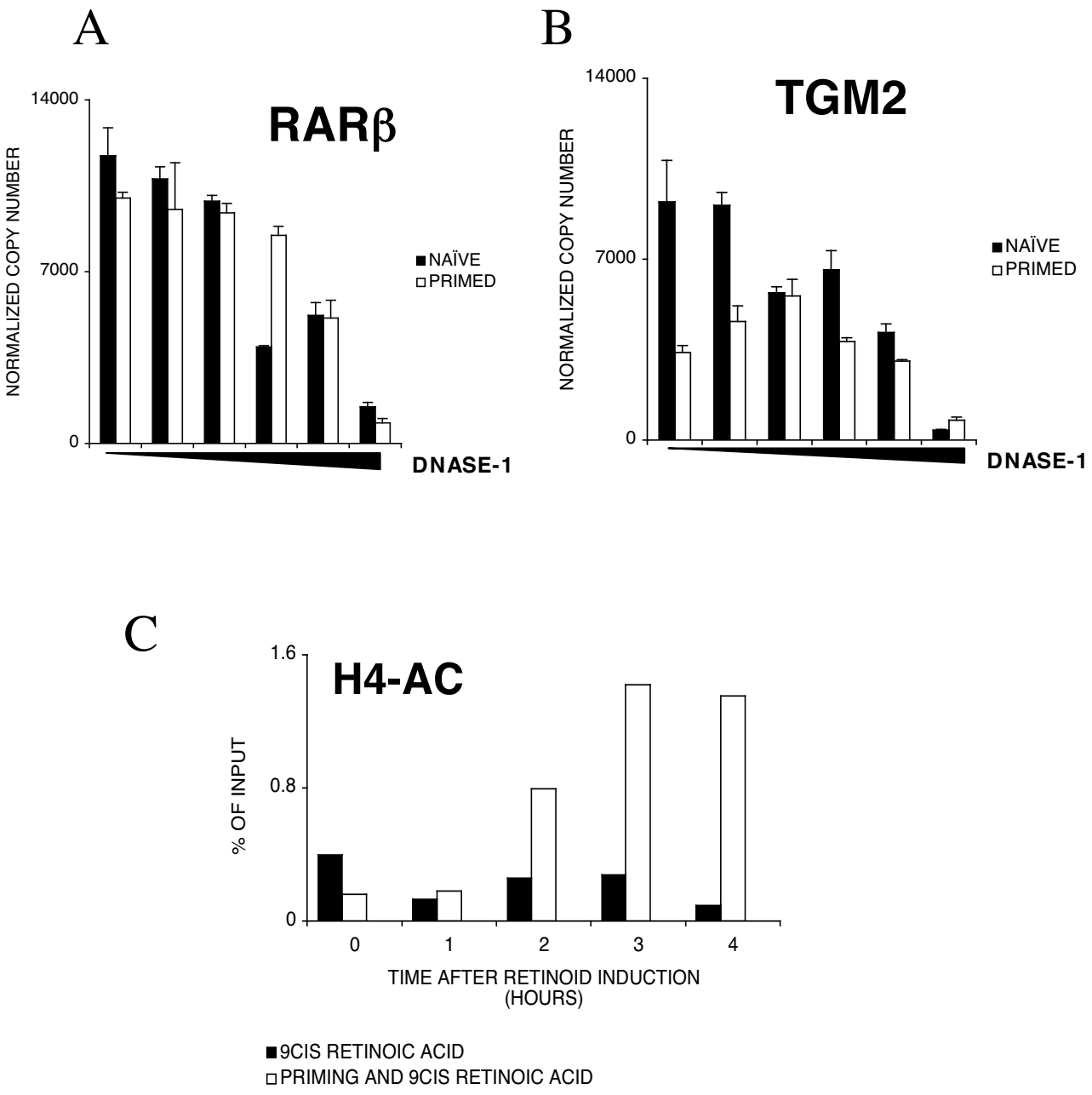
A
RARβ
14000
7000
0
NORMALIZED COPY NUMBER
NAÏVE
PRIMED
DNASE-1
B
TGM2
14000
7000
0
NORMALIZED COPY NUMBER
NAÏVE
PRIMED
DNASE-1
C
H4-AC
1.6
0.8
0
% OF INPUT
0
1
2
3
4
TIME AFTER RETINOID INDUCTION
(HOURS)
9CIS RETINOIC ACID
PRIMING AND 9CIS RETINOIC ACID

Fig. 4

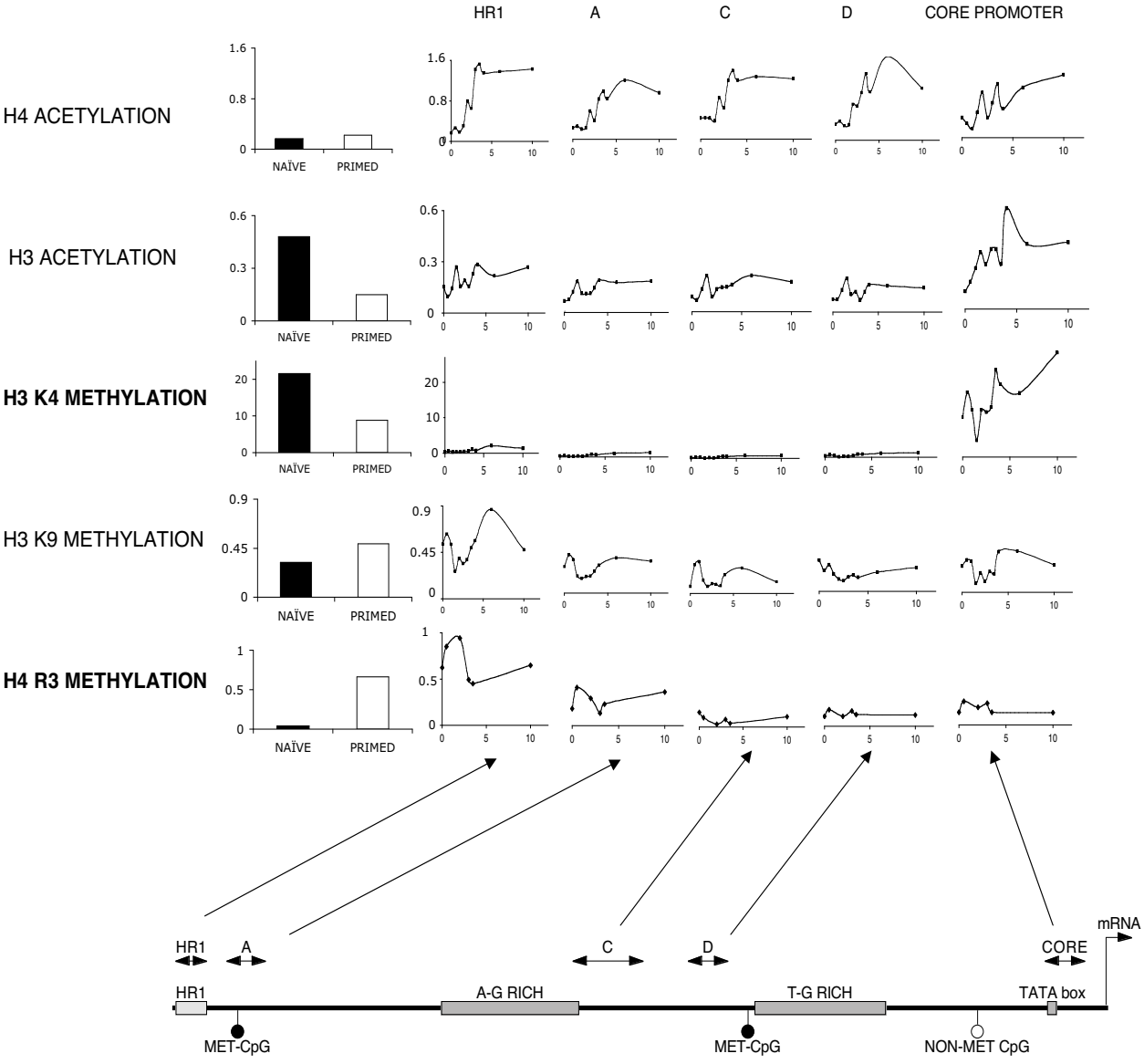
HR1
A
C
D
CORE PROMOTER
H4 ACETYLATION
H3 ACETYLATION
H3 K4 METHYLATION
H3 K9 METHYLATION
H4 R3 METHYLATION
NAÏVE
PRIMED
HR1
A
C
D
CORE
mRNA
HR1
A-G RICH
T-G RICH
TATA box
MET-CpG
MET-CpG
NON-MET CpG

Fig. 5

A

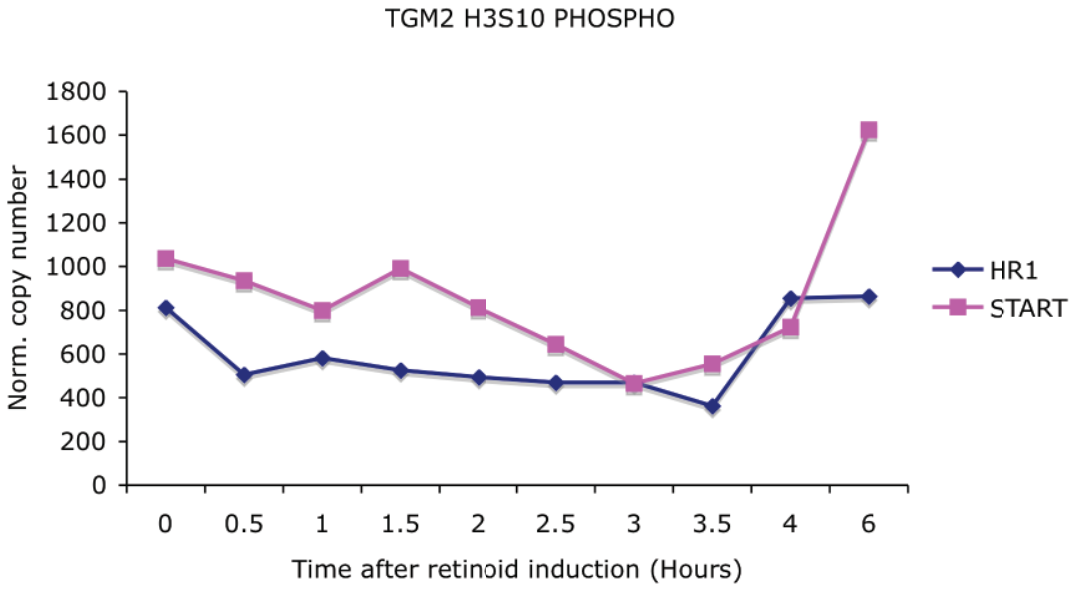
TGM2 H3S10 PHOSPHO
Norm. copy number
1800
1600
1400
1200
1000
800
600
400
200
0
0
0.5
1
1.5
2
2.5
3
3.5
4
6
Time after retinoid induction (Hours)
HR1
START

B

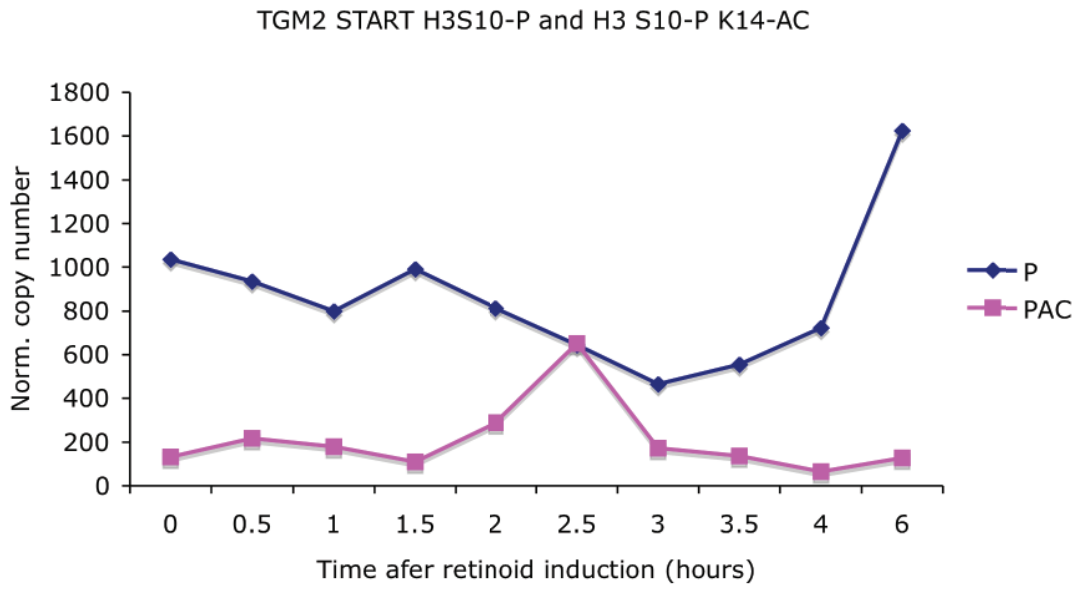
TGM2 START H3S10-P and H3 S10-P K14-AC
Norm. copy number
1800
1600
1400
1200
1000
800
600
400
200
0
0
0.5
1
1.5
2
2.5
3
3.5
4
6
Time afer retinoid induction (hours)
P
PAC

Fig. 6

A

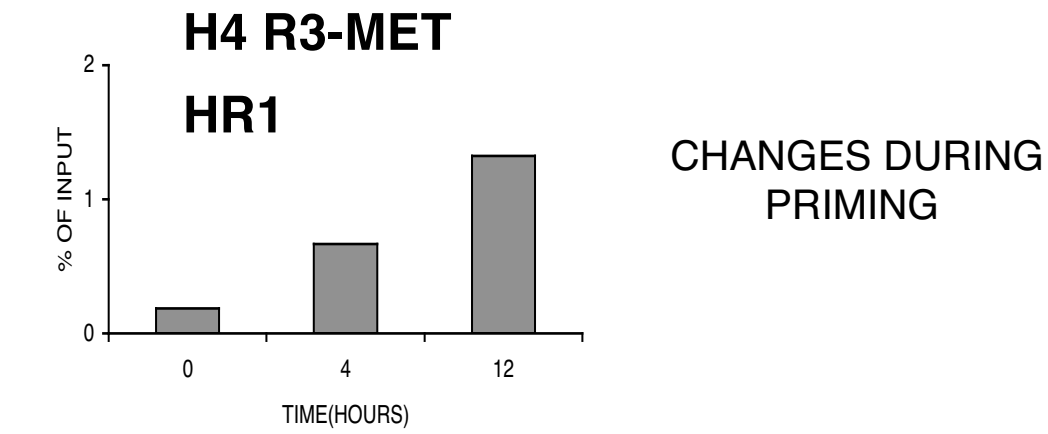
H4 R3-MET
HR1
% OF INPUT
2
1
0
0
4
12
TIME(HOURS)
CHANGES DURING
PRIMING

B

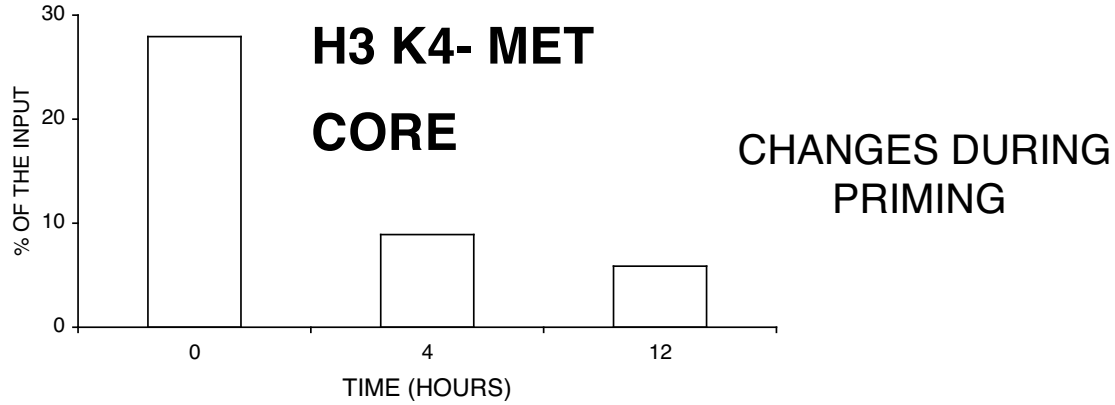
H3 K4- MET
CORE
% OF THE INPUT
30
20
10
0
0
4
12
TIME (HOURS)
CHANGES DURING
PRIMING

Fig. 7

A

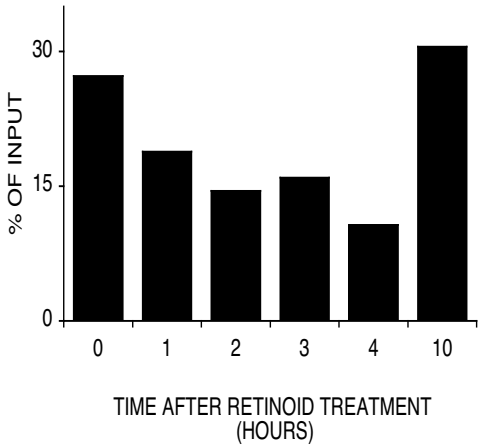

H3 K4-DI MET
IN NAÏVE CELLS

B

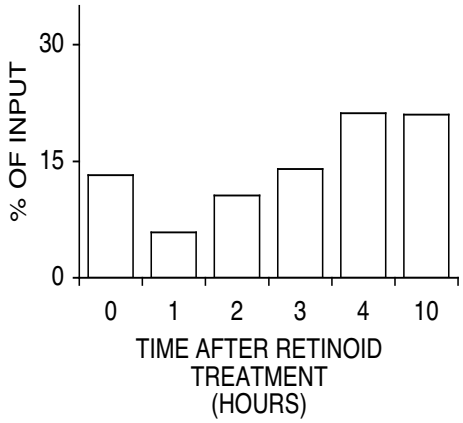

H3 K4-DI MET
IN PRIMED CELLS

C

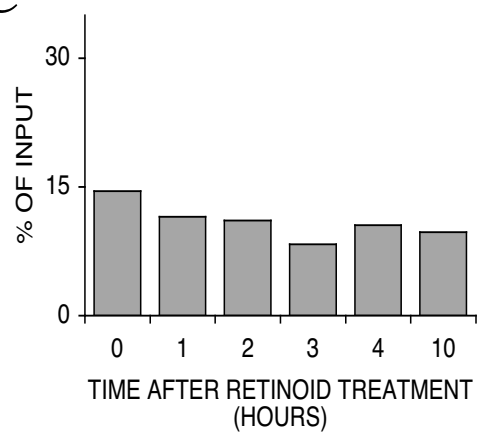

H3 K4-DI MET IN PRIMED
METHYLATION MUTE
CELLS

Fig. 8

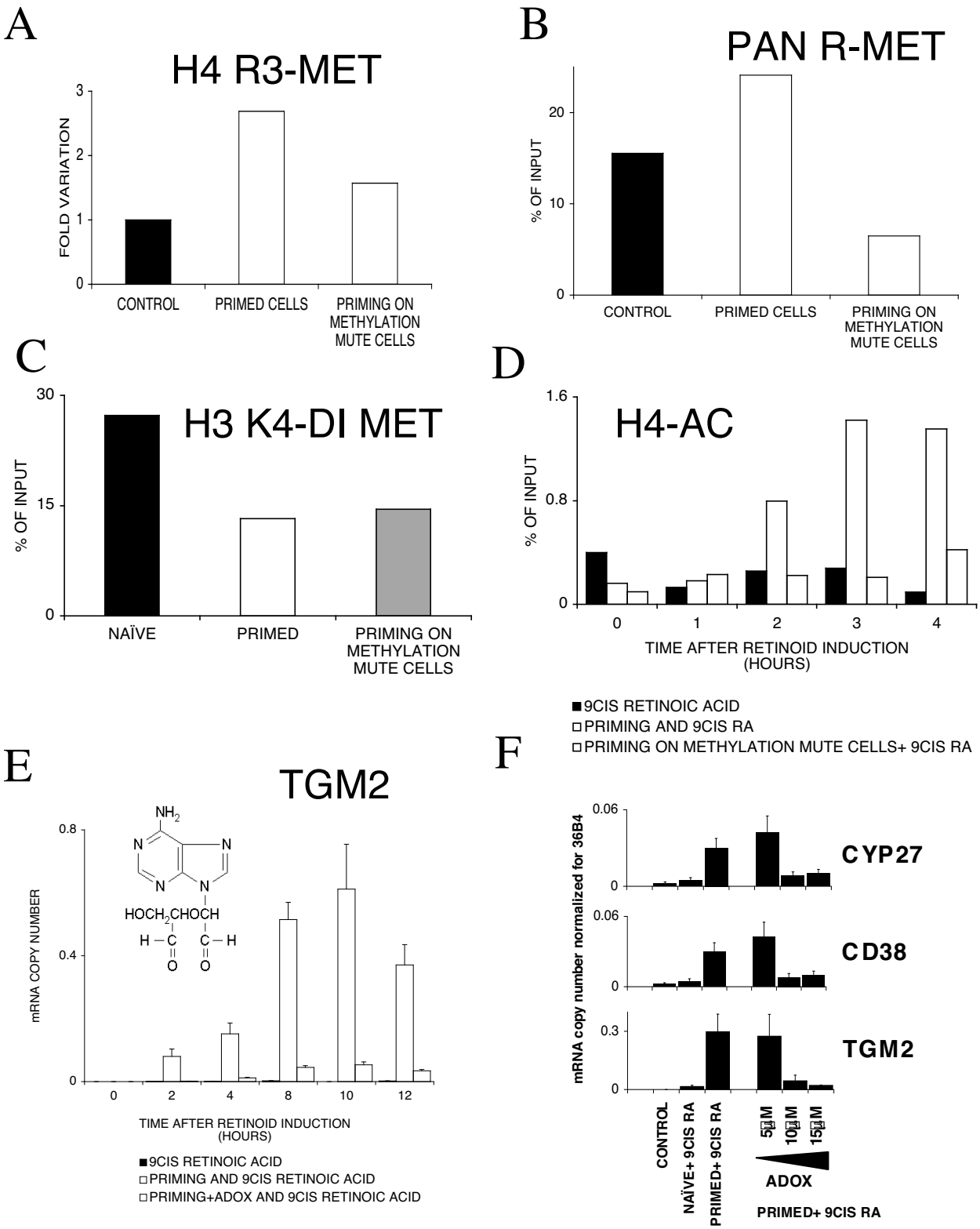
A
H4 R3-MET
FOLD VARIATION
CONTROL
PRIMED CELLS
PRIMING ON METHYLATION MUTE CELLS
B
PAN R-MET
% OF INPUT
CONTROL
PRIMED CELLS
PRIMING ON METHYLATION MUTE CELLS
C
H3 K4-DI MET
% OF INPUT
NAÏVE
PRIMED
PRIMING ON METHYLATION MUTE CELLS
D
H4-AC
% OF INPUT
TIME AFTER RETINOID INDUCTION (HOURS)
9CIS RETINOIC ACID
PRIMING AND 9CIS RA
PRIMING ON METHYLATION MUTE CELLS+ 9CIS RA
E
TGM2
mRNA COPY NUMBER
TIME AFTER RETINOID INDUCTION (HOURS)
9CIS RETINOIC ACID
PRIMING AND 9CIS RETINOIC ACID
PRIMING+ADOX AND 9CIS RETINOIC ACID
F
mRNA copy number normalized for 36B4
CYP27
CD38
TGM2
CONTROL
NAÏVE+ 9CIS RA
PRIMED+ 9CIS RA
5μM
10μM
15μM
ADOX
PRIMED+ 9CIS RA

Fig. 9

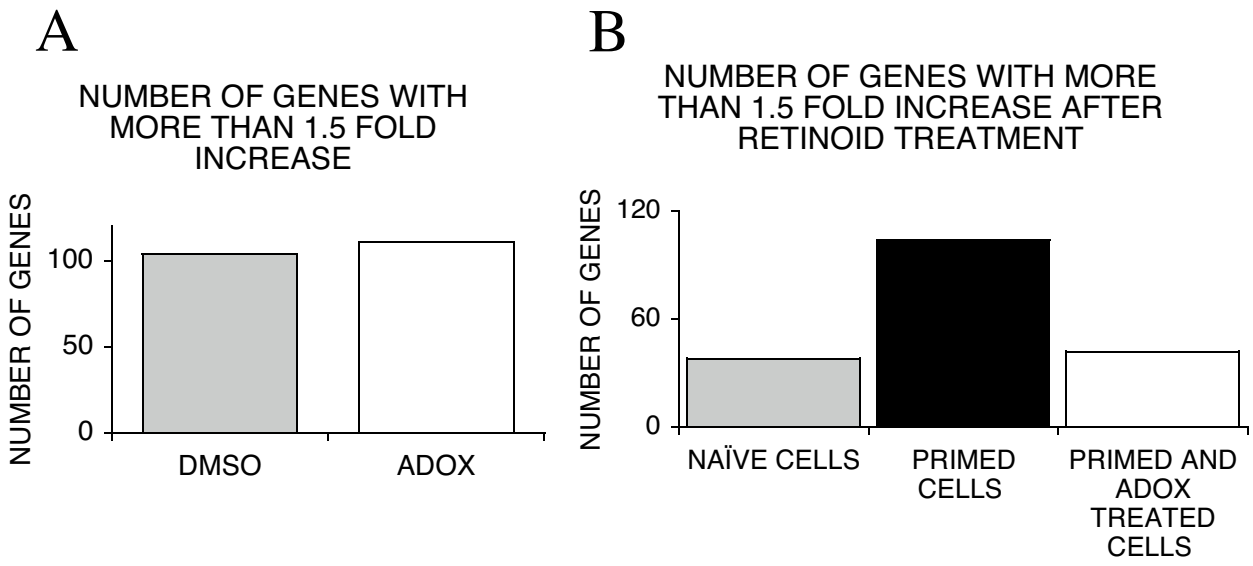
A
NUMBER OF GENES WITH MORE THAN 1.5 FOLD INCREASE
NUMBER OF GENES
100
50
0
DMSO
ADOX
B
NUMBER OF GENES WITH MORE THAN 1.5 FOLD INCREASE AFTER RETINOID TREATMENT
NUMBER OF GENES
120
60
0
NAÏVE CELLS
PRIMED CELLS
PRIMED AND ADOX TREATED CELLS

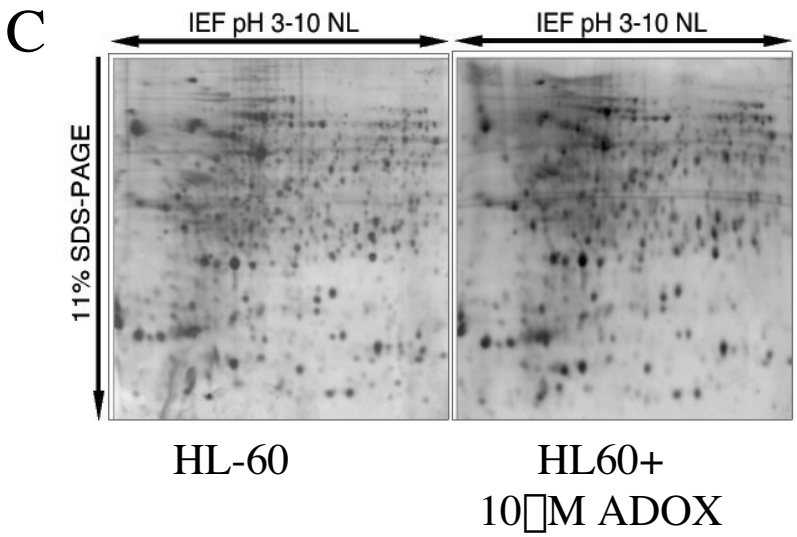
C
IEF pH 3-10 NL
IEF pH 3-10 NL
11% SDS-PAGE
HL-60
HL60+
10□M ADOX

Fig. 10

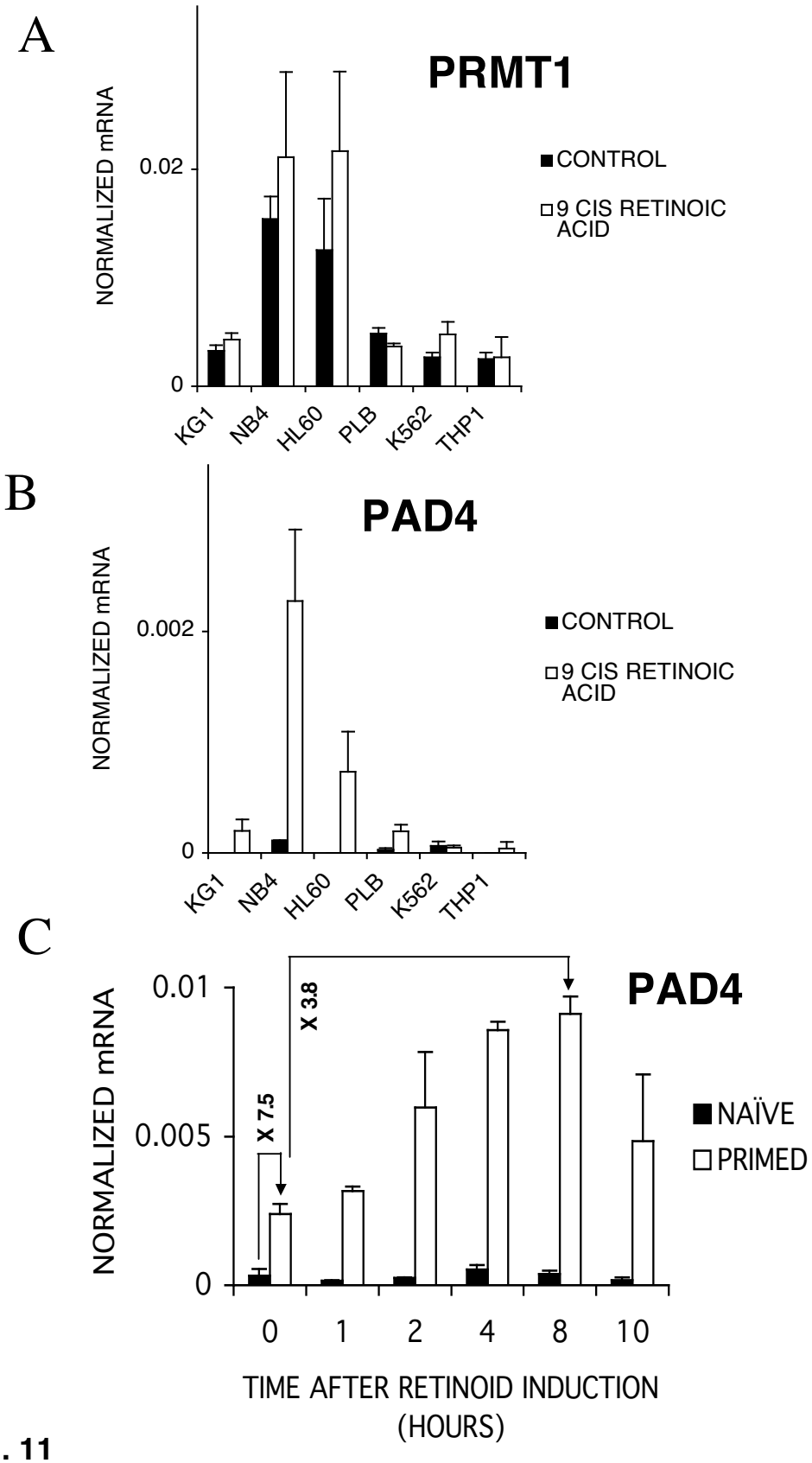
A
PRMT1
NORMALIZED mRNA
0.02
0
CONTROL
9 CIS RETINOIC ACID
KG1
NB4
HL60
PLB
K562
THP1
B
PAD4
NORMALIZED mRNA
0.002
0
CONTROL
9 CIS RETINOIC ACID
KG1
NB4
HL60
PLB
K562
THP1
C
PAD4
NORMALIZED mRNA
0.01
0.005
0
X 7.5
X 3.8
NAÏVE
PRIMED
0
1
2
4
8
10
TIME AFTER RETINOID INDUCTION (HOURS)

Fig. 11

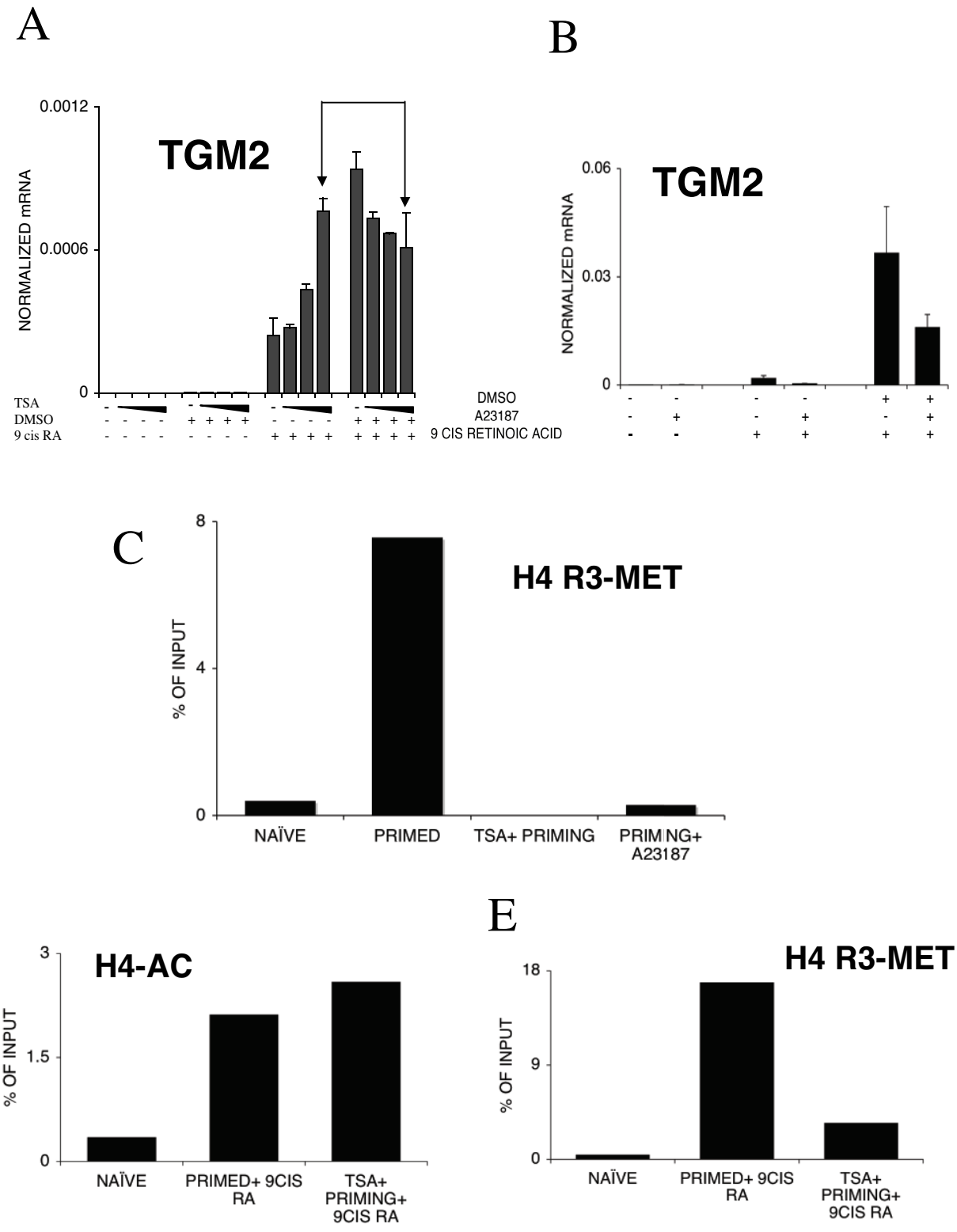
A
TGM2
NORMALIZED mRNA
0.0012
0.0006
0
TSA
DMSO
9 cis RA
B
TGM2
NORMALIZED mRNA
0.06
0.03
0
DMSO
A23187
9 CIS RETINOIC ACID
C
H4 R3-MET
% OF INPUT
8
4
0
NAÏVE
PRIMED
TSA+ PRIMING
PRIMING+ A23187
D
H4-AC
% OF INPUT
3
1.5
0
NAÏVE
PRIMED+ 9CIS RA
TSA+ PRIMING+ 9CIS RA
E
H4 R3-MET
% OF INPUT
18
9
0
NAÏVE
PRIMED+ 9CIS RA
TSA+ PRIMING+ 9CIS RA

Fig. 12

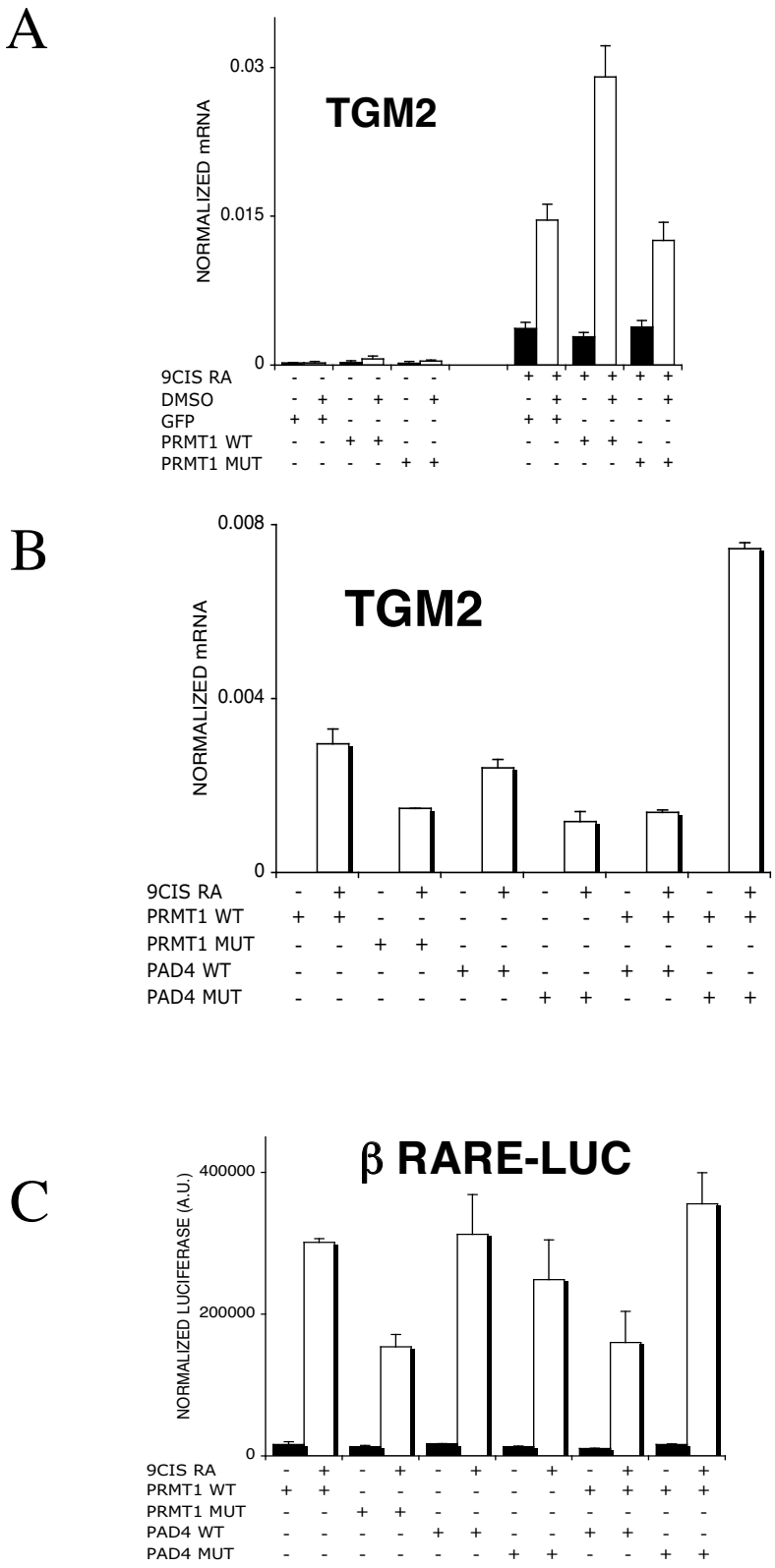
A
TGM2
NORMALIZED mRNA
0.03
0.015
0
9CIS RA
DMSO
GFP
PRMT1 WT
PRMT1 MUT
B
TGM2
NORMALIZED mRNA
0.008
0.004
0
9CIS RA
PRMT1 WT
PRMT1 MUT
PAD4 WT
PAD4 MUT
C
β RARE-LUC
NORMALIZED LUCIFERASE (A.U.)
400000
200000
0
9CIS RA
PRMT1 WT
PRMT1 MUT
PAD4 WT
PAD4 MUT

Fig. 13

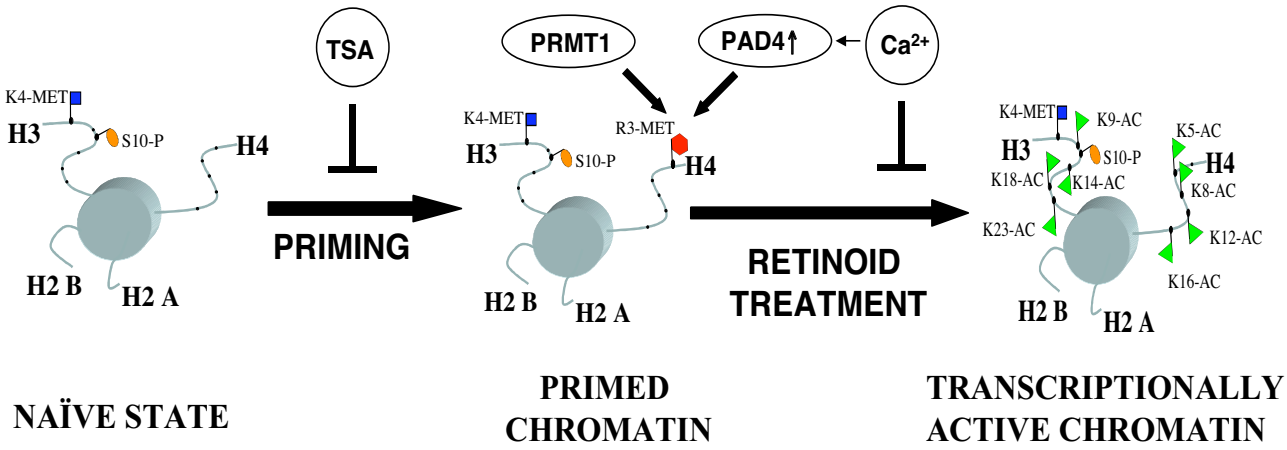
TSA
PRMT1
PAD4↑
Ca2+
K4-MET
H3
S10-P
H4
H2 B
H2 A
PRIMING
R3-MET
RETINOID
TREATMENT
K9-AC
K5-AC
K18-AC
K14-AC
K8-AC
K23-AC
K12-AC
K16-AC
NAÏVE STATE
PRIMED
CHROMATIN
TRANSCRIPTIONALLY
ACTIVE CHROMATIN

Fig. 14

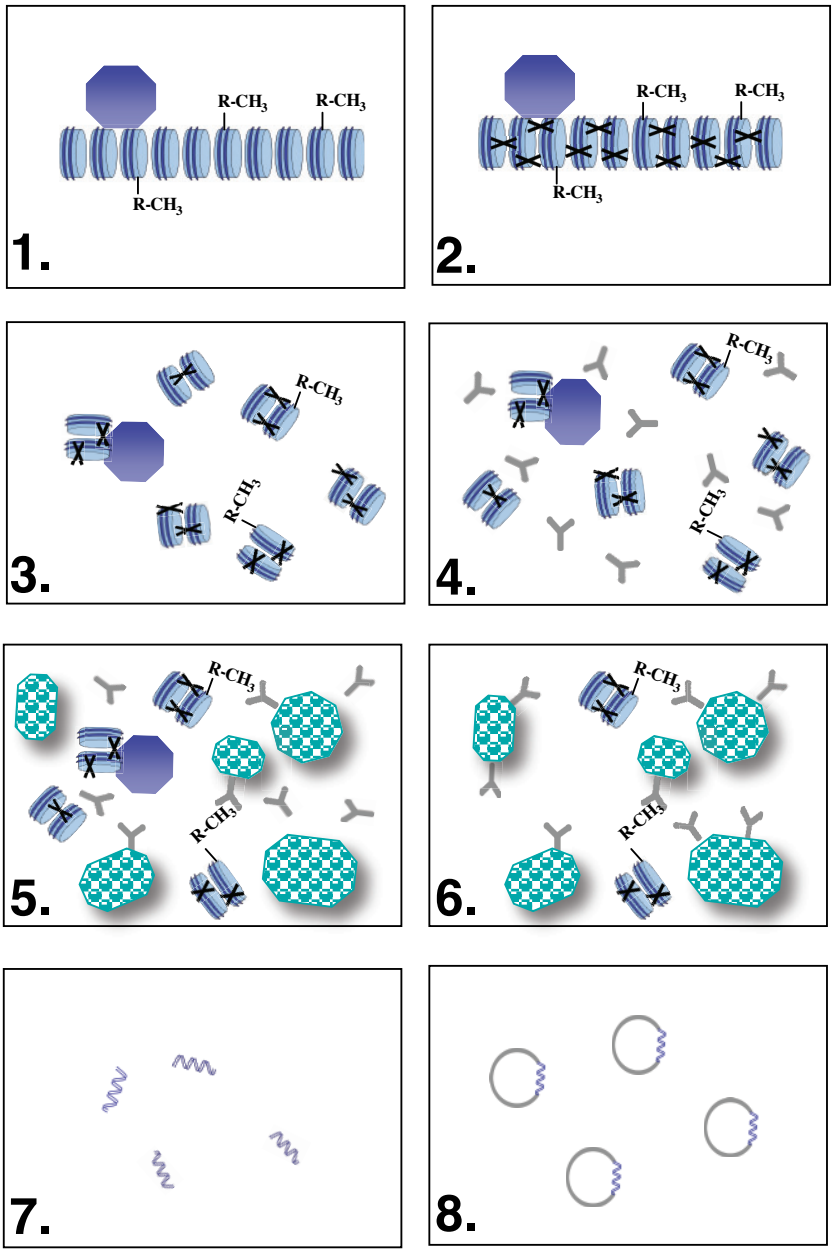
R-CH3
R-CH3
R-CH3
1.
R-CH3
R-CH3
R-CH3
2.
R-CH3
R-CH3
3.
R-CH3
R-CH3
4.
R-CH3
R-CH3
5.
R-CH3
R-CH3
6.
7.
8.

Fig. 15

A

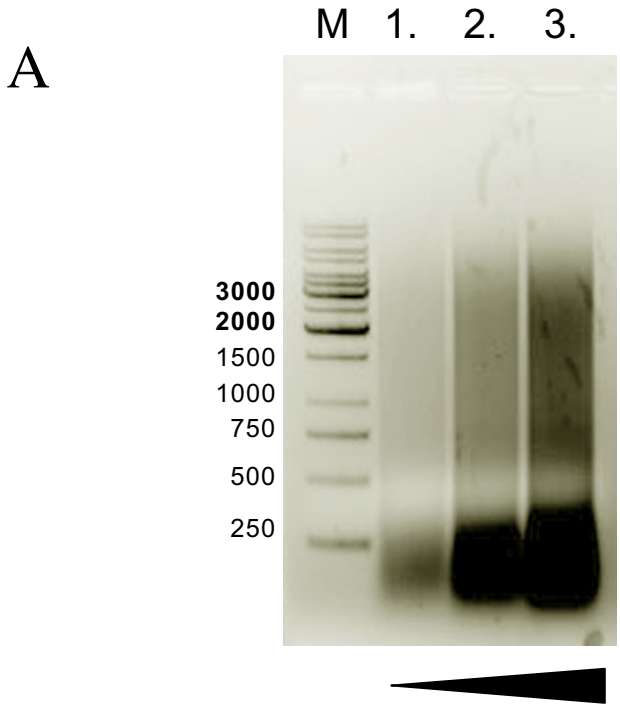
M 1. 2. 3.
3000
2000
1500
1000
750
500
250

B

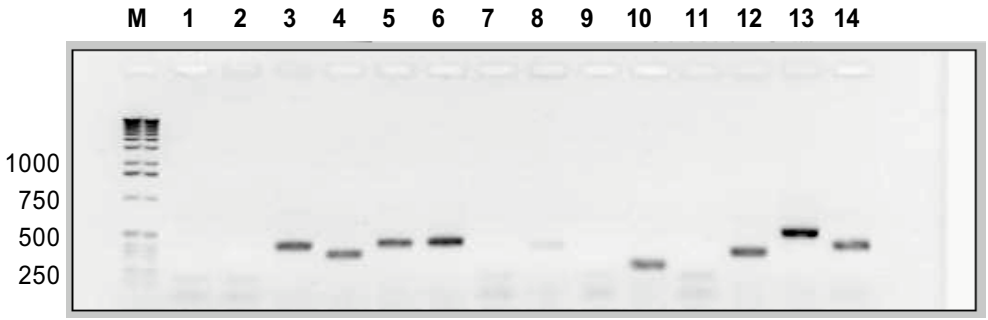
M 1 2 3 4 5 6 7 8 9 10 11 12 13 14
1000
750
500
250

Fig. 16

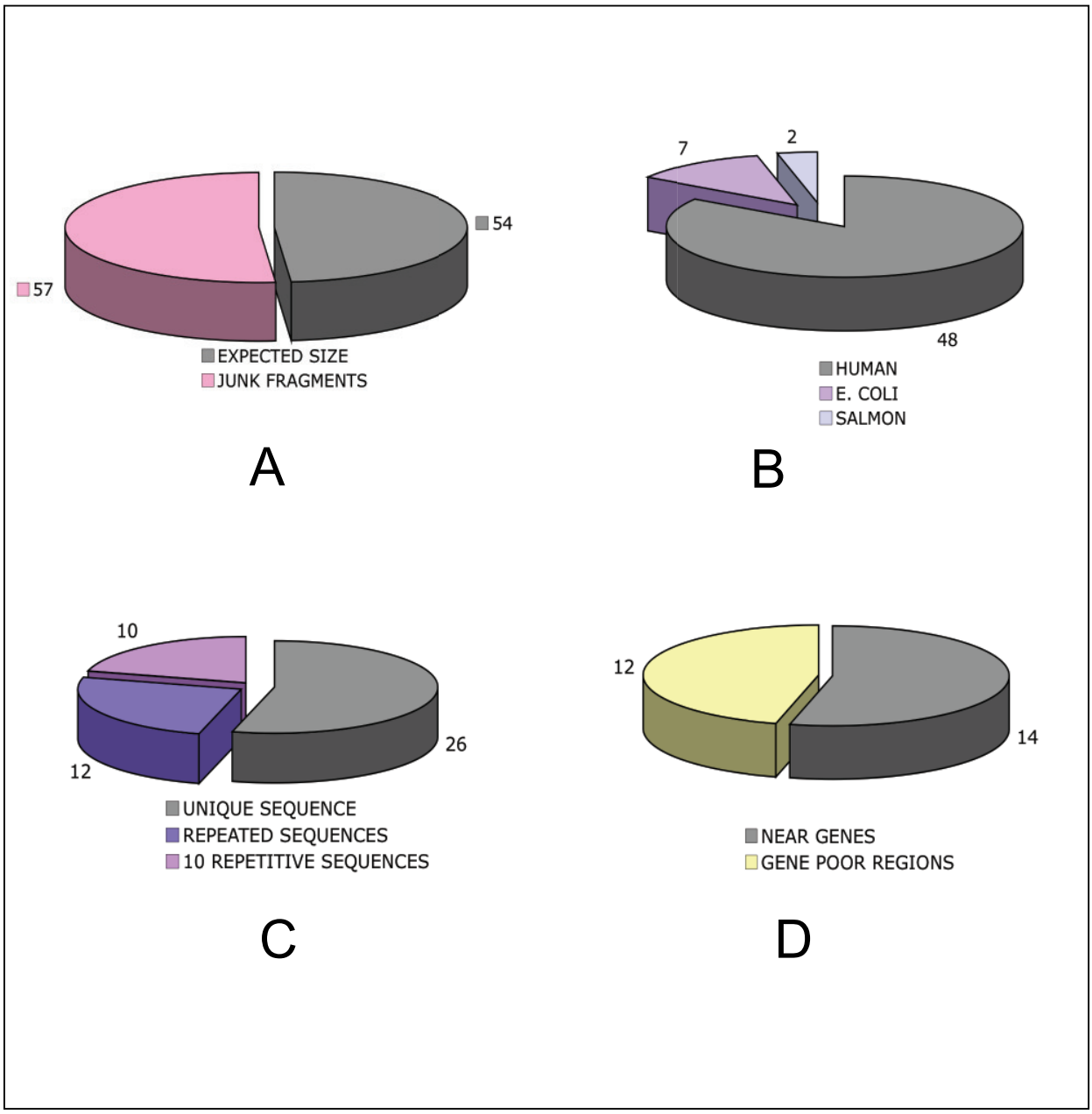
54
57
EXPECTED SIZE
JUNK FRAGMENTS
A
7
2
48
HUMAN
E. COLI
SALMON
B
10
26
12
UNIQUE SEQUENCE
REPEATED SEQUENCES
10 REPETITIVE SEQUENCES
C
12
14
NEAR GENES
GENE POOR REGIONS
D

Fig. 17

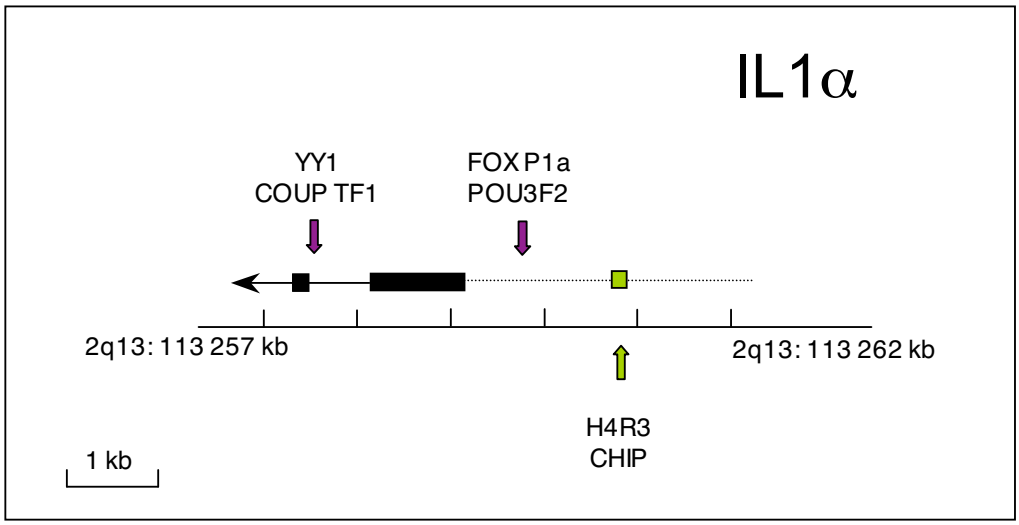
IL1α
YY1
COUP TF1
FOX P1a
POU3F2
2q13: 113 257 kb
2q13: 113 262 kb
H4R3
CHIP
1 kb

Fig. 18

A

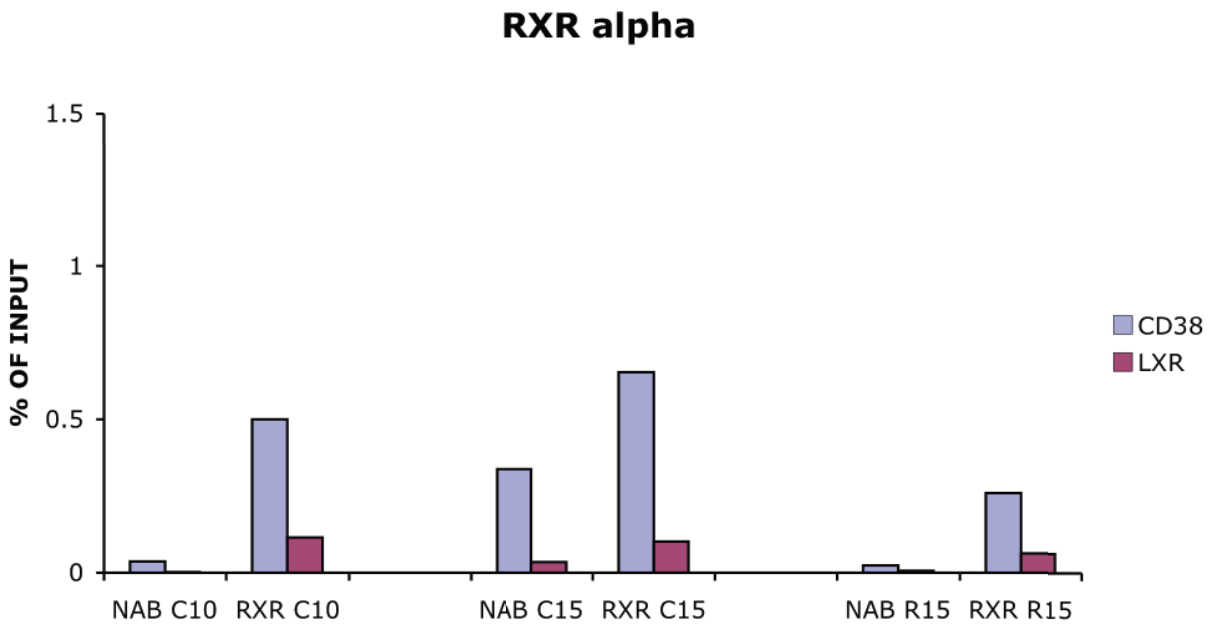
RXR alpha
1.5
1
0.5
0
% OF INPUT
CD38
LXR
NAB C10
RXR C10
NAB C15
RXR C15
NAB R15
RXR R15

B

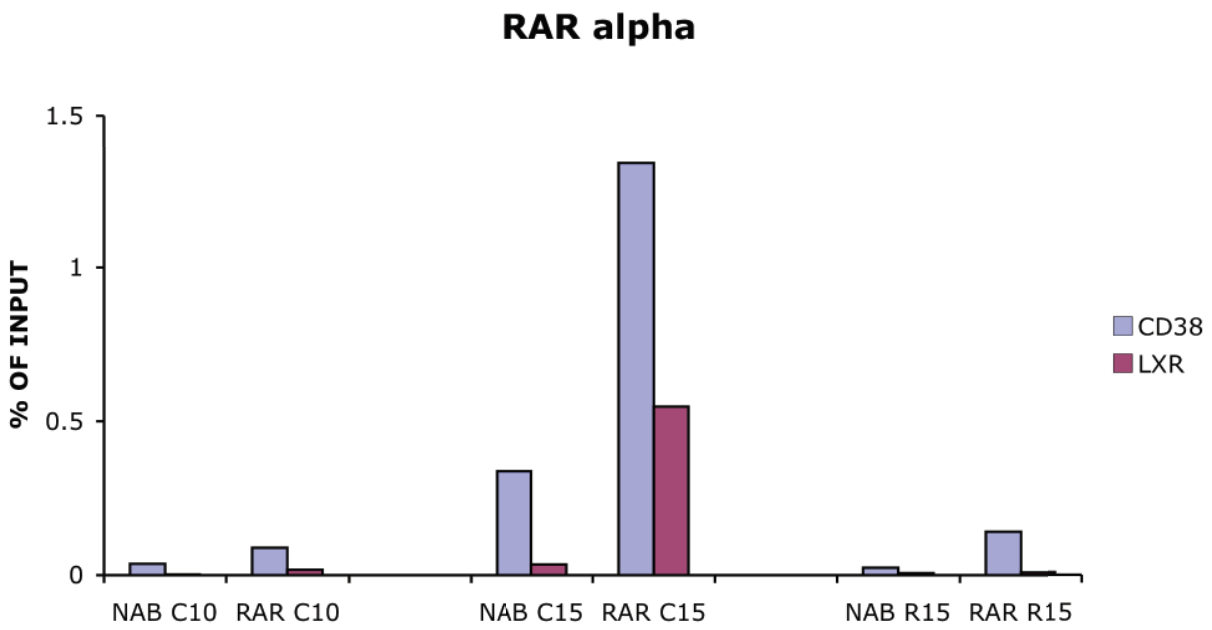
RAR alpha
1.5
1
0.5
0
% OF INPUT
CD38
LXR
NAB C10
RAR C10
NAB C15
RAR C15
NAB R15
RAR R15

Fig. 19

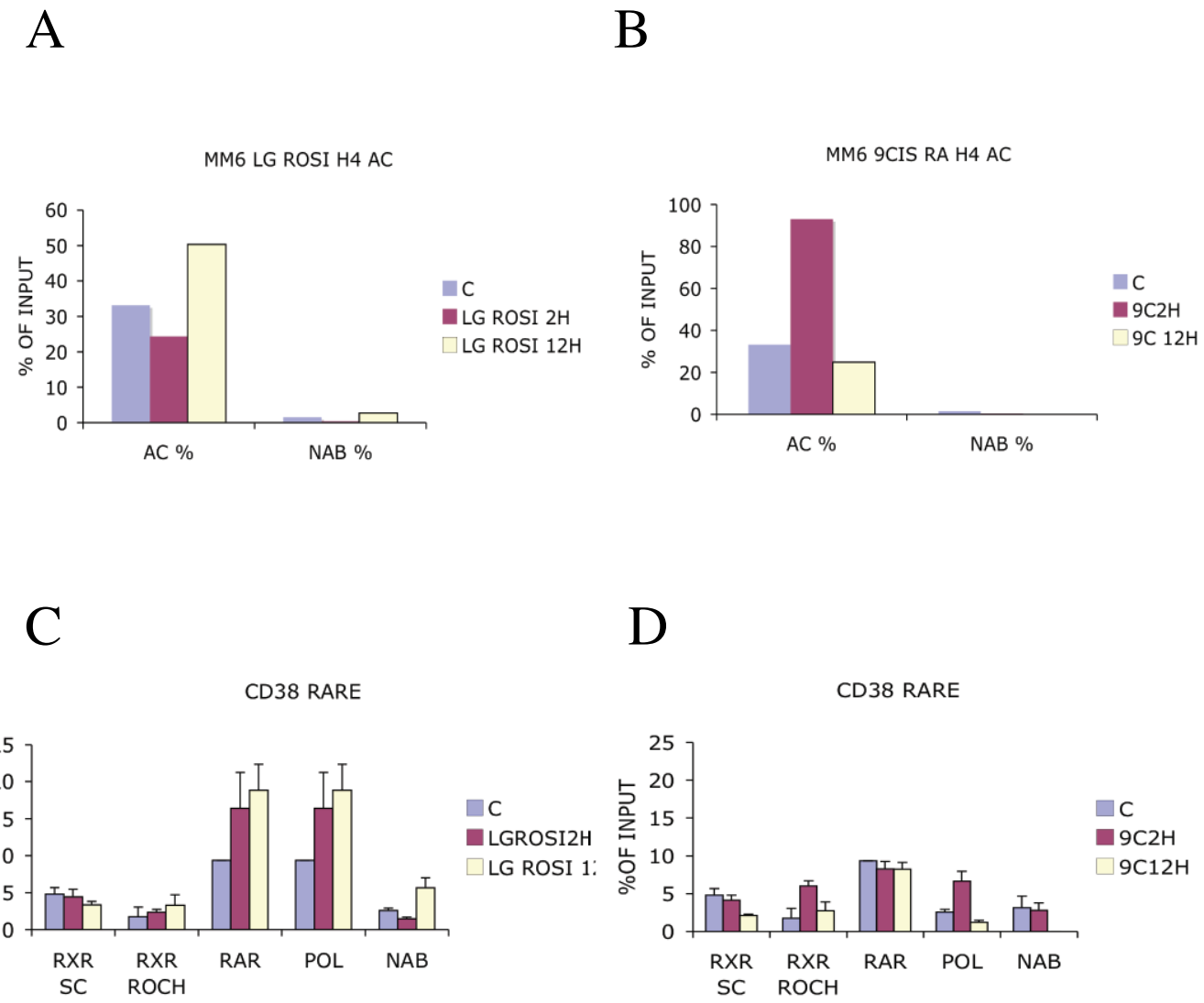
A
MM6 LG ROSI H4 AC
% OF INPUT
60
50
40
30
20
10
0
AC %
NAB %
C
LG ROSI 2H
LG ROSI 12H
B
MM6 9CIS RA H4 AC
% OF INPUT
100
80
60
40
20
0
AC %
NAB %
C
9C2H
9C 12H
C
CD38 RARE
25
20
15
10
5
0
RXR SC
RXR ROCH
RAR
POL
NAB
C
LGROSI2H
LG ROSI 1
D
CD38 RARE
%OF INPUT
25
20
15
10
5
0
RXR SC
RXR ROCH
RAR
POL
NAB
C
9C2H
9C12H

Fig. 20

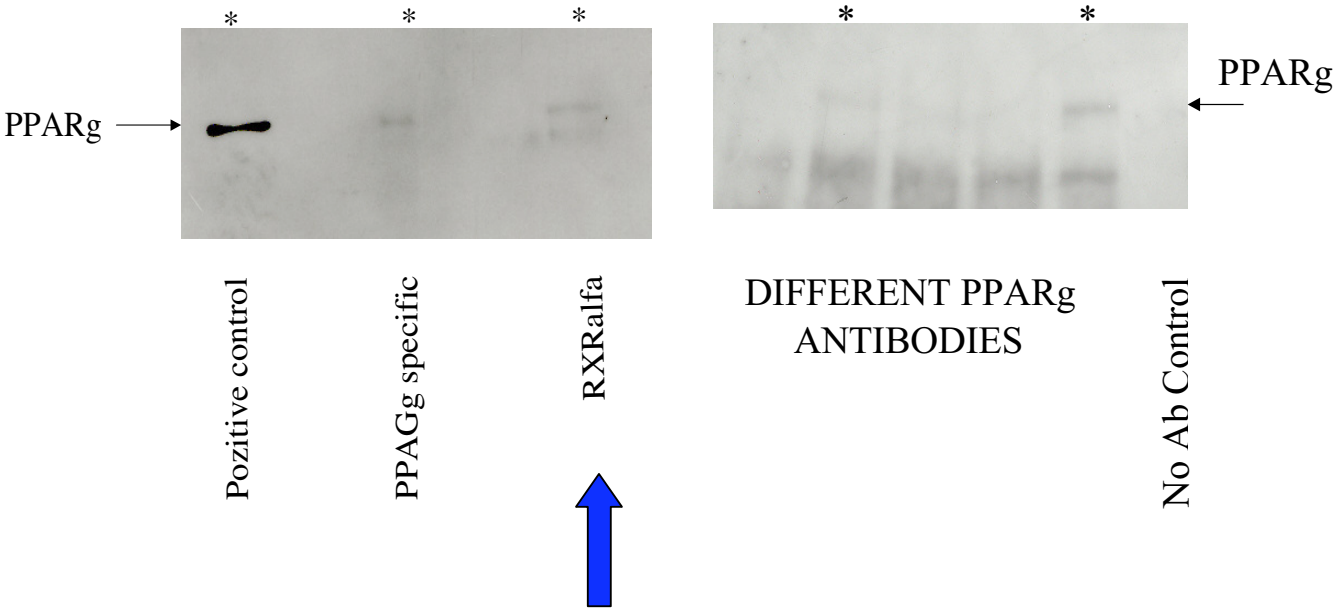
PPARg
PPARg
Pozitive control
PPAGg specific
RXRalfa
DIFFERENT PPARg ANTIBODIES
No Ab Control

Fig. 21

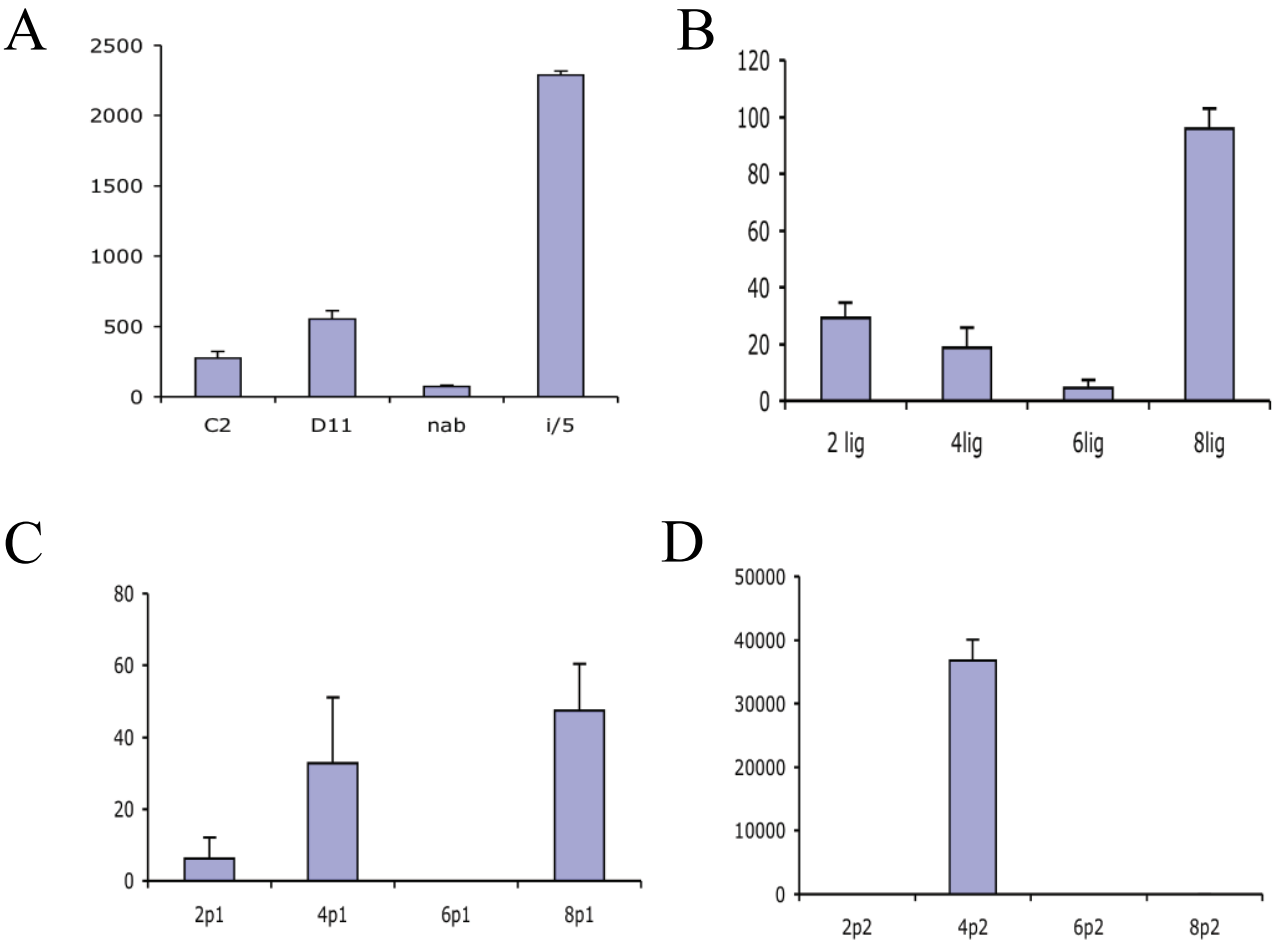

Farnham Lab protocol

1 . END FILL

T4 pol

2. LIGATION OF LINKER

Blunt end ligation with PEG

3. LINKER PCR

JW103	5’-GCGGTGACCCGGG AGA TCT GAA TTC-3’
JW102	3’-CT AGA CTT AAG-5’

Fig. 22

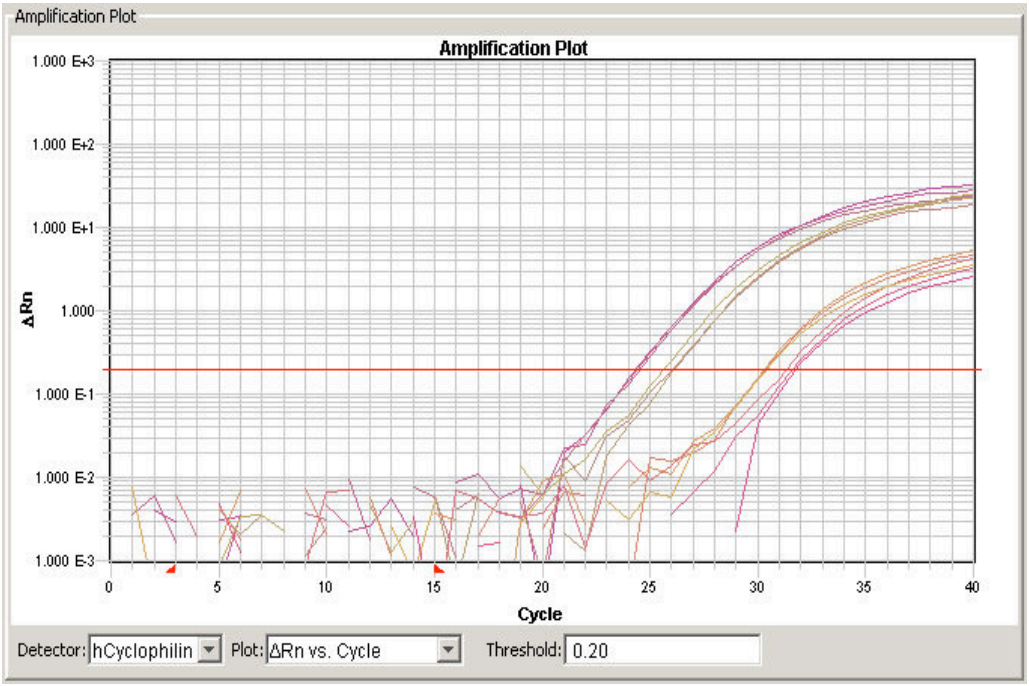

LM PCR
deRisi Lab protocol

1. Attach degenerated primer with Sequenase
   5'-GTT TCC CAG TCA CGA TCN NNN NNN NN-3'
   A, denature
   B, cool to 10 C
   C, slow ramp to 37 C
   D, denature
   E, add fresh enzyme and repeat from step A

2. Taq PCR with attached primer
   5'-GTT TCC CAG TCA CGA TC-3'

Fig. 23

A

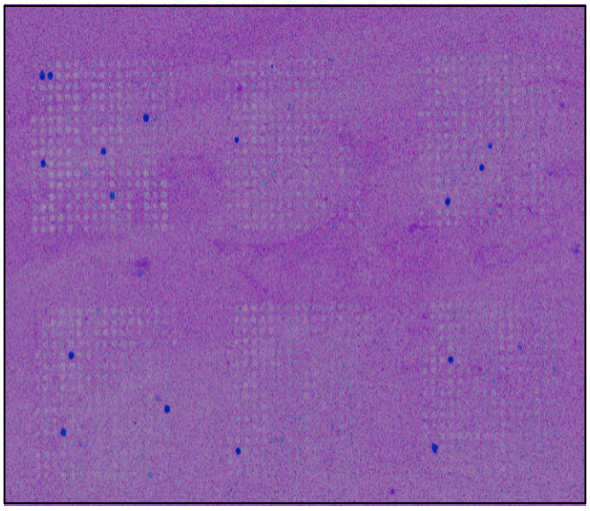

B

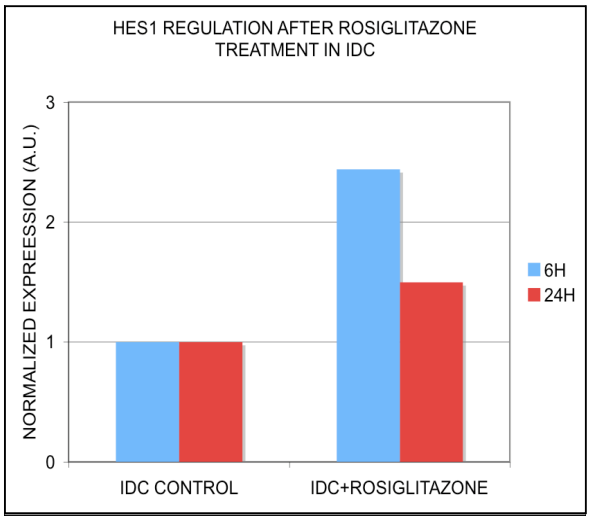
HES1 REGULATION AFTER ROSIGLITAZONE TREATMENT IN IDC
NORMALIZED EXPREESSION (A.U.)
3
2
1
0
6H
24H
IDC CONTROL
IDC+ROSIGLITAZONE

C

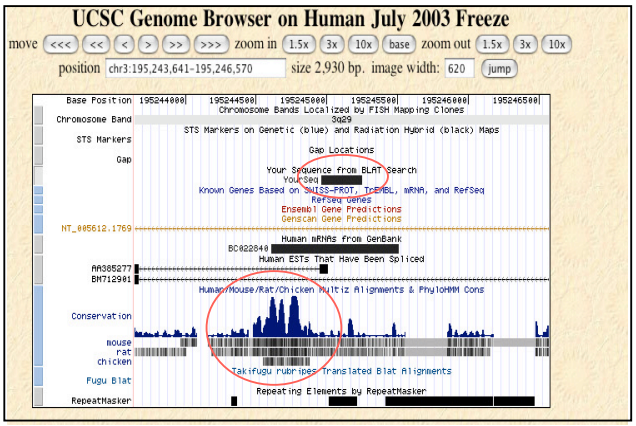
UCSC Genome Browser on Human July 2003 Freeze
move
zoom in
zoom out
position chr3:195,243,641-195,246,570
size 2,930 bp.
image width:
jump
Chromosome Band
STS Markers
Gap
Conservation
mouse
rat
chicken
RepeatMasker

D

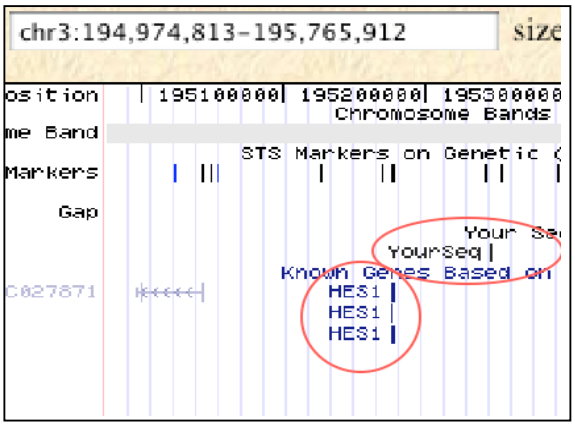
chr3:194,974,813-195,765,912
size
195100000
195200000
195300000
Chromosome Bands
STS Markers on Genetic
Gap
YourSeq
Known Genes Based on
HES1
HES1
HES1

E


HES1 DR1+DR1
GGG TCC CGG GAC AGA GCC CA
CCC AGG GCC CTG TCT CGG GT

Fig. 24

A

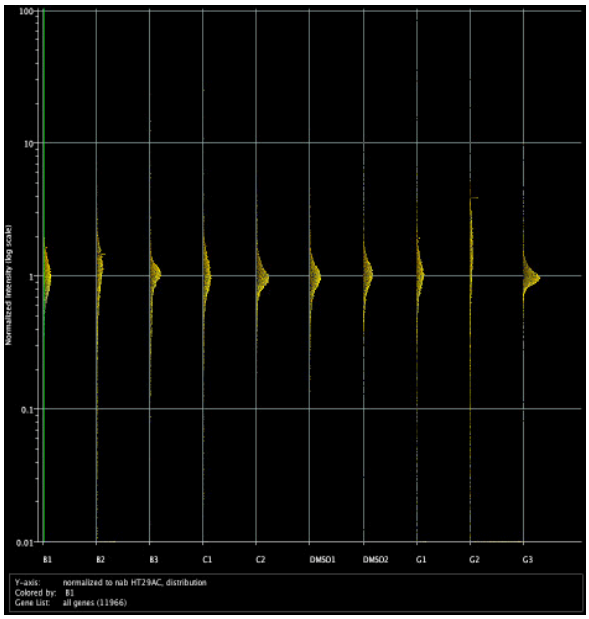
100
10
1
0.1
0.01
Normalized Intensity (log Scale)
B1
B2
B3
C1
C2
DMSO1
DMSO2
G1
G2
G3
Y-axis: normalized to nab HT29AC, distribution
Colored by: B1
Gene List: all genes (11966)

B

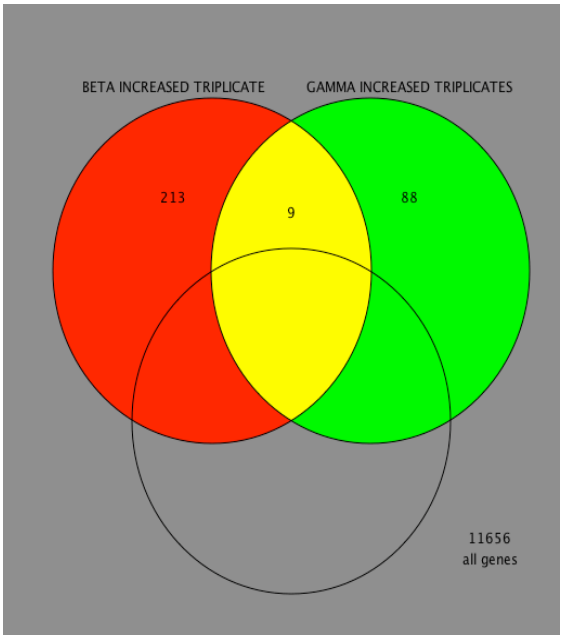
BETA INCREASED TRIPLICATE
GAMMA INCREASED TRIPLICATES
213
9
88
11656
all genes

C

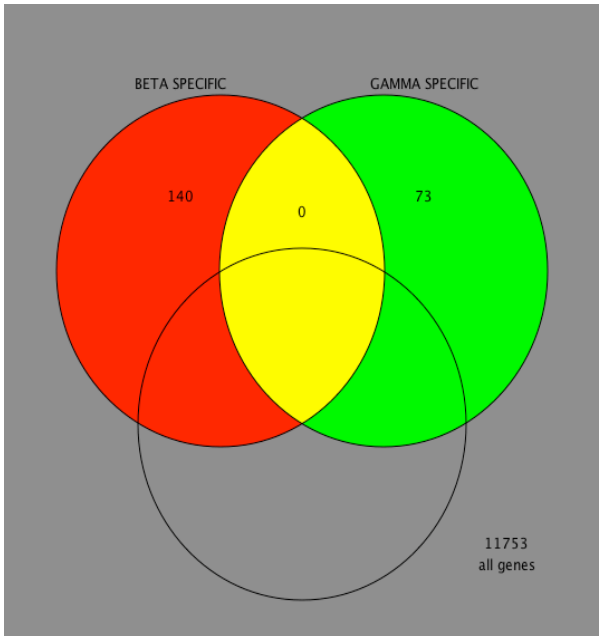
BETA SPECIFIC
GAMMA SPECIFIC
140
0
73
11753
all genes

Fig. 25

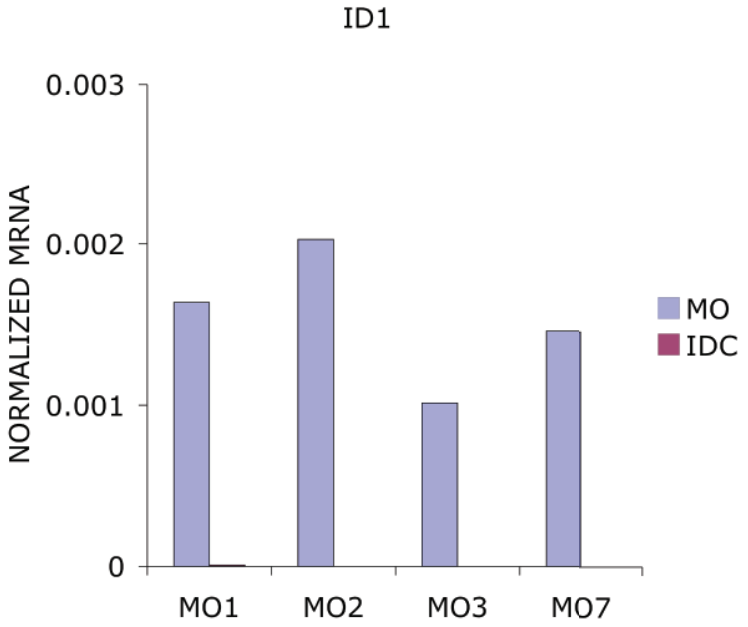
ID1
0.003
0.002
0.001
0
NORMALIZED MRNA
MO
IDC
MO1
MO2
MO3
MO7

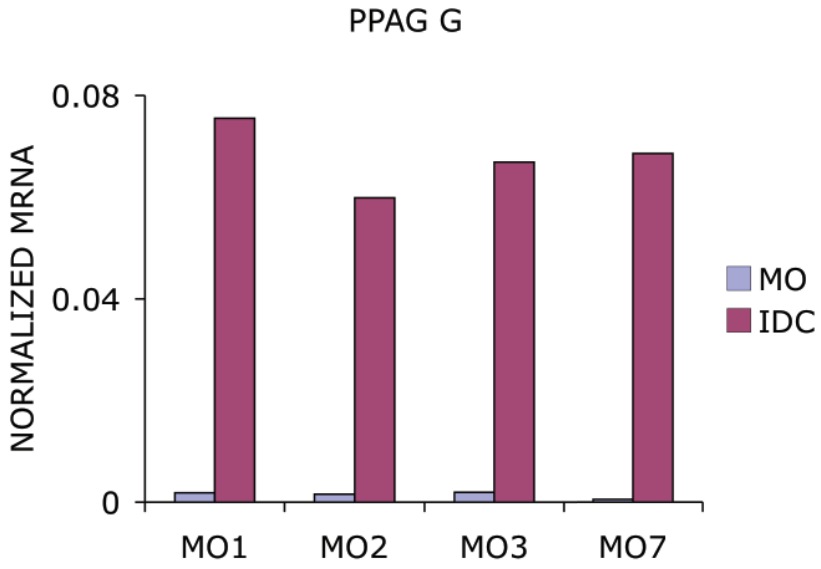
PPAG G
0.08
0.04
0
NORMALIZED MRNA
MO
IDC
MO1
MO2
MO3
MO7

Fig. 26

A

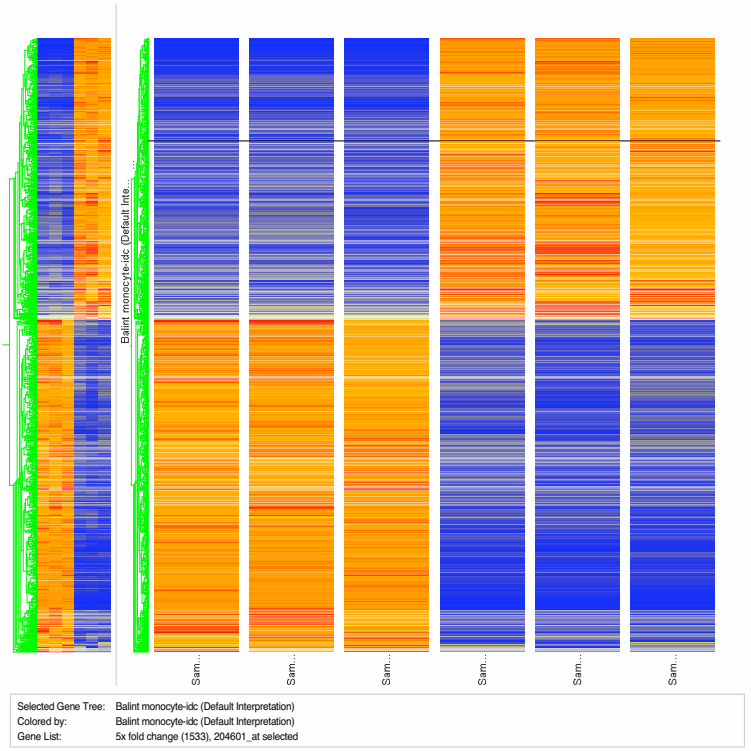
Balint monocyte-idc (Default Inte...
Sam...
Sam...
Sam...
Sam...
Sam...
Sam...
Selected Gene Tree: Balint monocyte-idc (Default Interpretation)
Colored by: Balint monocyte-idc (Default Interpretation)
Gene List: 5x fold change (1533), 204601_at selected

B

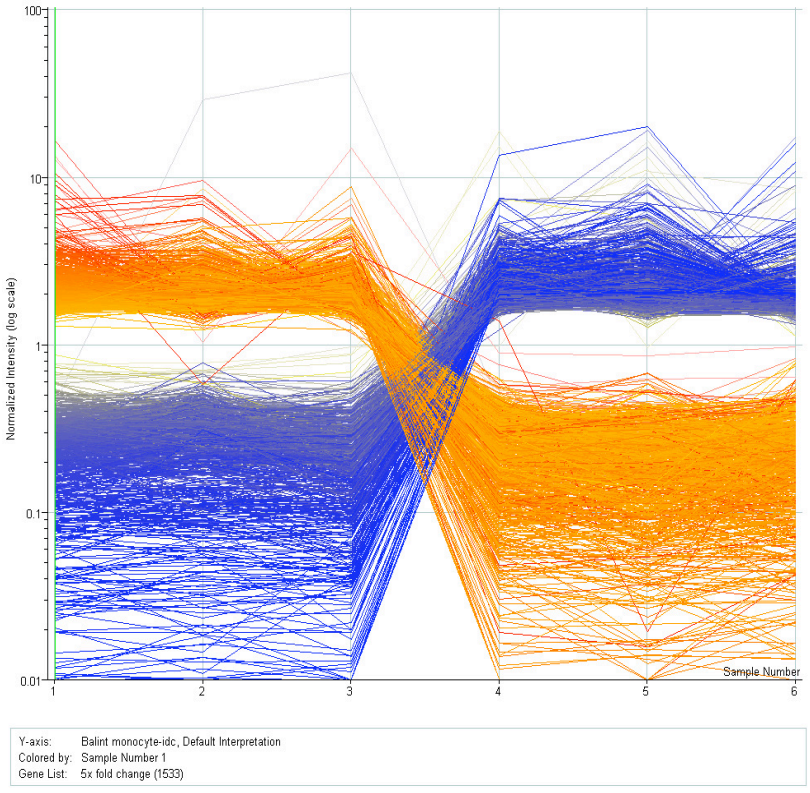
100
10
1
0.1
0.01
Normalized Intensity (log scale)
1
2
3
4
5
6
Sample Number
Y-axis: Balint monocyte-idc, Default Interpretation
Colored by: Sample Number 1
Gene List: 5x fold change (1533)

Fig. 27

Clusters of changing genes identified during monocyte/IDC transition

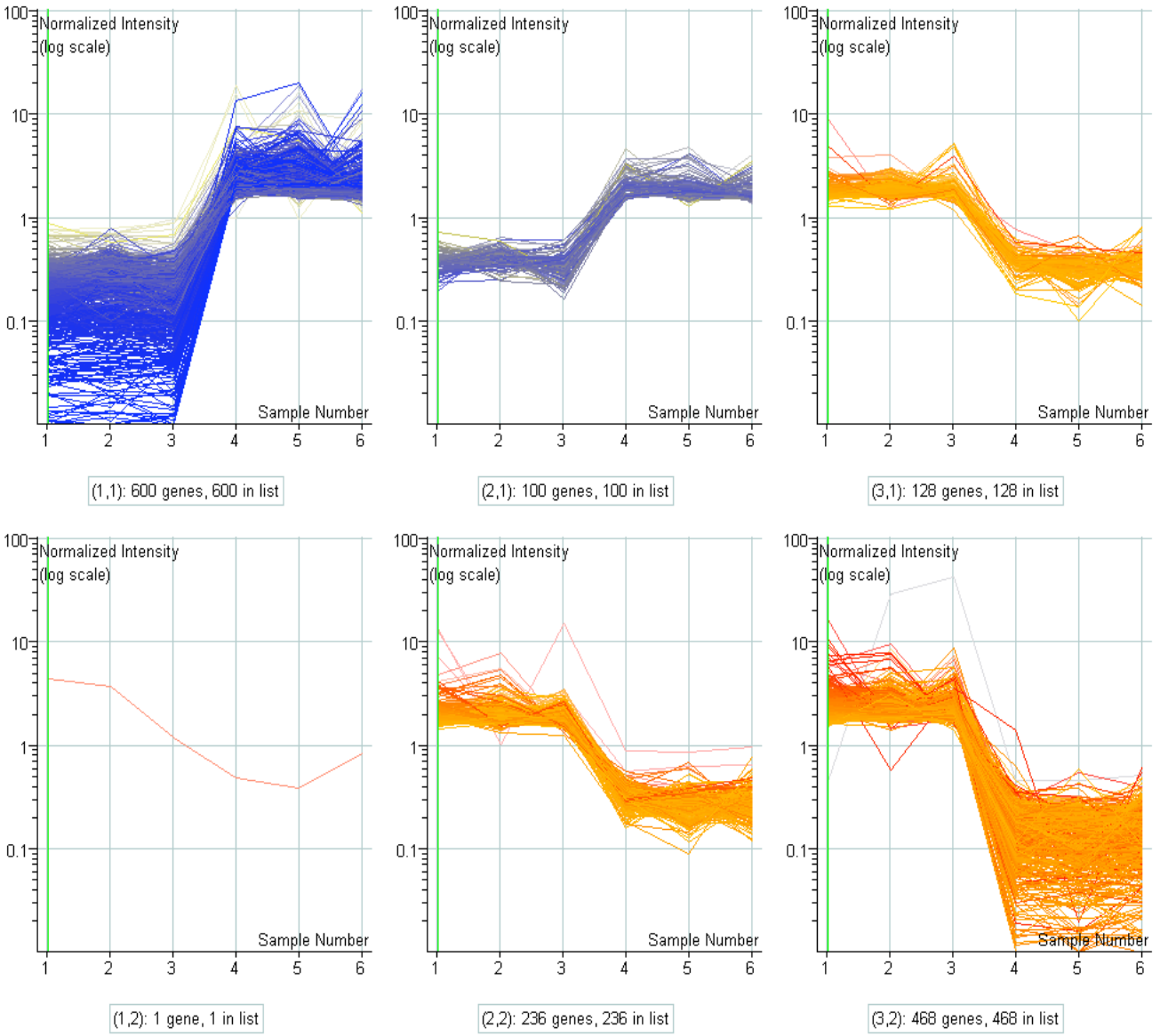

Fig. 28

A

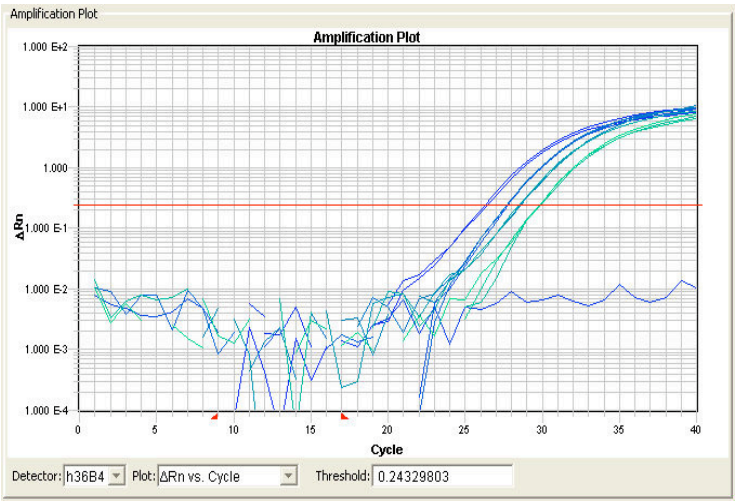

AMPLIFICATION PLOTS FROM 4000 TO 400 COPIES TAQMAN

B

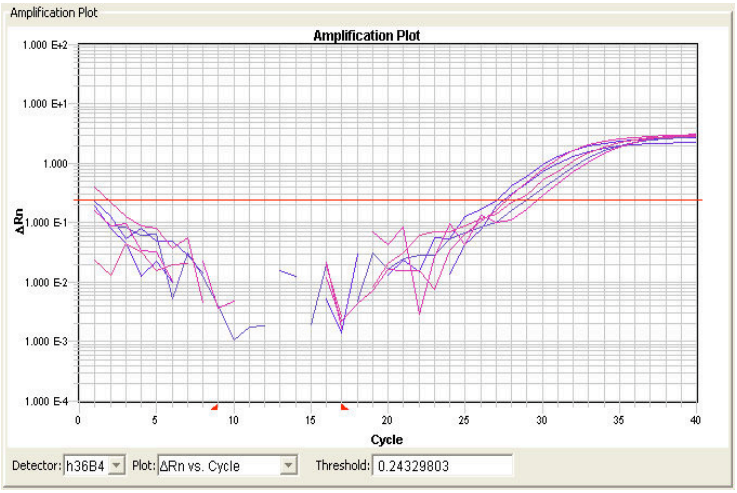

AMPLIFICATION PLOTS FROM 4000 TO 400 COPIES SYBR GREEN

C

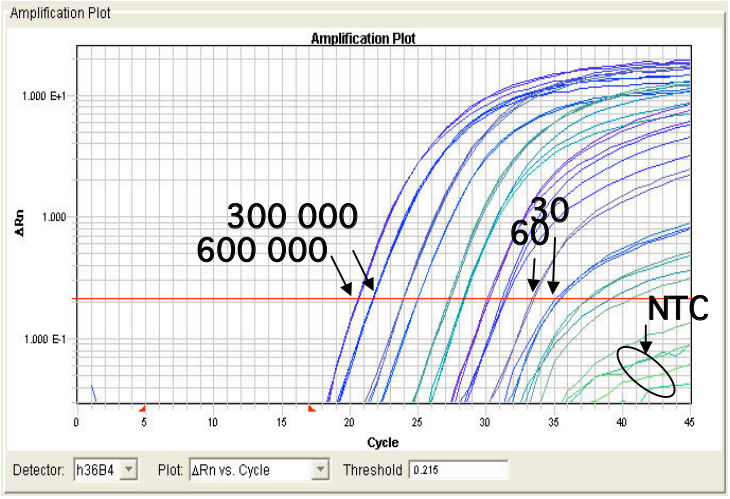

AMPLIFICATION PLOTS FROM 300 000 TO 3 COPIES AND THEIR DOUBLE QUANTITY

Fig. 29

GENOMIC ASSAYS	FW 5'-3'	REV 5'-3'	PROBE 5'-3'
TGM2-CORE	GAGACCCTCCAAGTGCGAC	CCAAAGCGGGCTATAAGTTAGC	FAM-CCGCCTCGGCAGTGCCA-TAMRA
TGM2-D	CAGACACACACCAGGACATAG	CTCTGGACACCTGCTCATCT	FAM-TGTGTGTGGCTCGCGGACAAGG-TAMRA
TGM2-C	ACACCAATGCCACTGTCAGAT	GTCTGTACCTGAGTCCATGCCTG	FAM-CTGTGGGTGCCCTCTCTGATTTTGGG-TAMRA
TGM2-B	GTCCTAGGCTGAGTCCCTGGA	TCCACTGAGCTTTCTTGAGGC	FAM-AGTCTTGCTCCTTTCTGGCACACAGTGGTAMRA
TGM2-A	GAGACTCCAGCCAGAGCCC	TCAGGGAAAACAACCCGTGT	FAM TTTGACCCAGGGAGAAATATCCACTGAAGC TAMRA
TGM2-HR1	TGCTCCCTGCAGCTGGT	CCTCTCGGTCGGGTGATT	FAM-TCCTCACGCTGCTCTTTCCTCCAA-TAMRA
RARb RARE	TGTCAGACTAGTTGGGTCATTTGAAG	TTGCCTAATATATGCGAGTGAACTTT	FAM-TTAGCAGCCCGGGTAGGGTTCACC-TAMRA
GENE EXPRESSION ASSAYS			
hCyclophilin	ACGGCGAGCCCTTGG	TTTCTGCTGTCTTTGGGACCT	FAM-CGCGTCTCCTTTGAGCTGTTTGCA-TAMRA
hCyp27	AGATGCACGTGAACCTGGC	TACTTTCCCTCTTGCCGCA	FAM-AGTGCCCCGCTCTTGGAGCAAGT-TAMRA
hRARa	CCAGCACCAGCTTCCAGTTA	GGGAGGGCTGGGCAC	FAM-CTCTTCAGAACTGCTGCTCTGGGTCTCAA-TAMRA
hRARb	GGAAACTTTCCCTTCACTCTGC	CCAGTCGGACTCGATGGTC	FAM-TGGGTAAATACACCACGAATTCCAGTGCTG-TAMRA
hRARg	TGCATCATCAAGATCGTGGAG	GTGATCTGGTCAGCAATGCTG	FAM-CCAAGCGGTTGCCTGGCTTTACA-TAMRA
hRXRa	GGCCTACTGCAAGCACAAGTA	CAGGCGGAGCAAGAGCTTA	FAM-CGAACCTTCCCGGCTGCTCTG-TAMRA
hRXRb	CCCATTCAGCAGGAGTAGG	CTCATGTCACGCATTTTGGA	FAM-TCTGTCAGCACCCGATCAAAGATGG-TAMRA
hRXRg	GGGAAGCTGTGCAAGAAGA	GGTAGCACATTCTGCCTCACT	FAM-AGACAGAGGAGCCGAGAGCGAG-TAMRA
hCD38	CGTCAAGTACACTGAAATTCATCCT	AATAAATGCACCCTTGAAAGCA	FAM-CCCATACACTTTGGCAGTCTACATGTCTCATCT -TAMRA
hRAOH	TTCTCCAGAAAGTGCGAGAAGAG	CTTAATAACACACCCGATGTATTTAAG	FAM-CAAATTTCCATGTCTAACTTGTTGTCTTGATTGCT-TAMRA
hTGM2	CTGGGCCACTTCATTTTGC	ACTCCTGCCGCTCCTCTTC	FAM-TCCAGGTACACAGCATCCGCTGGG-TAMRA
PREDESIGNED GENE EXPRESSION ASSAYS	Applera Assay I.D.		
hPADI4	Hs00202612_m1		
hPRMT1	Hs00266002_m1		

REAL TIME QUANTITATIVE PCR OLIGO SETS USED IN THE PRESENTED EXPERIMENTS

Table 1

GENE NAME	CHROMOSOMAL LOCATION	POSITION TOWARDS THE GENE	CONSERVED TFBS WITHIN 1KB
AMPH 1	7p14.1	intronic	V$ICSBP_Q6
Cadherin 23	10q22.1	intronic	V$S8_01, V$PAX2_01
Collagen 9 alpha 1	6q13	5‘	VFOX_Q2, VMEF2_01
DCAMKL1	13q13.3	intronic	-
DSU	2q35	intronic	V$RORA2_01
EYA3	1p35.3	intronic	-
IL1A	2q13	5‘	V$FOXP1_01, V$BRN2_01
IL1RAPL2	Xq22.3	intronic	-
KIAA0476	1q21.3	5‘ from predicted promoter	-
MGC27434	8q24.21	intronic	V$OCT1_B
PAPD1	10p11.23	intronic	V$HP1SITEFACTOR_Q6
ROBO1	3p12.3	intronic	V$SOX5_01
SLC36A1	5q33.1	5‘	-
SPAG16	2q34	intronic	-

Table 2

GENE NAME	PANTHER MOLECULAR FUNCTION	PANTHER BIOLOGICAL PROCESS	REFERENCE
AMPH 1	Membrane traffic regulatory protein	Endocytosis Transport Neurotransmitter release	(Shang, 2004)
Cadherin 23	Cadherin	Cell adhesion-mediated signaling Cell adhesion Oogenesis Embryogenesis Anterior/posterior patterning Heart development Cytokinesis Cell proliferation and differentiation	(Bolz, 2001)
Collagen 9 alpha 1	Extra cellular matrix structural protein	Cell structure	(Mayne, 1985)
DCAMKL1	Non-receptor serine/threonine protein kinase	Protein phosphorylation Calcium mediated signaling Neurogenesis Cell motility	(Sossey-Alaoui, 1999)
DSU	Unclassified	Unclassified	(O'Sullivan, 2004)

Table 3

GENE NAME	PANTHER MOLECULAR FUNCTION	PANTHER BIOLOGICAL PROCESS	REFERENCE
EYA3	Other hydrolase	Vision Developmental processes	(Li, 2003)
IL1A	Interleukin	Cytokine and chemokine mediated signaling pathway Ligand-mediated signaling Macrophage-mediated immunity Cytokine/chemokine mediated immunity Cell cycle control Cell proliferation and differentiation	(Lord, 1991)
IL1RAPL2	Interleukin receptor	Cytokine and chemokine mediated signaling pathway	(Khan, 2004)
KIAA0476	Guanyl-nucleotide exchange factor	Other signal transduction	-
MGC27434	Unclassified	Unclassified	(Storlazzi, 2004)
PAPD1	Unclassified	Unclassified	-
ROBO1	Immunoglobulin receptor family member Defense/immunity protein	Cell adhesion	(Rhee, 2002)
SLC36A1	Other transporter Amino acid transporter	Amino acid transport Transport	(Sagne, 2001)
SPAG16	Microtubule family cytoskeletal protein	Cell motility	-

Table 3 continued

TF BINDING MATRIX	TRANSCRIPTION FACTOR	NUMBER OF OCCURENCES
V$OCT1_B	POU2F1	6
V$MEF2_Q6_01	MEF-2	5
V$FREAC7_01	FOXL1	4
V$PAX4_04	Pax-4a	3
V$FOXO4_02	FOXO4	3
V$EVI1_05	Evi-1	3

Table 4